SHEAR STRENGTH OF SAND REINFORCED WITH SHREDDED WASTE TIRES

by

Gary J. Foose

A thesis submitted in partial fulfillment of

the requirements for the degree of

Master of Science

(Civil and Environmental Engineering)

at the

UNIVERSITY OF WISCONSIN-MADISON

1993

SHEAR STRENGTH OF SAND REINFORCED WITH SHREDDED WASTE TIRES

Gary J. Foose
Under the supervision of Assistant Professor Craig H. Benson
at the University of Wisconsin-Madison

Currently, the most common methods for disposing of waste tires are either landfilling or stockpiling. The objective of this study is to demonstrate the feasibility of using shredded waste tires as a means of soil reinforcement. There are several examples of field-scale projects using shredded tires as soil reinforcement. However, a key question still remains: "What is the shear strength of soil reinforced with shredded waste tires?"

Results of large-scale direct shear tests on mixtures of sand and shredded waste tires were analyzed. The influence of confining stress, reinforcement content, length of reinforcement, unit weight of the soil matrix, and orientation of reinforcement on shear strength were evaluated. Strength envelopes for 27 different mixtures of sand and shredded waste tires were developed and compared to the strength envelope of un-reinforced sand. Additionally, stress-displacement relationships were compared to study the effects of reinforcement on modulus and volume change during shear.

Results indicate that initial friction angles as high as 67° can be obtained by reinforcing sand with shredded waste tires. Initial friction angle tends to increase with increasing reinforcement content. The average initial friction angle of specimens with a unit weight of the soil matrix of 16.8 kN/m^3 was 15° higher than specimens with a unit weight of the soil matrix of 15.7 kN/m^3. Length of reinforcement and orientation of the reinforcement were not found to significantly effect shear strength sand reinforced with shredded waste tires.

ACKNOWLEDGMENTS

The author thanks Professor Craig H. Benson for his motivation, guidance, and interest in seeing his students excel. The author expresses appreciation to Professor Peter J. Bosscher for providing his insight and support to the project. The author would also like to thank Professors Tuncer B. Edil and Jeffrey S. Russell for serving on this committee.

Special thanks are expressed to Norm Severson for constructing the testing equipment for this project. The author and the many other graduate students that Norm has helped are indebted to him for his keen insight into testing soils and patients in working with eager students. Thanks are also extended to those fellow students who were involved in the completion of the project: Tarek Abichou, Milind Khire, Jerry Krueger, Senro Kuraoka and Jim Tinjum.

Financial support for the research described in this thesis has been provided by the State of Wisconsin's Solid Waste Research Council (SWRC). This support is greatly appreciated. The findings herein are those of the author and do not necessarily reflect the opinions of SWRC. This thesis has not been subjected to SWRC's review. Mention of trade names or commercial products does not constitute endorsement of recommendation for use.

TABLE OF CONTENTS

LIST OF FIGURES

LIST OF TABLES

SECTION 1
INTRODUCTION

There are nearly 250 million tires discarded per year in the United States (Bader, 1992). Most landfills do not allow the disposal of whole tires because they tend to float to the top of the fill and have poor compressibility (Bader, 1992). Some tires are shredded and disposed of in landfills, but many are simply stockpiled. These tires are detrimental to the environment because they provide a habitat for breeding mosquitoes and the potential for an uncontrollable fire.

Several alternatives to landfilling and stockpiling exist. Using waste tires as fuel is becoming a popular method of disposal. Environmental concerns with burning include emissions from combustion and the destruction of a non-renewable resources that are incorporated into tires. The disposal of shredded tires in landfills is also wasteful because a non-renewable resource is being eliminated from circulation.

Using recycled rubber from waste tires in low grade rubber products, such as truck bed liners and doormats, has recently become popular. However, the increased use of reinforcement (i.e. steel belts) in tires has complicated the process by which rubber can be broken down and recycled. Additionally, there have been several investigations into using shredded waste tires as a lightweight fill material and as reinforcing elements in soil (Edil and Bosscher, 1992; Humphrey and Manion 1992;. Minnesota Pollution Control Agency 1992). Flexibility, resiliency, inertness, high strength and resistance to degradation by friction are characteristics of shredded tires that are beneficial for their use in soil reinforcement.

The objective of this study is to demonstrate the feasibility of using shredded waste tires as a means of soil reinforcement. This objective was attained through the following steps:

(1) Identification of significant factors affecting reinforcing characteristics of shredded waste tires via analysis of variance.

(2) Selection of significant factors for further study.

(3) Comprehensive experimental investigation of significant factors and complete exploration of possible soil/reinforcement mixes.

(4) Development of tables and charts that aid in characterizing the strength of various mixtures of soil and shredded tires.

An initial identification of significant factors affecting the strength of soil/tire shred mixtures was accomplished using a 5 factor, 2-level, half-fraction factorial. This initial experiment identified 4 factors significantly affecting shear strength: (1) confining stress, (2) reinforcement content, (3) reinforcement dimensions, and (4) mix density. Over 200 direct shear tests were then performed to evaluate these factors. Shear strengths of the various mixtures were compared to the shear strength of un-reinforced soil assuming the strength of the mixtures of soil and shredded tires could be described by the Mohr-Coulomb failure criterion.

The data collected from the various mix designs are compared to identify those mixes that yield the greatest shear strength. The experimental results are also fit to a soil reinforcement model to determine its applicability to prediction of the shear strength of soil/tire shred mixtures.

SECTION 2
BACKGROUND AND LITERATURE REVIEW

2.1 SHREDDED WASTE TIRES AS A CONSTRUCTION MATERIAL

The use of shredded tires as a construction material is a developing concept. Current applications of shredded tires include road bed construction in soft soils, aggregate for leach beds in septic systems, and as an asphalt additive (Bader, 1992). Park et al. (1993) reported that tire chips have high sorptive capacity for organic compounds. They propose that tire chips could be used as a substitute for earthen materials in primary leachate collection systems and in cover systems to prevent volatile organic compounds from escaping from the landfill. Other selected references on use of shredded waste tires as a construction material are: Edil and Bosscher (1992), Hall (1991), Humphrey and Manion (1992), and Minnesota Pollution Control Agency (1992).

Humphrey and Manion (1992) investigated using shredded tires as lightweight fill. They reported that the maximum dry unit weight (modified Proctor energy) was 6.28 kN/m^3, making it much lighter than typical soils. Laboratory results presented by Humphrey and Manion (1992) showed that at confining stresses less than 170 kPa, the lateral earth pressure coefficient (K_o) was 0.4. For stresses greater than 170 kPa, K_o increased to about 1.0. Humphrey and Manion (1992) also investigated using shredded tires as pavement sub-grade with a linear elastic finite element program. They report that using shredded tires as fill material is possible, provided that enough soil or sub-grade material is placed over the shredded tires. Overburden is needed on the shredded tires to provide confinement. Overburden is also needed to provide enough stress on the

Construction and evaluation of an embankment built with shredded waste tires was conducted by Edil and Bosscher (1992). The test embankment was 5 meters wide, 60 meters long, and 2 meters high. Several sections were constructed to evaluate different compaction techniques and mixes of soil and shredded tires. With respect to overall settlement, the test section constructed with 1 layer of shredded tires at the base and a soil cover settled the least. Although initial settlements of the embankment were high in all test sections, after the first 60 days of traffic, none of the sections settled significantly.

Environmental monitoring of the test embankment was also conducted. Leachate was collected from two lysimeters installed under the embankment. Chemical analysis of the leachate from the embankment showed that it was not considered a hazardous waste as defined by the U.S. Environmental Protection Agency.

Edil and Bosscher (1992) concluded that embankments can be constructed with shredded waste tires using normal construction machinery. The embankment they constructed performed similar to most gravel roads after an initial period of adjustment. Edil and Bosscher (1992) reported that sections with adequate lateral and vertical confinement performed satisfactorily. However, shredded waste tires covered with 1 meter of soil performed better than sections covered with 0.3 meters of soil. This agrees with the results of the finite element investigation by Humphrey and Manion (1992).

In this study, the shear strength of mixtures containing soil and shredded tires is investigated using a large-scale direct shear machine. Before the investigation began, a literature review was conducted to evaluate how shear strength is affected by discontinuous reinforcing elements. The following sections describe the findings of this literature review.

2.2 METHODS OF SOIL REINFORCEMENT

There are several common techniques used to reinforce soils including addition of vegetation, metal strips, fabrics, plastic grids, and discontinuous inclusions. Each method has specific merits warranting application in a given situation. Site conditions often dictate the type of soil reinforcement that can be used.

Vegetation can have a beneficial effect on the stability of slopes. In addition to the advantageous effects of interception of rain water, soil moisture depletion, and buttressing, trees increase the shear strength of the soil by mechanically reinforcing it with their root system. There is a wealth of information on the subject of bio-technical slope protection presented by Gray and Lieser (1982).

Metal strips have been used in constructing reinforced earth structures by placing the soil and strips in alternating layers. The principles of this method are discussed by Vidal (1969). Almost any type of metal can be used as the reinforcing material providing it has a high enough tensile strength and can develop enough frictional resistance. A concern with this technique is longevity of the reinforcing materials.

With the development of geosynthetics, a multitude of products have been developed for use as soil reinforcement. Geogrids (plastic grids with large apertures) and geotextiles can be used to reinforce soil. Geogrids and geotextiles are placed in a manner similar to metal strips; i.e., in a layered soil/reinforcement system (Koerner, 1990).

There have been a number of studies conducted to characterize the effectiveness of discontinuous inclusions used as soil reinforcement (Andersland et al. 1979; Arenicz and Chowdury 1988; Edil and Bosscher 1992; Eldin and Senouci 1992; Freitag 1986; Gray and Al-Refeai 1986; Gray and Maher 1989; Gray and

Ohashi 1983; Hoare 1979; Lee et al. 1973; Lawton 1993; Maher and Gray 1990; Maher and Woods 1990; McGown et al. 1978; McGown et al. 1985; Noorany and Uzdavines 1989; Shewbridge and Sitar 1989; Verma and Char 1978). Small inclusions are mixed with the soil to form a reinforced system. They can be oriented in a preferred pattern or placed in a random arrangement.

2.3 EFFECT OF REINFORCEMENT ON SHEAR STRENGTH

2.3.1 General Effect of Reinforcement on Shear Strength

The effects of random fiber reinforcement on unconfined compressive strength have been demonstrated by Freitag (1986). Freitag (1986) reinforced a lean sandy clay (CL) with random inclusions of polypropylene rope fiber and a polypropylene olefin fiber intended for use in reinforced concrete. For samples compacted wet of optimum, he found that the unconfined compressive strength increased by about 25%. However, for samples compacted dry of optimum, there was no significant increase in unconfined compressive strength. Freitag (1986) states that the lack of an increase in shear strength dry of optimum may be a result of the fibers not being bonded with the soil.

Results of triaxial and direct shear tests on soils reinforced with a wide array of discontinuous reinforcing elements have been reported by Andersland and Khattak (1979), Benson and Khire (1992), Gray and Ohashi (1983), Gray and Al-Refeai (1986), Hoare (1979), Jewell (1987), McGown et al. (1985), Gray and Maher (1989), Maher and Gray (1989), Shewbridge and Sitar (1988), and Verma and Char (1978).

Larger gains in friction angle were reported by Andersland and Khattak (1979). For kaolinite reinforced with pulp fibers, they found that the consolidated-undrained strength increased by 30 kPa . Similarly, for consolidated-drained tests

Andersland and Khattak (1979) found that the undrained friction angle increased from 20° for un-reinforced kaolinite to 80° for reinforced kaolinite.

Hoare (1979) tested sandy gravel reinforced with strips of polypropylene/nylon (75%/25%) fabric and twisted polypropylene chopped staple fibers in a triaxial test. Hoare (1979) found that increasing reinforcement content resulted in increased shear strength.

Gray and Ohashi (1983) found several significant results from their tests on sand reinforced with reed fibers. They found that the Mohr-Coulomb envelop for sand reinforced with discontinuous reinforcing elements was bi-linear (Fig 2.1). The failure envelope exhibits an initial friction angle greater than the friction angle for the soil alone, but at a confining pressure greater than the "critical confining stress" the failure envelop changes slope and becomes parallel to the failure envelop for un-reinforced sand. Figure 2.1 illustrates a bi-linear failure envelop.

Gray and Ohashi (1983) also found that the increase in shear strength was directly proportional to the amount of reinforcement, at least up to a reinforcement area ratio of 1.7%. For reed fibers at a reinforcement area ratio of 1.7%, the shear strength, at the critical confining stress (48 kPa), increased from 36 kPa (for un-reinforced sand) to 74 kPa. For this test, the friction angle below the critical confining stress was 57° whereas the friction angle for un-reinforced sand was 37°. At confining stresses higher than 48 kPa, the friction angle for reinforced sand was 37°; i.e., the reinforced and un-reinforced sand had the same friction angle for confining stresses greater than the critical confining stress.

The influence of randomly oriented polymer mesh fibers on the shear strength of soil was studied by McGown et al. (1985) using consolidated-drained triaxial tests. Samples were tested with reinforcement contents of 0.09%, 0.18%

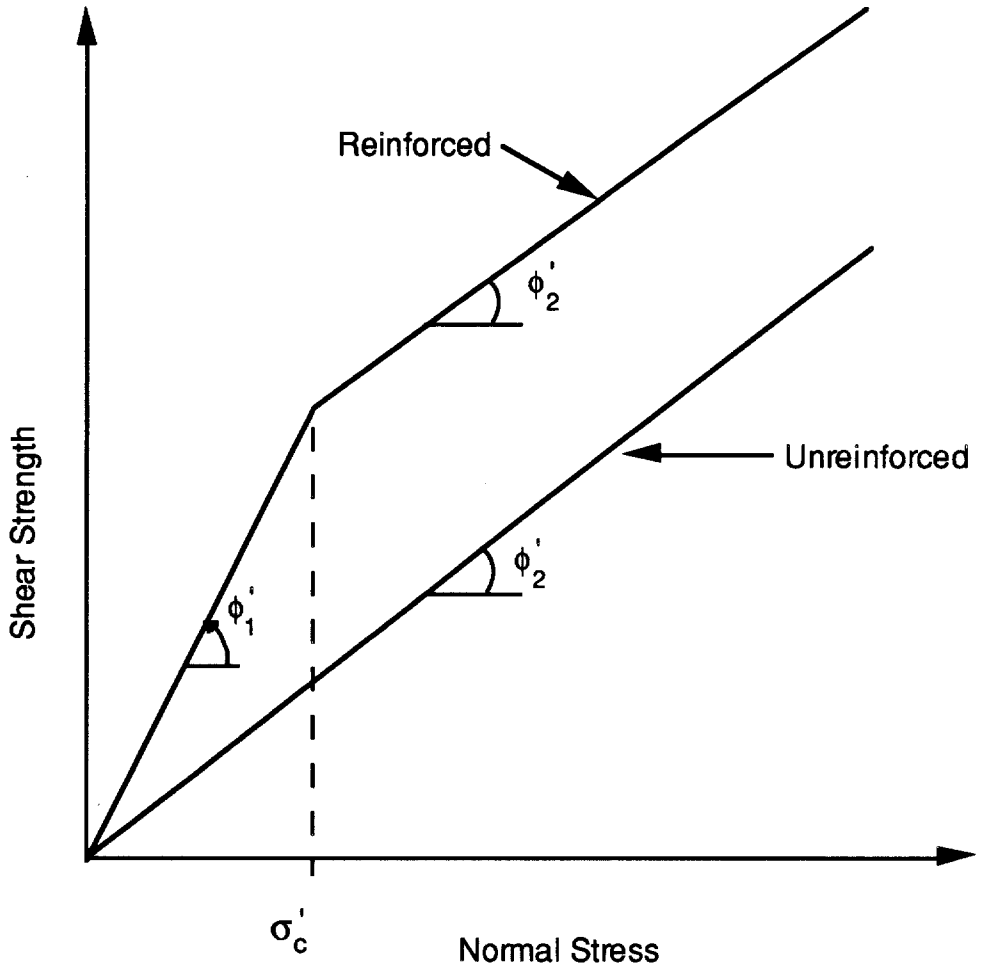

Figure 2.1. Bi-Linear Failure Envelope.

and 0.24% by weight. They found that the peak difference in principal stresses in reinforced soil was as much as 2 times greater than the peak difference in principal stresses in un-reinforced soil at a cell pressure of 25 kN/m^3. They also reported that increases in the peak difference in principal stresses at low confining stresses were more significant than increases at high confining stresses.

Verma and Char (1978) reported that addition of steel fibers (5 mm long and 1 mm wide) to sand increased its friction angle as much as 7°. For un-reinforced sand, the friction angle was 36°. When the reinforcement content was 1% (by weight), the friction angle did not increase. However, for reinforcement contents of 3% and 5%, the friction angles increased 1° and 4°, respectively. The greatest increase in friction angle noted in their study was 7° for a reinforcement content of 7% by weight.

Results presented by Shewbridge and Sitar (1989) show variability in the effect of increasing reinforcement content on the shear strength of reinforced soil. In sand reinforced with parachute cord, they found that increasing reinforcement content resulted in increased shear strength. However, the relationship between reinforcement content and shear strength was not linear as reported by Gray and Ohashi (1983). At a reinforcement area ratio of 0.2%, the shear strength increase was about 10%. For area ratios of 0.5% and 0.9%, increases in shear strength were 33% and 44%. For tests run on sand reinforced with wooden rods, there was no trend between reinforcement content and shear strength. In some cases, increasing the reinforcement content resulted in lower shear strengths. However, in all tests performed, addition of reinforcement did increase the shear strength above the strength of un-reinforced sand. Shewbridge and Sitar (1989) concluded from their tests that the relationship between increase in shear strength and

reinforcement content was non-linear and asymptotically approached an upper limit.

Benson and Khire (1992) reported the strength of sand reinforced with HDPE strips increased with increased reinforcement content. They also reported a bi-linear failure envelope. The highest reinforcement content in their tests was 4% (by weight). On average, a 1% percent increase in reinforcement content increased the shear strength by 15 kPa at confining stresses above the critical confining stress. Unlike the results shown by Gray and Ohashi (1983), the critical confining stress varied with different reinforcement contents.

The bi-linear failure envelope and the effects of reinforcement content on shear strength were also observed by Gray and Al-Refeai (1986). Results of their tests using glass fibers as reinforcement show that the relationship between reinforcement content and increase in shear strength is essentially linear up to a reinforcement content of 4% . For reinforcement contents greater than 4% (by weight) the increase in shear strength resulting from additional reinforcement approached an upper limit asymptotically. A summary of the effects of reinforcement content on shear strength is shown in Table 2.1

2.3.2 Effect of Reinforcement on Critical Confining Stress

Gray and Maher (1989) performed triaxial tests on sand reinforced with several types of reinforcement. They found that the failure envelopes were either curved or bilinear, with the break in slope called the critical confining stress. From tests in which all conditions were held constant except the reinforcement aspect ratio, they found that increasing the aspect ratio decreased the critical confining stress. Results from Benson and Khire (1992) do not support the conclusion by Gray and Maher (1989). Benson and Khire (1992) found that for sand reinforced

Table 2.1. Effect of Reinforcement Content on Shear Strength.

Reference	Test	Soil	Reinforcement	Reinforcement Content Tested	Effect of Reinforcement Content on Shear Strength
Hoare (1979)	triaxial	sandy gravel	polypropylene fibers	increasing content	increased
Gray and Ohashi (1983)	direct shear	sand	reed fibers	up to 1.7% by weight	directly proportional to reinforcement content
McGown (1985)	CD triaxial	sand	polymer mesh	up to 0.24% by weight	increased up to 2 times greater than un-reinforced sand
Shewbridge and Sitar (1988)	direct shear	sand	parachute cord	up to 0.9% by area ratio	increased and approached asymptotically an upper limit
			wooden rods	up to 0.9% by area ratio	no trend
Benson and Khire (1992)	direct shear	sand	HDPE strips	up to 4% by weight	directly proportional to reinforcement content
Gray and Al-Refeai (1986)	triaxial	sand	glass fibers	up to 6% by weight	increased linearly and approached asymptotically an upper limit beyond 4% content

with HDPE strips at aspect ratios of 4, 8, and 12 kPa, the critical confining stresses were 35, 103 and 69 kPa, respectively.

Results from Benson and Khire (1992) indicate that the critical confining stress increased with increased reinforcement content. The study performed by Gray and Maher (1989) does not support this finding. They found no significant trends with respect to reinforcement content.

Gray and Maher (1989) also investigated the effects of varying grain size and sphericity of the sand being reinforced on the critical confining stress. They found that increasing the sphericity of the particle resulted in increased critical confining stress. They also found that increasing sphericity resulted in less contribution to the strength by the reinforcement. Increasing grain size was not found to have an effect on the critical confining stress but it did decrease the contribution of reinforcement to shear strength.

2.3.3 Effect of Modulus of Reinforcement on Shear Strength

The effect of the modulus of reinforcing fibers on shear strength has been studied by Gray and Ohashi (1983), Jewell (1987), McGown et al. (1978), Gray and Maher (1989), and Shewbridge and Sitar (1989). McGown et al. (1978) identified two distinct cases with respect to relative extensibility of inclusions. Inclusions having rupture strains less than the maximum tensile strain of un-reinforced soil were identified as "relatively inextensible." Relatively inextensible inclusions may or may not rupture during shear depending on the strain in the soil. Inclusions having rupture strains greater than the maximum possible soil strain were identified as "relatively extensible" inclusions. It is not possible for these inclusions to rupture regardless of the load on the shearing plane because the soil gripping the

reinforcement will fail first. Inextensible and extensible inclusions can further be broken down into two classes, strong and weak (McGown et al., 1978).

McGown et al. (1978) concluded that for weak inclusions the increase in shear strength would be minimal. For strong inclusions, they concluded that the increase in shear strength would be significant. From the model proposed by McGown et al. (1978), strong extensible and strong inextensible inclusions would increase shear strength by the same amount.

Gray and Ohashi (1983) presented failure envelopes for sand reinforced with a wide variety of inclusions at similar reinforcement contents. For the materials they tested, they found that inextensible copper wire was most effective; it increased the shear strength, at the critical confining stress, by 24 kPa. Tests performed using more extensible fibers (palmyra, plastic, and reeds) showed less significant gains in shear strength.

Jewell (1987) found that increases in shear strength depended on the modulus of reinforcement. For fibers having the same dimensions, he reported that inextensible reinforcement was more effective at increasing the shear strength than extensible reinforcement. A limited amount of data was presented to support this conclusion.

Shewbridge and Sitar (1989) support the conclusions by Jewell (1987), McGown et al. (1978), and Gray and Ohashi (1983). They found that inclusions with higher modulus yielded the greatest increase in shear strength. Direct shear tests were conducted on sand reinforced with bungy cord, parachute cord, wooden rods, wooden dowels, steel rods, and aluminum rods (listed in order of increasing stiffness). They reported that increasing reinforcement modulus increases shear strength.

Results from Gray and Maher (1989) also show that inclusions with higher modulus are more efficient at increasing shear strength. They showed that addition of reed fibers, with a modulus of 33 MPa, increased the shear strength by 85.5 kPa at the critical confining stress. Addition of Buna-N rubber (modulus of 9.8 MPa) increased the shear strength less than 1 kPa. Addition of palmyra fibers (17 MPa) increased the shear strength by 93.4 kPa. Maher and Gray (1989) concluded that fibers with low modulus do little to increase shear strength. A summary of the effects of reinforcement modulus on shear strength is shown Table 2.2

2.3.4 Effect of Aspect Ratio of Reinforcement on Shear Strength

The effects of varying the aspect ratio of fiber reinforcement on shear strength has been investigated by Benson and Khire (1992), Gray and Al-Refeai (1986), Gray and Ohashi (1983), Gray and Maher (1989), and Verma and Char (1978). Verma and Char (1978) reported that increasing aspect ratio increased shear strength. For sand reinforced with mild steel fiber, having an aspect ratio of 2, an increase in friction angle was not observed. However, for steel fibers with an aspect ratio of 5, the increase in friction angle was as much as 7°.

Gray and Ohashi (1983) found that for a variety of fibers the improvement in shear strength was greater for fibers with higher aspect ratios. The materials studied ranged from reed fibers with aspect ratios up to 130 (length=24 cm) to copper wires with aspect ratios up to 240 (length=24 cm).

For glass fibers, Gray and Al-Refeai (1986) also found that increasing the aspect ratio of the reinforcing fiber increased shear strength. For glass fibers with an aspect ratio of 42, the effect of the reinforcement was negligible. When 3% fibers by weight, having an aspect ratio of 125 were used as reinforcement, shear

Table 2.2. Effects of Reinforcement Modulus on Shear Strength.

Reference	Test	Soil	Reinforcement	Effect of Reinforcement Modulus on Shear Strength
McGown et al. (1978)	triaxial	sand	strong extensible and strong inextensible	both types of reinforcement have the same effect
Gray and Ohashi (1983)	direct shear	sand	reed fibers and copper wire	increasing reinforcement modulus increases strength
Jewell (1987)	direct shear	sand	extensible and inextensible	inextensible reinforcement was most effective at increasing strength
Shewbridge and Sitar (1989)	direct shear	sand	ranging from bungy cord to steel rods	increasing reinforcement modulus increases strength
Gray and Maher (1989)	triaxial	sand	ranging from rubber to reed fibers	increasing reinforcement modulus increases strength

strength at the critical confining stress increased by 33 kPa. However, the increase in shear strength was not found to be directly proportional to aspect ratio.

Gray and Maher (1989) found that increasing the aspect ratio of reinforcement resulted in greater increases in shear strength. They reported that the friction angle was 67° for mortar sand reinforced with fibers having an aspect ratio of 125 mixed at 3% by weight. For the same type of fibers with an aspect ratio of 60, the friction angle was 60°.

Benson and Khire (1992) did not find that varying the aspect ratio of reinforcement altered initial friction angle. For reinforcement content of 4% (by weight), they tested reinforcements having aspect ratios of 4, 8, and 12. Benson and Khire (1992) found that the friction angles calculated for the reinforced samples varied only 2 degrees across the range of aspect ratios tested. However, strips with an aspect ratio or 8 had the highest shear strength because of they had the highest critical confining stress. The effects of varying aspect ratio on shear strength are summarized in Table 2.3.

2.3.5 Effect of Orientation of Reinforcement on Shear Strength

The effect that orientation of reinforcement has on shear strength has been considered by Jewell and Wroth (1987), Gray and Al-Refeai (1986), and Gray and Ohashi (1983). Gray and Ohashi (1983) tested sand reinforced with reed fibers placed at different orientations. They found that the optimum angle to place reinforcement was 60° to the shear plane. Gray and Ohashi (1983) also reported that reinforcement oriented at 90° increased shear strength by the same amount as reinforcement that was randomly oriented. Jewell and Wroth (1987) state that for optimal increases in shear strength, reinforcing fibers should be oriented in the direction of the principle incremental strain in the soil, which for most sands in

Table 2.3. Effects of Varying Aspect Ratio on Shear Strength.

Reference	Test	Soil	Reinforcement	Effect of Aspect Ratio on Shear Strength
Verma and Char (1978)	triaxial	sand	steel fibers	increasing aspect ratio increased shear strength
Gray and Ohashi (1983)	direct shear	sand	reed fibers and copper wires	increasing aspect ratio increased shear strength
Gray and Al-Refeai (1986)	triaxial	sand	glass fibers	increasing aspect ratio increased shear strength
Gray and Maher (1989)	triaxial	sand	glass fibers	increasing aspect ratio increased shear strength
Benson and Khire (1992)	direct shear	sand	HDPE strips	varying aspect ratio had no significant effect

direct shear is about 60°. This orientation results in the fibers becoming loaded with the maximum possible tension.

2.3.6 Stress-Strain Properties

Freitag (1986) found that the modulus for lean sandy clay (CL) reinforced with random inclusions of polypropylene fibers was slightly lower than the modulus for un-reinforced sandy clay tested in unconfined compression. Conversely, Verma and Char (1978), Benson and Khire (1992), and Gray and Al-Refeai (1986) have found that addition of reinforcing inclusions increases the modulus.

Verma and Char (1978) reinforced sand with mild steel fibers. The modulus for the reinforced soil was approximately 10% greater than the modulus for the un-reinforced soil. Increases in modulus were observed by Gray and Al-Refeai (1986) in triaxial tests on sand reinforced with reed fibers. For a reed fiber content of 1% (by weight), the tangent modulus increased by approximately 30% over un-reinforced sand.

Jewell and Wroth (1987) did not find any difference in modulus for sand reinforced with inextensible inclusions. The effect of reinforcement on the stress-strain properties of the soil were seen only at strains greater than the strain corresponding to failure for un-reinforced sand. The effects of discontinuous reinforcement on modulus are summarized in Table 2.4.

For tests on reinforced sand performed in a direct shear device, Gray and Ohashi (1983) found that the initial modulus for a reinforced sand to be less than that for an un-reinforced sand (Gray and Ohashi 1983). Gray and Ohashi (1983) attributed their findings to the testing procedures that were used. When the confining stress was applied, the reinforcing fibers were loaded in compression. Therefore, displacement was required before the reinforcement could be loaded in

Table 2.4. Effects of Discontinuous Reinforcement on Modulus.

Reference	Test	Soil	Reinforcement	Effect on Modulus
Freitag (1986)	unconfined compression	clay	polypropylene fibers	decreased
Verma and Char (1978)	triaxial	sand	mild steel fibers	increased
Gray and Al-Refeai (1986)	triaxial	sand	reed fibers	increased
Benson and Khire (1992)	direct shear	sand	HDPE strips	increased
Gray and Ohashi (1983)	direct shear	sand	reeds, copper wire, and palmyra	decreased
Shewbridge and Sitar (1989)	direct shear	sand	parachute cord	increased
Andersland and Khattak (1979)	triaxial	clay	pulp fibers	increased
Jewell and Wroth (1987)	direct shear	sand	inextensible inclusions	none

tension. Benson and Khire (1992) and Shewbridge and Sitar (1989) did not observe decreases in initial modulus in their experiments.

The effect of increasing reinforcement content on modulus has been reported by Andersland and Khattak (1979), Benson and Khire (1992), Gray and Al-Refeai (1986), Gray and Ohashi (1983), Shewbridge and Sitar (1989), and Verma and Char (1978). Triaxial tests by Andersland and Khattak (1979) showed that addition of pulp fibers to kaolinite significantly increased the modulus of the kaolinite. The increase in modulus cannot be quantified because the tests on un-reinforced specimens were conducted at a much higher effective stress (343 kPa) than the tests on reinforced specimens (294 kPa).

Results from direct shear tests performed by Benson and Khire (1992) do not show a clear relationship between reinforcement content and modulus. For plain rectangular and kinked HDPE strips, they found that increasing the reinforcement content resulted in an increase in modulus. However, for punched strips the modulus did not depend on the reinforcement content.

Results from triaxial tests performed by Gray and Al-Refeai (1986) show that increasing the reinforcement content increased the modulus. For sand reinforced with reed fibers at reinforcement contents between 0% and 1% (by weight), the modulus increased proportionally with reinforcement content. This is in contrast to earlier findings by Gray and Ohashi (1983), who found that modulus decreased when the reinforcement area ratio was increased from 0.25% to 1.67% when reed fibers of equal tensile strength, modulus, and diameter were used as reinforcement.

Shewbridge and Sitar (1989), who tested sand reinforced with parachute cord in direct shear, found that increasing the reinforcement content from 14 to 60 pieces of cord increased the tangent modulus slightly. However, when they used

wooden rods as reinforcement, no change in modulus was apparent when the reinforcement content was changed.

The effect on modulus caused by increasing the content of mild steel fibers in reinforced sand was shown by Verma and Char (1978). For reinforcement contents between 0% and 7%, they found that the modulus at failure increased slightly. They found that the modulus at failure for a reinforcement content of 0.5% (by weight) was 8.7 MPa. For 7% reinforcement content, the secant modulus at failure was 12.8 MPa.

The effects of varying the aspect ratio of discontinuous reinforcing inclusions have been presented by Benson and Khire (1992) and Verma and Char (1978). Benson and Khire (1992) reinforced sand with shreds of HDPE that varied in aspect ratio from 4 to 12. Their results show that the highest modulus was obtained for reinforcements having an aspect ratio of 8 and a 4% reinforcement content (by weight). Verma and Char (1978) report that the modulus at failure increased when the aspect ratio of their mild steel fiber was increased. For fibers with an aspect ratio of 5, the modulus was 25% higher than the modulus obtained when fibers having an aspect ratio of 2 were used.

2.3.7 Effect of Reinforcement on Type of Failure

McGown et al. (1978) proposed a conceptual model describing how inclusions having different strength and stiffness affect the strength and stress-strain properties of soil. Figure 2.2 illustrates the model of behavior proposed by McGown et al. (1978). They suggest that weak inextensible inclusions will generally increase the shearing resistance of soil, but the mixture will fail at strains less than the strain at failure for plain soil. This causes the soil/reinforcement composite to be more brittle than un-reinforced soil. Strong inextensible inclusions

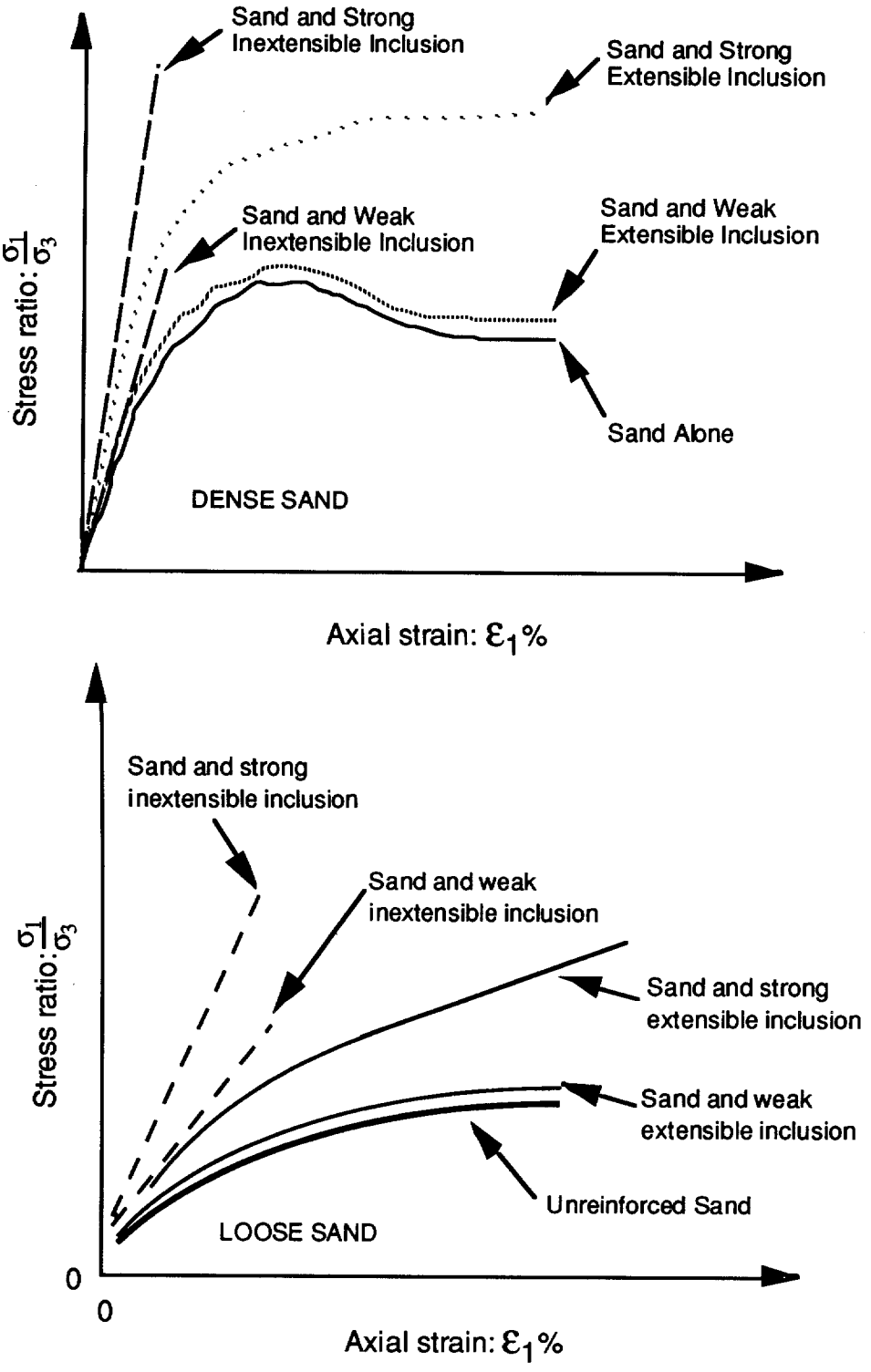

Figure 2.2. Conceptual Model by McGown (1978).

will increase the shearing resistance of sand more than a weak inextensible inclusion, but will still exhibit a brittle behavior. Weak and extensible inclusions will increase the shearing resistance and make the composite behave more plastically. Strong and extensible inclusions will increase the shearing resistance and the mixture will behave in a much more plastic manner than un-reinforced sand or sand reinforced with weak extensible inclusions.

Freitag (1986) found that the strain at failure increased from 6% (un-reinforced) to 10% for samples that were reinforced with polypropylene fibers. Andersland and Khattak (1979) also found that kaolinite reinforced with pulp fibers were more plastic than un-reinforced kaolinite. For un-reinforced kaolinite the strain at failure was 15%, whereas for the reinforced soil the strain at failure was 20%. An increase in strain at failure was also noted by Gray and Al-Refeai (1986). They found that the strain at failure for un-reinforced sand tested in a triaxial cell was about 2%, whereas the sand reinforced with 1% reed fibers failed at a strain of 6%.

Saran et al. (1978) reported that specimens reinforced with aluminum foil rings that were tested in a triaxial cell exhibited brittle failure. The strain at failure for the un-reinforced sand was approximately 6%, whereas for reinforced sand the strain at failure was approximately 4%. Similar results were reported by Verma and Char (1978) for triaxial tests. They found that samples reinforced with metal fibers failed at a strain of approximately 4%, whereas un-reinforced sand failed at a strain of approximately 6%.

Shewbridge and Sitar (1989) show results from direct shear tests on sand reinforced with a variety of materials. For the un-reinforced sand used in their study, the displacement at failure was approximately 10 mm. For sand reinforced with steel rods, the strain at failure was slightly greater than 10 mm. Sand

reinforced with wooden rods failed at a displacement of approximately 40 mm. The sand reinforced with parachute cord failed at a strain of approximately 30 mm and sand reinforced with bungy cords failed at a strain of approximately 40 mm. From their results, it appears that strain at failure increased with increasing modulus of the reinforcement.

Gray and Ohashi (1983) report results from several direct shear tests on sand reinforced with reeds, palmyra fibers, and copper wire. Addition of reed fibers increased the displacement at failure to 30 mm for the highest reed content tested. Displacement at failure for un-reinforced sand was approximately 1 mm. For sand reinforced with copper wire at an area ratio 0.25%, the displacement at failure was approximately 2 mm. Reinforcing the sand with palmyra fibers at an area ratio of 0.23% increased the displacement at failure to approximately 1.6 mm.

Results from direct shear tests by Benson and Khire (1992) show that, at a confining stress of 69 kPa, the addition of strips of HDPE to the sand increased the lateral strain at failure from 2.2% to 3.5% when 1% reinforcement was used (by weight). The increase in failure strain decreased with a reduction in confining stress. At a confining stress of 11.7 kPa, the increase in lateral strain at failure was not noticeable. A summary of the effects of reinforcement on strain at failure is shown in Table 2.5.

2.3.8 Effects of Reinforcement on Post-Peak Behavior

The effect of discontinuous reinforcement on limiting post-peak reductions in strength has been reported by Andersland and Khattak (1979), Gray and Ohashi (1983), Gray and Al-Refeai (1986), McGown et al. (1978), and Shewbridge and Sitar (1989). Andersland and Khattak (1979) reported a 100% reduction in post-peak loss in shear strength for kaolinite reinforced with pulp fibers.

Table 2.5. Effect of Reinforcement on Strain at Failure.

Reference	Test	Soil	Reinforcement	Stain at Failure (Un-Reinforced)	Stain at Failure (Reinforced)
Freitag (1986)	unconfined compression	clay	polypropylene	6%	10%
Andersland and Khattak (1979)	triaxial	clay	pulp fibers	15%	20%
Gray and Al-Refeai (1986)	triaxial	sand	reed fibers	2%	6%
Saran et al. (1978)	triaxial	sand	aluminum foil rings	6%	4%
Verma and Char (1978)	triaxial	sand	metal fibers	6%	4%
Shewbridge and Sitar (1989)	direct shear	sand	wooden rods	10 mm	40 mm
Benson and Khire (1992)	direct shear	sand	HDPE strips	2.2% lateral displacement	3.5% lateral displacement
Gray and Ohashi (1983)	direct shear	sand	reed	1 mm	3 mm

Gray and Ohashi (1983) found that increasing the reinforcement content decreased the post-peak reduction in strength for sand reinforced with reed fibers. For un-reinforced sand, the reduction in strength after peak stress was 22 kPa. At a fiber content of 0.5% (by area ratio), the reduction in strength was 9.5 kPa. For a fiber content of 1.7% (by area ratio), no loss in strength was observed. Gray and Al-Refeai (1986) reported similar results for sand reinforced with reed fibers were had a larger diameter than those used by Gray and Ohashi (1983) (1.75 mm compared to 1.25 mm).

Shewbridge and Sitar (1989) found that addition of discontinuous reinforcement limited post-peak reductions in strength. For the un-reinforced sand used in their study, the post-peak reduction in strength was about 0.5 kPa. Samples reinforced with parachute cord did not show any post-peak reduction in strength. For wooden rods placed at an area ratio of 0.2%, the post-peak loss in strength was minimal. However, when the area ratio was 0.5%, the post-peak reduction in strength was 1 kPa.

McGown et al. (1978) suggest that the mechanical properties of the inclusions should affect post-peak losses in strength. They show a loss in strength will occur after peak strength has occurred, but the loss will not be as large as would occur in un-reinforced soil. For a strong extensible inclusion, no distinct loss in post-peak strength will occur.

In contrast to McGown et al. (1978), Shewbridge and Sitar (1989) reported that the amount of post-peak reduction in strength was not related to the type of reinforcing material. Steel rods (inextensible inclusions) and bungy cords (extensible inclusions) did not have significantly different post-peak strengths.

The orientation of reinforcement has been found not to affect post-peak loss in strength. At a reed fiber content of 0.456% (by weight), Gray and Ohashi (1983)

found that the post-peak loss of strength was similar for reinforcements oriented at 30, 60, 90, 120, and 150° from the shear plane.

Reductions in post-peak losses in strength were not observed by Jewell and Wroth (1987). They added extensible and inextensible inclusions to sand an tested the specimens in direct shear. Post-peak losses in strength were observed in specimens regardless of type of reinforcement. However, the post-peak loss of strength for sand reinforced with extensible inclusions was less than the loss that occurred in un-reinforced soil. Sand reinforced with inextensible inclusions had a higher peak strength than un-reinforced soil. However, post-peak losses in strength of the reinforced soil were equal to the post-peak losses in un-reinforced soil. Beyond peak stress, sand reinforced with inextensible inclusions showed the same behavior as un-reinforced sand and the improvement in strength of reinforced sand compared to un-reinforced sand remained constant. Figure 2.3 illustrates this behavior.

Gray and Al-Refeai (1986) and Gray and Maher (1989) observed the failure mode (slip plane, bulging, etc.) for specimens of reinforced sand tested in a triaxial apparatus. In both studies, addition of discontinuous reinforcing elements resulted in a slip-type failure. In most tests, the slip plane was oriented close to the plane that would be predicted by Coulomb theory ($45^o + \phi/2$). From their observations, Gray and Al-Refeai (1986) and Gray and Maher (1989b) concluded that soil reinforced with random inclusions does not have preferential failure planes and behaves isotropically. A summary of the effects of reinforcement on post-peak reduction in strength is shown in Table 2.6.

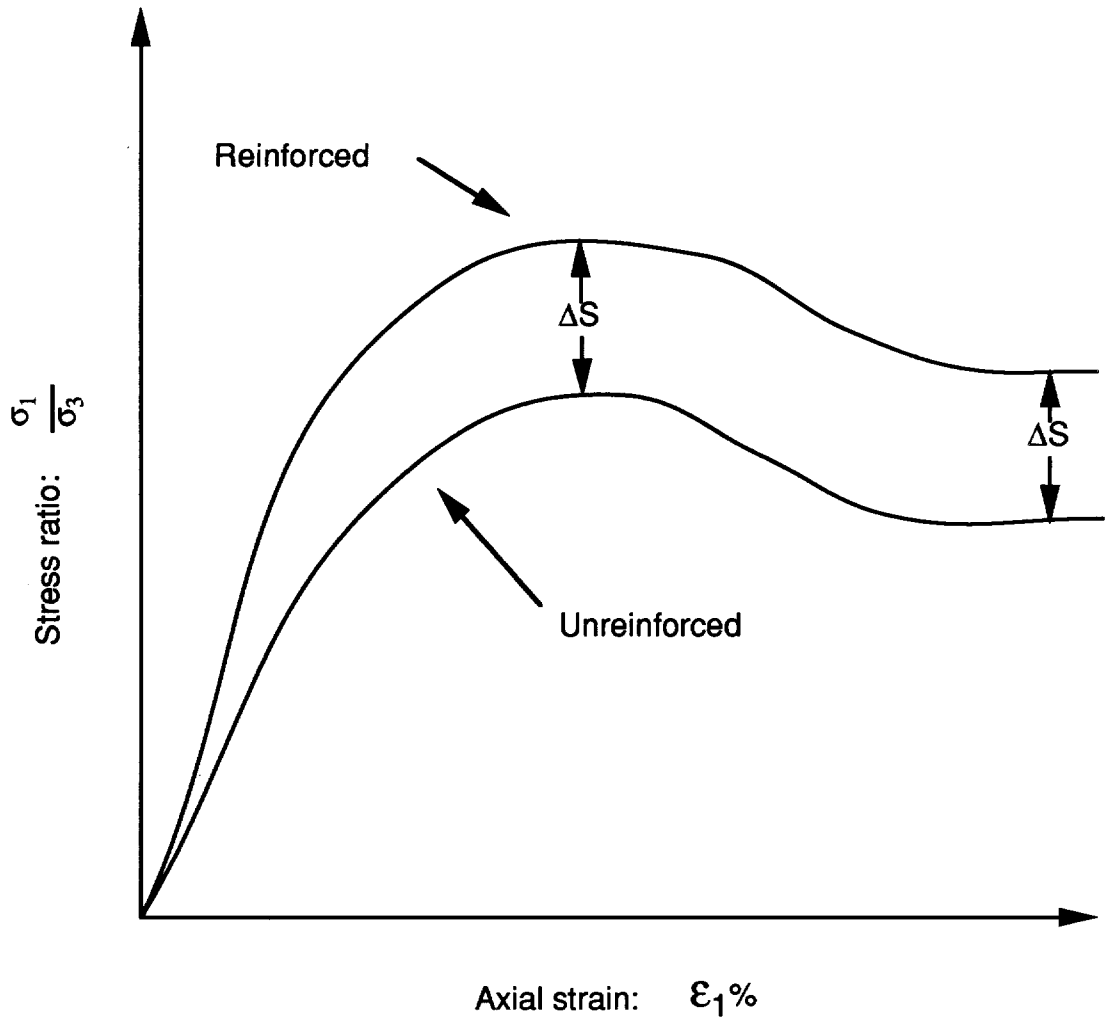

Figure 2.3. Observation by Jewell and Wroth (1987) for Sand Reinforced With Inextensible Inclusions.

Table 2.6. Effects of Reinforcement on Post-Peak Reduction in Strength.

Reference	Test	Soil	Reinforcement	Post- Peak Loss In Shear Strength [kPa]	
				Un-Reinforced	Reinforced
Andersland and Khattak (1979)	triaxial	clay	pulp fibers	10.3	0
Gray and Ohashi (1983)	direct shear	sand	reed fibers	22	9.5
Gray and Al-Refeai (1986)	triaxial	sand	reed fibers	3.4	0
Shewbridge and Sitar (1989)	direct shear	sand	Parachute Cord	0.5	0

2.4 MODELS TO PREDICT INCREASE IN SHEAR STRENGTH

Methods have been proposed to model the behavior of soil reinforced with discontinuous inclusions (Gray and Ohashi 1983; Jewell and Wroth 1987; Maher and Gray 1990). The model proposed by Jewell and Wroth (1987) is a limit equilibrium analysis. The force on the shear plane from reinforcement is separated into tangential and normal components. Equation 2.1 is used to predict the increase in shear strength (τ_{EXT}) where P_R is the tensile force in the reinforcement, θ is the angle of the reinforcement relative to the shear plane, and ϕ is the internal angle of friction of the un-reinforced soil. Figure 2.4 is an illustration of the forces on the shear plane.

$$\tau_{EXT} = \frac{P_R}{A_S}(\cos\theta \tan\phi + \sin\theta) \qquad (2.1)$$

To use the model, the tensile force in the reinforcement must be known. Jewell and Wroth (1987) made these measurements using radiographic observations. To verify their model, they took data from one set of tests and determined the plane strain friction angle of the reinforced specimens. They used this information to back-calculate the un-reinforced plane strain friction angle of the sand used in their study. The plane stain friction angle back-calculated by Jewell and Wroth (1987) equaled that of the un-reinforced sand.

The model proposed by Gray and Ohashi (1983) (Fig. 2.5) is for a long fiber crossing both sides of a potential slip plane. The fiber under consideration can be at any orientation. The tensile force mobilized in the reinforcing element is separated into two components, one parallel to the shear plane and another perpendicular to the shear plane. The component parallel to the shear plane

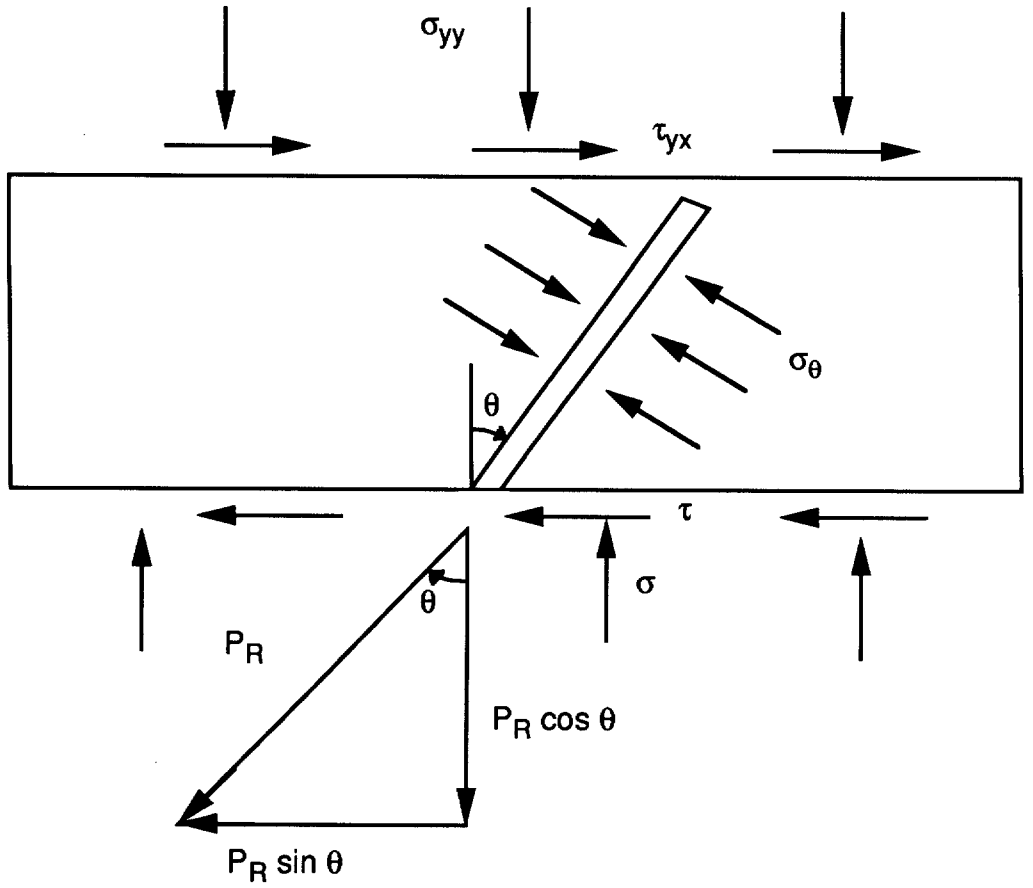

Figure 2.4. Forces on the Shear Plane for Model Proposed by Jewell and Wroth (1987).

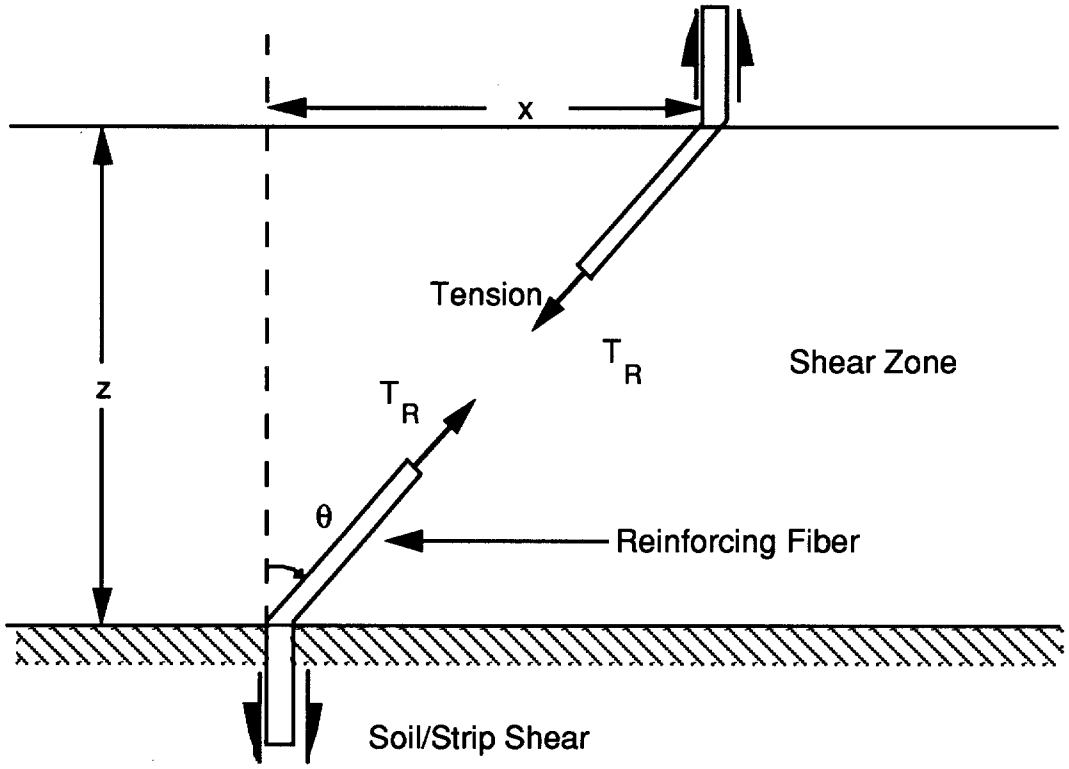

Figure 2.5. Model by Gray and Ohashi (1983).

directly resists shear deformation. The component normal to the shear plane increases the confining stress on the sand along the shear plane and thus increases the shear strength. Multiple elements crossing the shear plane can be considered using the ratio of area of reinforcement to area of sand (i.e., the "area ratio").

Equation 2.2 can be used to predict the increase in shear strength (ΔS_r) from reinforcement oriented perpendicularly to the shear plane based on the mobilized tensile strength per unit area of soil (t_R), angle of shear distortion (θ), and friction angle (ϕ):

$$\Delta S_r = t_R[\sin\theta + \cos\theta \tan\phi] \qquad (2.2)$$

The mobilized tensile strength per unit area (t_R), is defined by:

$$t_r = \left(\frac{A_R}{A}\right)\sigma_R \qquad (2.3)$$

where A_R is the cross-sectional area of reinforcement in the shear plane, A is the area of the shear plane, and σ_R is the tensile stress developed in the fiber at the shear plane.

For reinforcing fibers with an initial orientation (i) with respect to the shear surface (Fig. 2.6), Eq. 2.4 can be used to predict the increase in shear strength:

$$\Delta S_r = t_R[\sin(90-\psi) + \cos(90-\psi)\tan\phi] \qquad (2.4)$$

The parameter ψ is defined as:

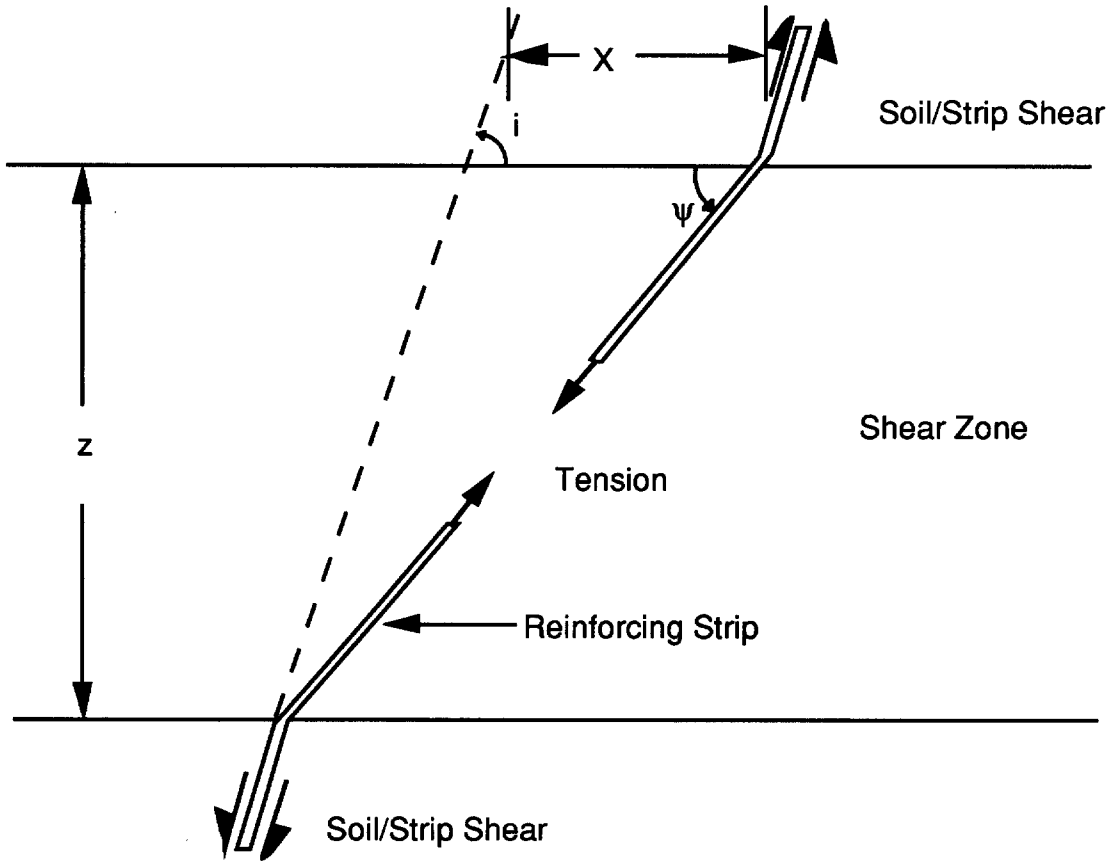

Figure 2.6. Gray and Ohashi (1983) Model for Fiber with Initial Orientation (i).

$$\psi = \tan^{-1}\left[\frac{1}{k + (\tan^{-1} i)^{-1}}\right] \qquad (2.5)$$

where

$$k = \frac{x}{z} \qquad (2.6)$$

In Eq. 2.6, x is the horizontal displacement and z is the thickness of the shear zone.

Maher and Gray (1990) further developed the model proposed by Gray and Ohashi (1983). Maher and Gray (1990) applied statistical theory to characterize the orientation of fibers randomly distributed across the shear plane. They found that, on average, the fibers are perpendicular to the shear plane. This leads to the applicability of the model by Gray and Ohashi (1983), which is only useful for fibers oriented in one direction. Results from Gray and Ohashi (1983) support the finding that the fibers are, on average, vertical. They found shear strengths for soil reinforced with vertically oriented fibers was roughly equal to the shear strength of soil containing randomly oriented fibers.

Maher and Gray (1990) proposed that the increase in shear strength for sand reinforced with randomly oriented inclusions can be computed using Eq. 2.7:

$$\Delta S_R = N_s\left(\pi\frac{d^2}{4}\right)(2\sigma_{crit}\tan\delta)(\sin\omega + \cos\omega\tan\phi)(\zeta) \qquad (2.7)$$

where d is the diameter of reinforcement, σ_{crit} is the critical confining stress, and δ is the friction angle between the reinforcement and sand. The parameter N_s in Eq. 2.7 is defined as:

$$N_s = \frac{2\beta_f}{\pi d^2} \qquad (2.8)$$

where β_f is the volume fraction of reinforcement and ω is defined by Eq. 2.9:

$$\omega = \tan^{-1}\left(\frac{x}{z}\right) \qquad (2.9)$$

where x is the shear displacement and z thickness of shear zone.

Results from tests on soil reinforced with discontinuous inclusions were analyzed by Maher and Gray (1989) to verify this model. Close agreement between the model and experimental data was found.

2.5 EFFECT OF REINFORCEMENT ON CBR TESTS

2.5.1 Effect on CBR

Studies have shown that discontinuous soil reinforcing elements can significantly improve the California Bearing Ratio (CBR) of soil (Benson and Khire 1992; Fletcher and Humphrey 1991; Lawton et al. 1993). Benson and Khire (1992) reported that CBR of a sand reinforced with 4% (by weight) HDPE strips increased by 5 times over un-reinforced sand. For sand reinforced with polypropylene elements at a reinforcement content of 10% (by volume) the un-reinforced sand had a CBR of 6.9. Lawton et al. (1993) reported that the stress at a penetration of 2.5 cm was 4 times greater than the stress at a penetration of 2.5 cm for un-reinforced sand. Fletcher and Humphrey (1991) found that adding polypropylene fibers increased the CBR as much as 2 times over the un-reinforced CBR when the reinforcement content was 1% by weight.

The effects of increasing reinforcement content on CBR are different in each study. Benson and Khire (1992) show increases in CBR for increasing

reinforcement content. However, their study was limited to reinforcement contents of 4% by weight. Fletcher and Humphrey (1991) reported an optimum reinforcement content of 1%. Any addition or reduction in reinforcement content resulted in lower CBR. Lawton et al. (1992) have suggested that an asymptotic relationship exists between reinforcement content and CBR for reinforced silty sand. They reported that the CBR increased more for changes in reinforcement content from 0% to 1% than for increases in reinforcement content from 1% to 2%. This was also true for increases from 2% to 3% reinforcement content.

There is also variability in the effect that the shape and roughness of reinforcement have on CBR. Benson and Khire (1992) reported that flat and kinked reinforcing strips had similar CBR. Benson and Khire (1992) also report that the optimal aspect ratio (length/width) for their reinforcement was 8. At aspect ratios of 4 and 12, a lower CBR was measured. Fletcher and Humphrey (1991) report that increasing the aspect ratio of reinforcement decreased the CBR. However, results for a wide range of aspect ratios were not reported. Lawton et al. (1992) investigated the effects of reinforcement surface roughness on the CBR. For both Ottawa and silty micaceous sand, they found that smooth jacks resulted in the largest increases in CBR.

2.5.2 Load-Deformation Relationships

The addition of discontinuous reinforcing elements has been shown to decrease the tangent modulus of soil in the CBR test (Benson and Khire 1992; Lawton et al. 1992). Benson and Khire (1992) found that increasing the reinforcement content resulted in a decrease in initial modulus. However, at larger depths of penetration, increasing the reinforcement content resulted in an increase in modulus. For sand alone, Benson and Khire (1992) reported that the modulus

was 27,000 kN/m^3. The average modulus reported for reinforcement contents of 1% to 2% (by weight) at 2.5 centimeters of penetration were 34,000 kN/m^3 and 72,000 kN/m^3.

Similar results were reported by Lawton et al. (1992) using polypropylene elements shaped like jacks. At shallow penetrations (penetrations < 0.5 cm), they found that specimens reinforced with 10% jacks (by volume) had lower initial modulus than the initial modulus for un-reinforced sand. They suggested that the reduction in initial modulus resulted from the initial deformation required to mobilize friction between the soil and reinforcing elements. However, the initial modulus for sand reinforced with 5% jacks by weight was slightly greater than the initial modulus of un-reinforced sand. Lawton et al. (1992) also reported that the modulus increased for increasing polypropylene fiber content.

2.6 EFFECTS OF REINFORCEMENT ON DYNAMIC PROPERTIES

Dynamic properties of soil have been found to improve with the addition of discontinuous reinforcement (Maher and Woods 1990; Noorany and Uzdavines 1989). Noorany and Uzdavines (1989) conducted cyclic triaxial tests on saturated sand reinforced with two types of polypropylene fibers. They reported that addition of discontinuous reinforcement increased the sands resistance to liquefaction. Additionally, they found improvements in the dynamic behavior of a reinforced saturated sand. For a given cyclic stress ratio and number of load applications, pore pressures and axial strains were lower in reinforced sand than in un-reinforced sand.

Maher and Woods (1990) reported that the dynamic modulus of reinforced sand increased with increases in fiber aspect ratio and modulus. They also found that the damping capacity increased when the soil was reinforced with

discontinuous fibers. It was also discovered that the increase in rigidity, resulting from reinforcement, was more evident at lower confining stresses.

SECTION 3
MATERIALS AND METHODS

3.1 INTRODUCTION

To investigate soil reinforcement with shredded waste tires, mixtures of Portage sand and shredded tires were tested using a large-scale direct shear machine. Thirty-five mix designs were tested, each having a unique reinforcement content, mix density, reinforcement orientation, and reinforcement size. A hydraulically driven direct shear machine was used; it was connected to a computerized data acquisition system that recorded data describing displacements and load. Results obtained from the direct shear tests included: (1) shear stress vs. horizontal displacement, (2) vertical deformation during shear, and (3) strength envelopes.

3.2 PORTAGE SAND

The soil selected for use in this study was Portage sand. Sand was selected because its density can be controlled and nearly identical specimens can replicated easily. Portage sand is uniformly graded and composed of rounded quartz particles. The particle size distribution curve for Portage sand is shown in Fig. 3.1. Table 3.1 summarizes the properties of Portage sand.

3.3 SHREDDED WASTE TIRES

The shredded waste tires used in this study were selected from shredded tires remaining from a previous study performed at the University of Wisconsin-Madison (Edil and Bosscher, 1992). The storage pile included a mixture of different types of tires (reinforced and un-reinforced) that were shredded at different

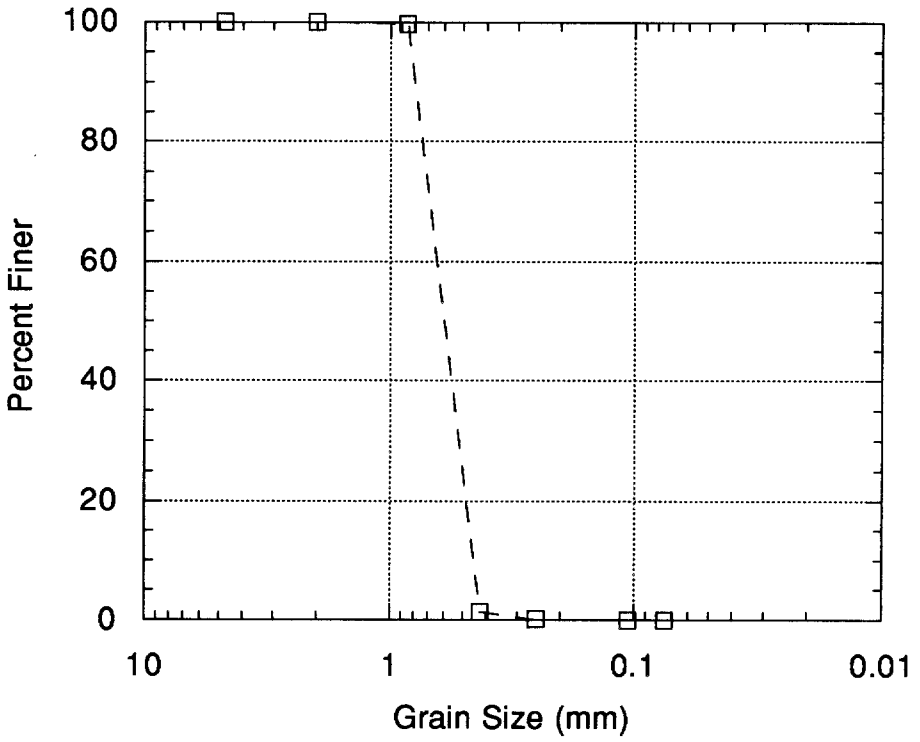

Figure 3.1. Particle Size Distribution Curve for Portage Sand.

Table 3.1. Characteristics of Portage Sand.

Property	ASTM Testing Method	Value
Coefficient of Uniformity, C_u	-	1.0
Coefficient of Curvature	-	1.0
Specific Gravity, G_s	D854	2.68
Maximum Dry Unit Weight, γ_{min}	D4253	17.7 kN/m^3
Minimum Void Ratio, e_{min}	-	0.48
Minimum Dry Unit Weight, γ_{min}	D4254	15.5 kN/m^3
Maximum Void Ratio, e_{max}	-	0.69
USCS Classification	-	SP

sites with various machinery. Criteria used to select the shreds were based on dimension, surface texture, and reinforcement type.

3.3.1 Grouping Shredded Tires by Size

The tire shreds were grouped into three classifications based on length: < 5 cm; 5-10 cm; and 10-15 cm. The maximum length of 15 cm was used because it was believed that mixtures containing shreds larger than this size could be affected by boundary effects when sheared. Shreds were selected and placed into one of three groups. The dimension recorded as the length of the shred was its longest dimension. For shreds with curved shapes, the dimension was recorded as the un-flattened maximum dimension. Care was taken to maintain a symmetric distribution of length and to have a wide range of surface textures (e.g., treaded and side-wall) in each group.

Within each group, the shreds had several notable characteristics. Figure 3.2 is a photograph of the three groups. The group of shreds with a maximum dimension ≤ 5 cm was the most unique. As is shown in Fig. 3.2, the majority of shreds ≤ 5 cm long had no metallic reinforcement. It is assumed that this was the result of reinforcement being pulled or torn out during the shredding process. For most shreds in this group, it was not apparent which surface was the exterior of the tire, or whether the rubber was from the rolling surface of the tire or the side wall. The shreds less than 5 cm long looked more like chunks of rubber than shredded tires.

Shredded tires with maximum dimensions between 5 cm and 15 cm (Fig. 3.2) were readily recognized as portions of tires. Many shreds still had reinforcement in them. Three basic types of reinforcement were identified: large

Figure 3.2 Samples of Shredded Tires Used in Study

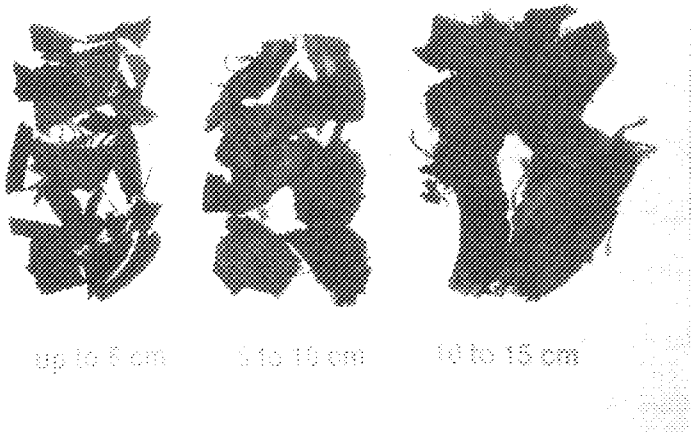

Figure 3.2 Samples of Shredded Tires Used in Study

metal wires roughly 1 mm in diameter, fine metal wires with a diameter less than 0.5 mm, and fabric. For all tire shreds in this group, it was possible to determine from which part of the tire the shred was from and whether it was from the exterior or interior of the original tire. As shown in Fig. 3.2, several of the shreds had metal reinforcement protruding from the rubber mass that was in a tangled and twisted state.

Histograms for random samples, collected from each group of shreds, are shown in Fig. 3.3. For the group with lengths ≤ 5 cm (Fig. 3.3), the average shred length was 3.16 cm. The minimum shred length was 0.6 cm. Having tire shreds less than 0.6 cm in length was not desirable because of the difficulty in separating the sand and tire shreds after shearing. For the group with lengths between 5 and 10 cm (Fig. 3.3), the average length was 7.8 cm. The distribution of length of shred in this group was nearly symmetric. For the group with lengths between 10 and 15 cm (Fig. 3.3), the average length was 12.3 cm and the distribution had a pronounced positive skew.

3.3.2 Properties of Shredded Waste Tires

3.3.2.1 *Specific Gravity*

In this study, mixtures of sand and shredded waste tires were identified by volume. To calculate the volume of shreds with a known weight, an average specific gravity was determined for each size group using a modified version of ASTM D854. Two specific gravity tests were performed for each group. A sample from each group was selected randomly and consisted of a handful of shredded tires (typically about 7 N). The flask used in the specific gravity test was 20 cm in diameter and 16 cm in height. A seal between the cap and the flask was maintained with an O-ring. Care was taken to evacuate as much air from the water

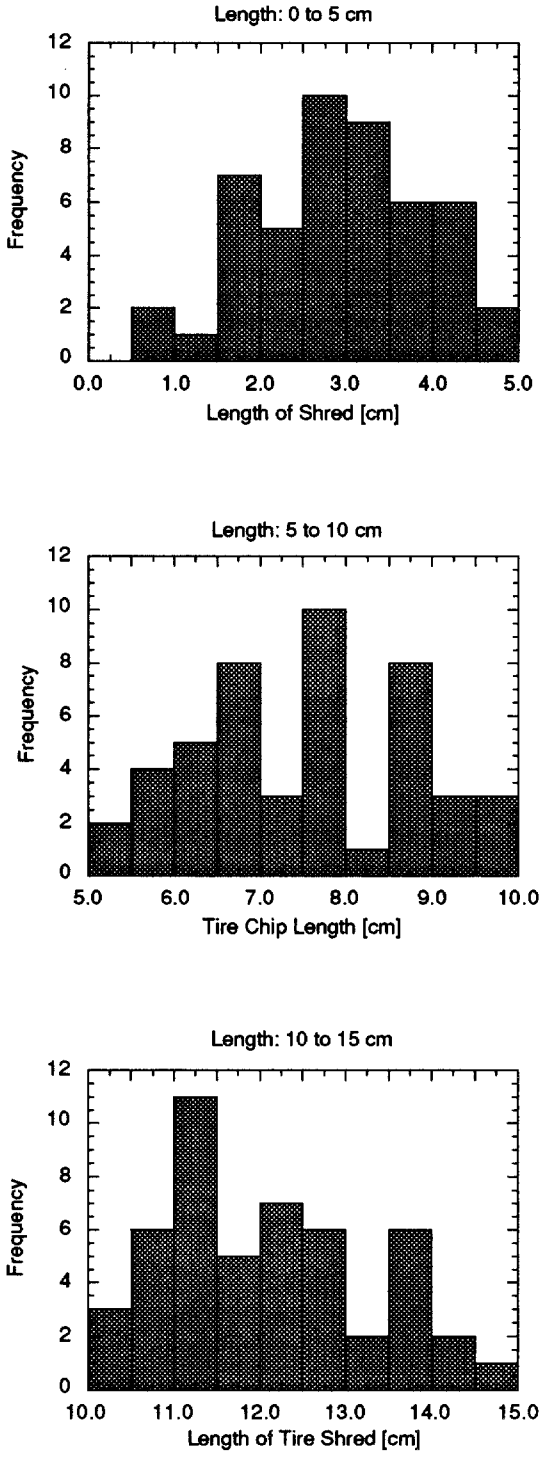

Figure 3.3. Histograms for Groups of Shredded Tires.

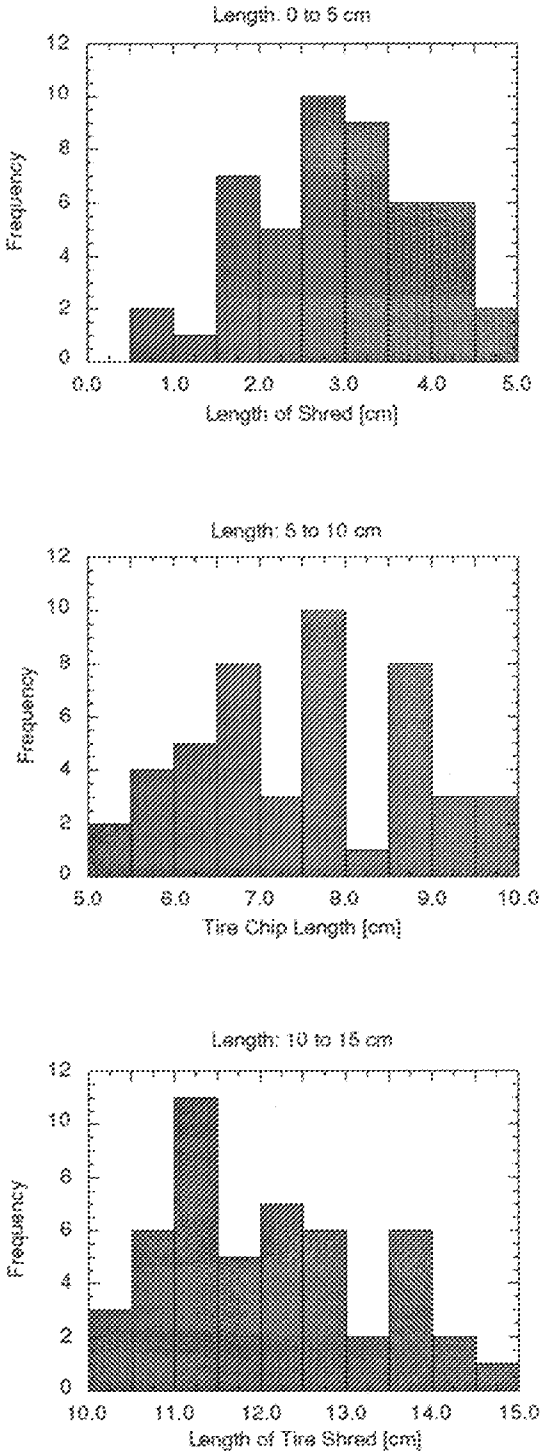

Figure 3.3. Histograms for Groups of Shredded Tires.

-tire chip mixture as possible. A summary of the specific gravity tests is in Table 3.2. The average specific gravity for shreds with lengths less than 5 cm was 1.21. For lengths of shreds between 5 and 10 cm, the average specific gravity was 1.25. The average specific gravity for shreds with length between 10 and 15 cm was 1.27.

3.3.2.2. *Interface Friction Between Portage Sand and Shredded Tires*

Interface friction between the shredded waste tires and Portage sand was measured in direct shear. Specimens were cut from shredded tires and placed in a direct shear ring with a diameter of 6.35 cm. The surface of the tire was set level with the shear plane by mounting it on a disk of plywood. Three small nails were used to attach the tire shred to the plywood. A photograph of a shredded tire ready to be mounted in the direct shear ring is shown in Fig. 3.4.

Two specimens were tested. Specimen "A" was set in the ring so that the shearing surface would be the exterior of an intact tire. Specimen "B" was placed in the ring with what would normally be the interior of a tire as the shearing surface. The objective of varying the shearing surface was to measure an average friction angle for the interface between tire shreds and sand.

Procedures in ASTM D3080 were used to perform the tests. Three different unit weights of sand were used. These unit weights were used throughout the study. A summary of results from the tests is shown in the Table 3.3. The average interface friction angle was 34^{o} when the unit weight of the soil matrix was 15.2 and 15.7 kN/m^{3}. The average interface friction angle between tire shreds and Portage sand at a unit weight of 16.8 kN/m^{3} was 39^{o}.

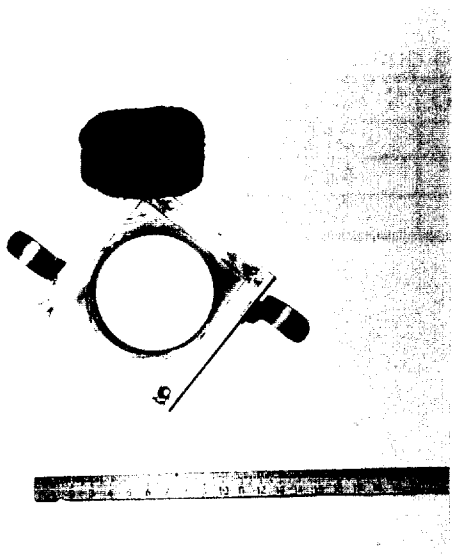

Figure 3.4. Setup for Determining Interface Friction Between Shredded Tire and Sand.

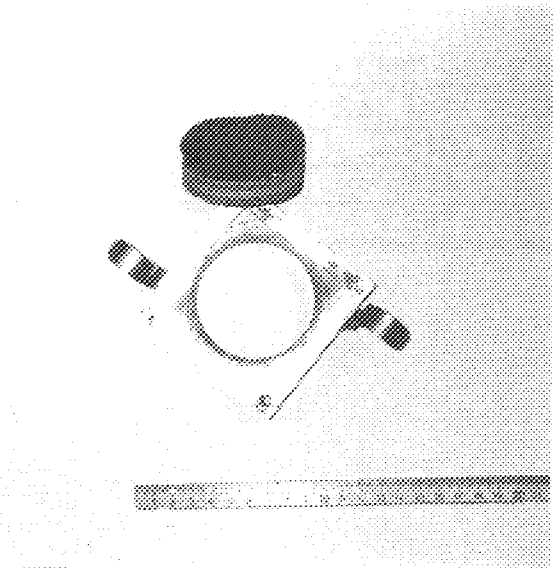

Figure 3.4. Setup for Determining Interface Friction Between Shredded Tire and Sand.

Table 3.2. Specific Gravity for Each Group of Shreds.

SAMPLE	G_S, Trial 1	G_S, Trial 2	G_S, average
0 - 5 cm	1.210	1.210	1.21
5 - 10 cm	1.253	1.254	1.25
10 - 15 cm	1.274	1.267	1.27

Table 3.3. Average Sand to Shredded Tire Interface Friction Angle.

Unit Weight of Sand on Shearing Surface [kPa]	Average Interface Friction Angle [degrees]
15.2	34
15.7	34
16.8	39

3.4 LARGE-SCALE DIRECT SHEAR MACHINE

3.4.1 General Aspects

A large-scale direct shear machine was constructed to determine the shearing properties of soil reinforced with shredded waste tires. A large-scale machine was used to reduce the effects of boundary conditions. Specimens of sand reinforced with shredded waste tires were prepared in the shear ring. Confining stress was applied with a pneumatic system and the shearing force was applied with an oil-driven diaphragm system. Load on the shear plane was measured with a load cell. Horizontal and vertical deformations were measured with linearly variable differential transducers (LVDTs) and a computerized data acquisition system recorded the data. Figure 3.5 is a photograph of the direct shear machine and the associated data acquisition equipment.

The frame for the large scale direct shear testing machine was constructed out of 7.6x7.6x30.4 section of steel channel. A triangular joist was attached at one end of the channel to transfer loads from the shear ring to the frame. Four metal slats were bolted perpendicular to the frame in a square pattern as a means for supporting the device applying the confining stress on the shear ring.

3.4.2 Shear Ring

The shear ring had an inner diameter of 27.9 cm and a height of 31.4 cm. The ring was made from stainless steel pipe with a wall thickness of 1.27 cm. The top and bottom halves of the shear ring were both 15.7 cm in height.

A photograph of the direct shear ring is shown in Fig. 3.6. Grooved flanges were attached on opposite sides of both the top and bottom rings parallel to the direction of shear plane. Plastic races with ball bearings (diameter = 1.27 cm), were set between the grooved flanges and separated the upper and lower halves

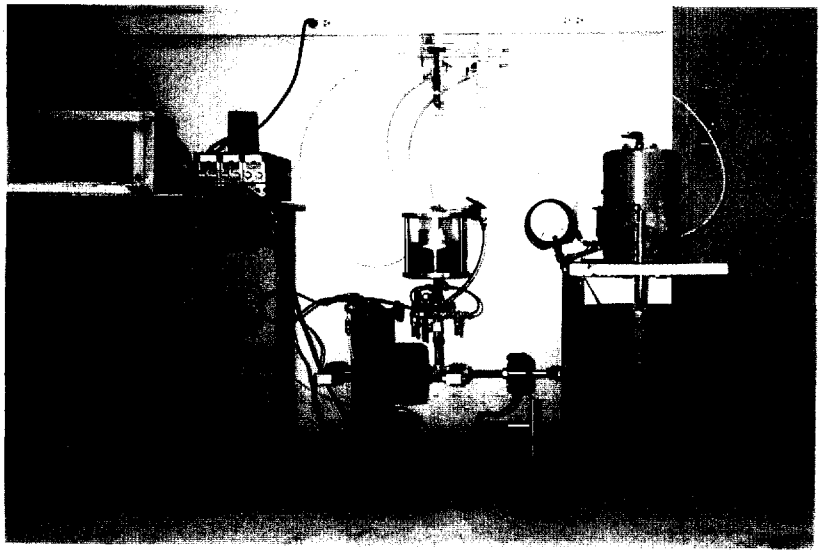

Figure 3.5. Large-Scale Direct Shear Machine.

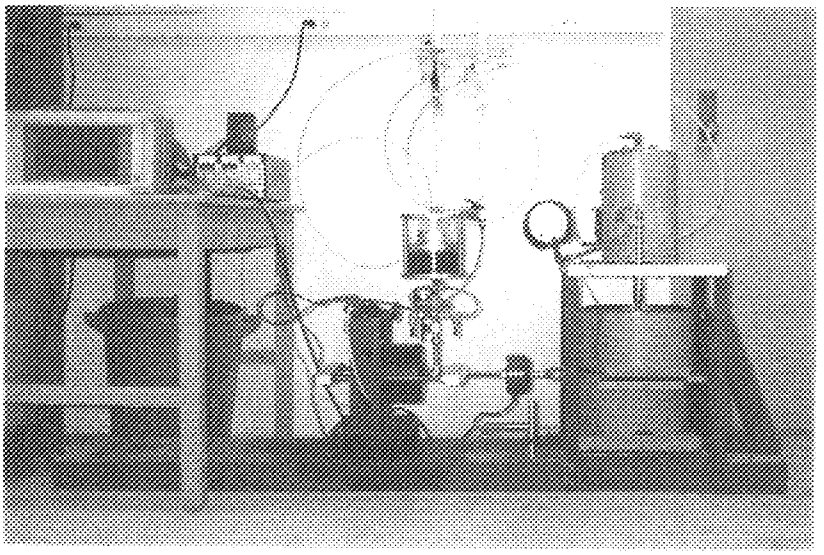

Figure 3.5. Large-Scale Direct Shear Machine.

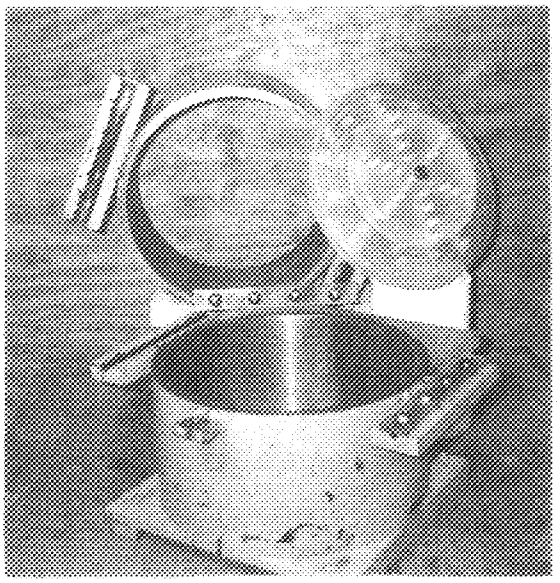

Figure 3.6. Direct Shear Ring and Top Plate.

Figure 3.6. Direct Shear Ring and Top Plate.

of the ring by less than 1.0 mm. This provision helped minimize the resistance from the ring halves sliding against one another.

A stainless steel plate was welded to the bottom ring. Another set of runners was set parallel to the direction of shear and bolted into the bottom steel plate. The runners were paired with a set of flanges bolted to the frame and races of ball bearings were set between the flanges. This set-up allowed the bottom of the shear ring to be pulled with minimal frictional resistance.

A stainless steel tab (2.5 cm x 2.5 cm x 1.2 cm thick) was welded 2.5 cm below the shearing plane. A hole (diameter =0.95 cm) was drilled into the tab to connect the bottom of the shear ring with the loading apparatus. A clevis pin was used for the connection. A triangular joist was used to transfer load from the top ring to the frame. Two steel bolts (diameter = 0.64 cm) with 2.5 cm spacers connected the top ring to the triangular joist.

A plastic plate was attached flush with the top of the bottom ring to keep the contents from the top half of the ring from spilling out when the rings displaced (Fig. 3.6). The plate was long enough for the sample to be sheared slightly more than 2.5 cm without a spill occurring from the top of the shear box.

3.4.3 Application of Confining Stress

A Bellofram® air cylinder was used to apply confining stress to the sample. The inside diameter of the air cylinder was 17.3 cm and the stroke was 15.2 cm. The air cylinder was bolted on a square stainless steel plate (2.5 cm thick) with a hole for the piston. The plate was bolted to the metal slats discussed in Section 3.4.2, which transferred load from the plate to the frame of the machine. The calibration curve for the Bellofram® is shown in Fig. 3.7.

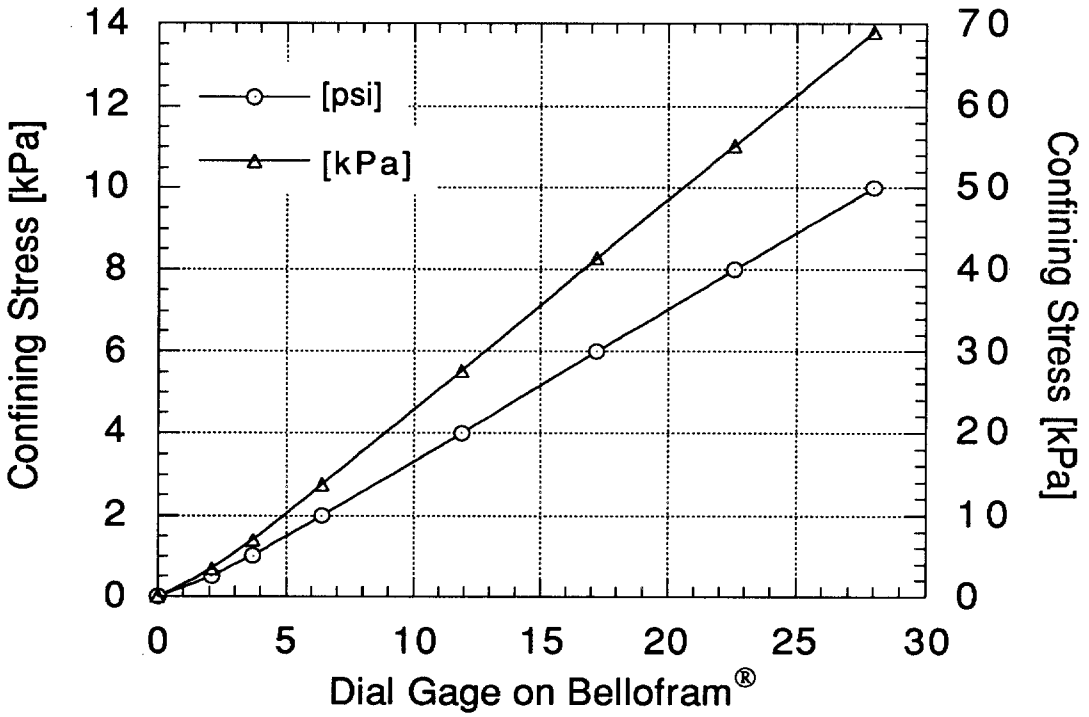

Figure 3.7. Calibration of Bellofram®

A ball bearing was used to transfer the load from the Bellofram® to the plastic top plate shown in Fig. 3.6. The plastic top plate had a diameter of 27.7 cm. The surface in contact with the specimen was 2.54 cm thick and had concentric circular grooves approximately 2.0 mm deep. A smaller circular plate was mounted on top of the plastic plate to act as a stiffener. The stiffener had a steel mount for the ball bearing.

3.4.4 Application of Shear Force

A cylinder with an air-to-oil interface was used to pressurize the oil (Fig 3.5). The inner diameter of the air-to-oil cylinder was 15.2 cm. Hydraulic fluid was routed out of the cylinder and through a flow regulator. The regulator allowed the rate of displacement to be controlled accurately, down to 0.0003 cm/sec. The pneumatic actuator (diameter = 15.2 cm and stroke = 5 cm) was connected to the regulator using steel pipe (diameter = 0.64 cm). The actuator was bolted to a 25.4 x 7.62 cm section of channel. A steel plate was welded to the channel and bolted to the machine frame. Load applied by the actuator was transferred to the lower ring of the shear ring through a double-yoke system connected to the lower ring of the shear ring (Fig. 3.5).

A shut-off valve was placed between the regulator and the actuator so that as much oil as possible could be pressurized before pressure was applied to the actuator. This helped to limit the amount of time required for the loading system to reach full capacity. Tests run without this shut-off valve system and required approximately 7 seconds for the loading system to begin moving steadily after air pressure was applied. With the valve installed, about 3 seconds was required. This time between application of air pressure and load was the biggest deficiency of the large-scale direct shear machine.

The double-yoke system was necessary because the actuator being used could be driven in only one direction (pushed out of the cylinder) whereas the design of the machine required that the bottom half of the shear ring be pulled to shear. Two holes were drilled in the channel to allow the yoke system to pass through. The end of the yoke (pulling the bottom of the shear ring) was connected to a 1.91 cm diameter piece of threaded rod. A load cell was mounted to the threaded rod and another piece of threaded rod connected the load cell to the shear ring via a clevis pin.

3.4.5 Data Acquisition

An electronic data acquisition system (EDAS) was used to retrieve and store data on a computer diskette. Instrumentation connected to the EDAS consisted of two LVDTs and a load cell. A software package titled "Easy Sense" (Validyne Engineering Corp.) and a UPC601-G Strain Gage PC Interface Card (by Validyne Engineering Corp.) were used with a Toshiba 386 portable computer. A TRYGON three channel DC power supply with a capacity +/- 32 volts supplied power to the LVDTs. The voltage was checked before each test with a Micronta voltmeter having a precision of 0.001 volts. Power for the load cell was supplied by the computer board.

The LVDT measuring vertical displacement was mounted in a hole drilled in the metal plate supporting the Bellofram®. An O-ring, on the LVDT, was used to hold it at an elevation such that the voltage reading was near zero at the beginning of the test. The hole for the vertical LVDT was 12.7 cm from the center of the top plate. Mounting the LVDT directly of the center of the plate would have been more desirable, but this was not possible because of the location of the Bellofram®. The LVDT used for measuring vertical displacement was a Type 1000 DC-D, 5-wire-

Table 3.4. Wiring Configuration for Vertical Measuring LVDT.

LVDT Wire	Connection to UPC601-G Strain Gage PC Interface Card
green	common
red	channel B (positive)
black	channel C (negative)
yellow	A-in
green	B-in

type, with a 5.5 cm stroke. It was manufactured by Schaevits Engineering. The voltage applied to the LVDT was 15 volts. The wiring scheme for the vertical LVDT is listed in Table 3.4. The vertical LVDT was calibrated with a micrometer accurate to 0.0003 cm. Eight replicate calibrations were run and found to yield 3.733 volts/cm, on average.

The LVDT measuring horizontal displacement was mounted to the frame of the machine so it was in contact with the bottom plate of the shear ring. The center line of the LVDT was set 3.2 cm off center from the bottom plate. Setting the LVDT on the center line of the shear box was not believed to be critical because construction of the shear box did not permit any side-to-side wobble or tilting. The horizontal LVDT was a DC Model 7308-X3-40 (4 wire, 3.8 cm stroke) with a spring-mounted core manufactured by Pickering & Co. The wiring scheme for the horizontal LVDT is listed in Table 3.5. The horizontal LVDT was calibrated with a micrometer accurate to 0.0003 cm. Eight replicate calibrations were conducted. The average calibration was 0.441 volts/cm.

The load cell was a model 1210-AJ manufactured by Interface Inc. The load cell was calibrated at 0.8256 mv/v/cm. The calibration factor, supplied by the manufacturer, was used to convert resistance measurements to loads. The load cell was connected to a 4 volt DC terminal on the computer board with the configuration listed in Table 3.6. A check of the calibration was made in an MTS loading frame and found to be within 1.0% at loads of less than 90 N and 0.1% at a load of 6.7 kN (Fig. 3.8).

3.4.6 Data Acquisition Software

Software, titled "Easy Sense," was provided with the Validyne UPC601-G Strain Gage PC Interface Card (Validyne Engineering Corp.). The software

Table 3.5. Wiring Configuration for Horizontal Measuring LVDT.

LVDT wire	Connection to UPC601-G Strain Gage PC Interface Card
black	common
red	+4 volt source
white	channel 4 A-in
green	channel 4 B-in

Table 3.6. Wiring Configuration for Load Cell.

Load Cell Wire	Connection to UPC601-G Strain Gage PC Interface Card
red-white/red	channel 1 4 volt DC
green	channel 1 A-in
white-white/yellow	channel 1 B-in
black-white/black	channel 1 ground

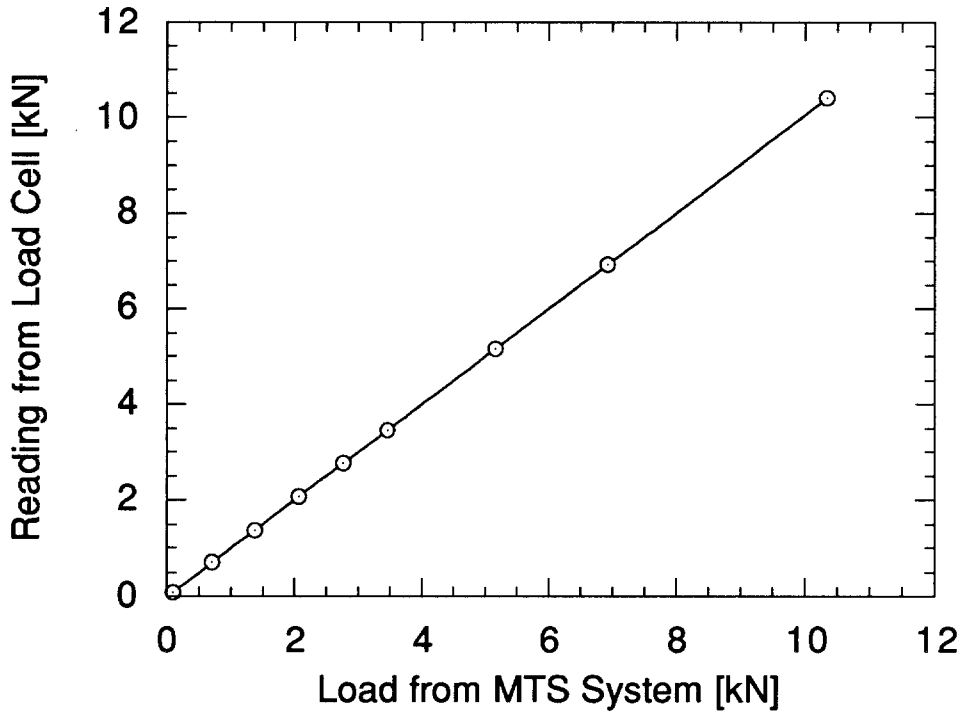

Figure 3.8. Evaluation of Calibration of Interface Model 1210-AJ Load Cell

allowed a high degree of flexibility with respect to configuration, calibration, and output. The software configuration for converting load cell readings to loads was used so that loads on the specimen and machine could be monitored easily. However, for the LVDTs only voltages were displayed and recorded. Setting up the LVDTs in this manner permitted more flexibility in positioning the LVDT's, required less set up time prior to each test, and simplified data reduction.

The software was configured to update 5000 times per second. Data was output to both the computer video display and a diskette. To minimize noise from the electronic sensors, the software was set to average readings taken over two seconds (i.e., 10,000 measurements) for display and recording. Output to the computer diskette was load, horizontal displacement, and vertical displacement.

3.4.7 Data Reduction

Careful positioning of the LVDTs was necessary to ensure the LVDT's operated near the center of their measuring span. The vertical LVDT was set so that the voltage reading prior to application of the confining stress was slightly less than zero. The horizontal LVDT was set so that the initial voltage reading was approximately +0.50 volts. Consistent initial settings for the LVDT's permitted the use of a single set of equations to reduce the data recorded via a spreadsheet.

A portion of a set of data, as recorded on diskette, is shown in Fig. 3.9. Equation 1 converts the voltage measurement from the horizontal LVDT into horizontal displacement:

$$h = (h_o - h_n)\, 2.270 \qquad (3.1)$$

UPC data log file			
T I M E	Load	Vertical Displacement	Horizontal Displacement
10:46:40:30	-1.7446	-0.8650001	0.6
10:46:46:28	-8.43223	-0.8700001	0.6
10:46:52:27	-15.7014	-0.87625	0.6
10:46:58:26	-24.13363	-0.8825001	0.59875
10:47:04:24	-31.98432	-0.8875	0.59875
10:47:10:23	-39.83502	-0.89125	0.59875
10:47:16:22	-49.13955	-0.8962501	0.5975
10:47:22:21	-57.86255	-0.9	0.5975
10:47:28:19	-68.33015	-0.9025	0.59625
10:47:34:18	-77.92545	-0.905	0.595
10:47:40:17	-87.81151	-0.9075	0.595
10:47:46:15	-98.27911	-0.91	0.59375
10:47:52:14	-108.45593	-0.9125	0.5925
10:47:58:13	-119.50507	-0.915	0.59125
10:48:04:11	-130.26343	-0.9175	0.59
10:48:10:10	-140.44026	-0.92	0.58875
10:48:16:09	-152.94322	-0.92125	0.5875

Figure 3.9. Sample Output as Recorded on Diskette.

where h is horizontal displacement (cm), h_o is the horizontal voltage reading at the start of the test, and h_n is the voltage reading at a given horizontal displacement.

Equation 3.2 converts the voltage measurement from the vertical LVDT into vertical displacement:

$$v = (v_n + v_o)\ 0.2679 \tag{3.2}$$

where v is vertical displacement (cm), v_o is the vertical voltage reading at the start of the test, and v_n is the voltage reading at a given vertical displacement.

Because the surface area of the shear plane constantly changes during the direct shear test, a corrected area was determined using Eq. 3.3:

$$A = A_o\left[\left(\frac{1}{90}\right)\cos^{-1}\left(\frac{\Delta h}{D}\right) - \left(\frac{2}{\pi}\right)\left(\frac{\Delta h}{D}\right)\left[1 - \left(\frac{\Delta h}{D}\right)^2\right]\right] \tag{3.3}$$

where A is the corrected area, A_o is the initial area of the ring, Δh is the horizontal displacement, and D is the diameter of the ring.

Volumetric strain (ε_v) was calculated using Eq. 3.4:

$$\varepsilon_v = 0.09189\ v \tag{3.4}$$

where v is vertical displacement (cm).

Shear stress on the specimen was calculated using Eq. 3.5, where P was the load on the specimen in newtons.

$$\tau = \frac{P}{A} \tag{3.5}$$

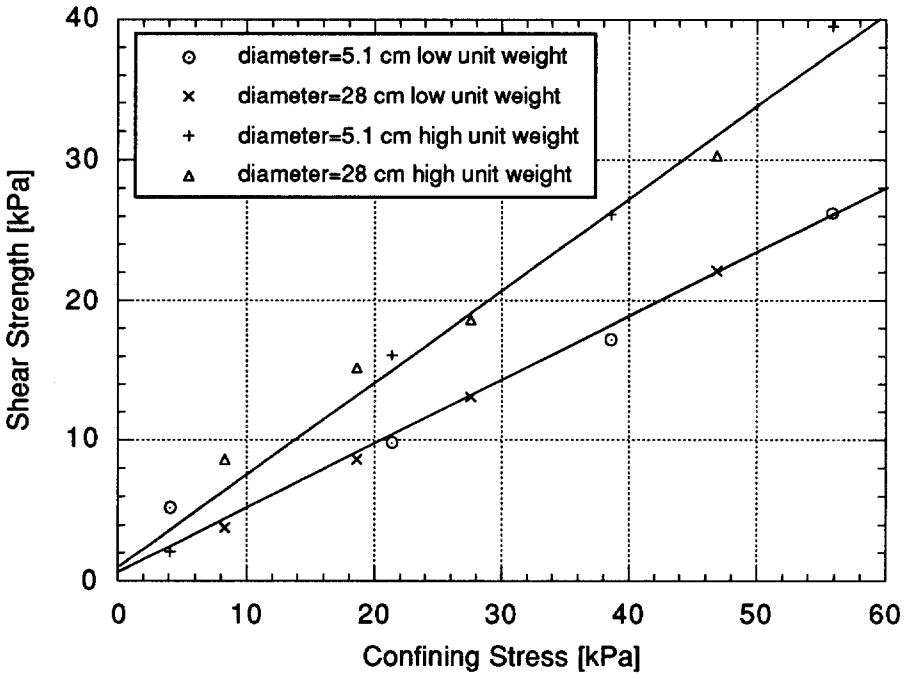

Figure 3.10. Failure Envelopes from Direct Shear Tests on Portage Sand Using Standard and Large-Scale Direct Shear Machines

3.4.8 Comparison of Large and Small Direct Shear Machines

Direct shear tests for an un-reinforced sand were performed in both the large-scale direct shear machine and a Wykeham-Farrance direct shear machine (Model No. 25301). The Wykeham-Farrance machine had a cylindrical shear ring with a diameter of 6.35 cm and a height of 2.54 cm. Mohr-Coulomb failure envelopes from both tests are shown in Fig. 3.10. These results indicate that, for Portage sand, the strength envelope determined using the large-scale machine is essentially the same as that from the standard size machine.

3.5 PREPARATION OF SPECIMENS

Prior to construction of the specimen, the shear ring was disassembled and wiped clean with a paper towel. Ball bearings supporting the top ring were rinsed and then sprayed with a light coating of silicon lubricant. The surfaces between the two halves of the shear ring were also coated lightly with silicon lubricant. Care was taken to neatly apply the lubricant to prevent the silicon from contacting the specimen. After lubrication, the top and bottom rings were assembled and aligned. C-clamps were used to clamp the flanges holding the two rings together to prevent movement rings during construction of the specimen.

3.5.1 Volume Calculation

The volume of sand (V_S) in each sample was calculated using:

$$V_S = (100–CSR)\ V \qquad (3.6)$$

where CSR is the reinforcement content by percent volume and V is the volume of specimen (V = 0.01687 m^3 for all tests). The volume of reinforcement (V_r) for each specimen was calculated using Eq. 3.7.

$$V_r = (CSR)\, V \tag{3.7}$$

The weight of reinforcement (W_r) was determined using Eq. 3.8:

$$W_r = \frac{V_r}{G_s \gamma_w} \tag{3.8}$$

where G_s is the specific gravity of the shreds being tested, and γ_w is the unit weight of water.

3.5.2 Construction of Specimens with Low Unit Weight

Constructing specimens with low unit weight (14.7 kN/m^3) required special procedures. The specimens were constructed in the shear ring while it was set in the machine. Depending on the reinforcement content, an appropriate portion of tire shreds was placed in the bottom of the ring. The amount of reinforcement to be placed in the bottom of the ring was determined "by eye." For reinforcement contents of 20% and 30%, an initial quantity of reinforcement was placed about 15 cm high in the shear ring, whereas the 30% mixture was packed more densely. For the 10% mixtures, some sand was poured in the bottom of the ring and tires shreds were placed in the sand as randomly as possible. After several practice specimens were prepared, it was possible to maintain a uniform distribution of reinforcement throughout the specimen.

The sand was poured into the shear ring with a funnel using a circular motion starting at the center. To obtain the loosest possible sand, the height of fall from the bottom of the cone was kept at about 0.5 cm. The procedure used was similar to the method of placement of a granular soil in a minimum density test. After the level of the sand was almost up to the level of the reinforcement, reinforcement was added to the ring. More sand was then poured into the ring with the funnel. This process was repeated until all the sand and shredded tires were in the ring.

During preparation of the specimens, two checks on the unit weight of the soil matrix were made. When the specimen was half-way completed, the weight of remaining sand and shredded tires was checked to ensure that the unit weight of the soil matrix and reinforcement content were correct. If the sample was not satisfactory, the shear ring was emptied and another attempt at constructing the specimen was made. After all the sand and shredded tires were mixed the top surface was gently smoothed by hand. In some cases, one or two pieces of reinforcement would interfere with leveling of the top of the specimen. These shreds were subsequently removed. The writer believes that a level surface for application of the confining stress was much more important than a piece of reinforcement more than 10 cm from the shear plane. After the top surface was level, the plastic top plate was placed on the reinforced soil.

Another check on unit weight of the soil matrix was performed by measuring the distance from the upper surface of the top plate to the top of the shear ring. For specimens prepared at the proper unit weight, this distance was 1.4 cm. If a distance greater than 1.4 cm was measured, the unit weight of the soil matrix was too high. Under these circumstances, the shear ring was emptied and another specimen was constructed. If the specimen was too loose (i.e. the measured

distance was less than 1.4 cm), the top plate was removed and a rod (diameter = 0.3 cm) was pressed into the specimen in several locations. Only a few of the specimens were prepared too loosely. The top plate was replaced and the same measurement was repeated. If the distance measured was 1.4 cm, the sample was deemed ready for testing. If it was still less than 1.4 cm, the rodding procedure was repeated.

3.5.3 Construction of Specimens with Medium or High Unit Weight

Samples with medium and high unit weight of the soil matrix were constructed in a manner similar to those having low unit weight of the soil matrix. However, the specimen was prepared with the shear ring removed from the machine frame and a vibrator was used to obtain higher unit weight. The sand and shredded tires were placed in the shear ring in the same manner as was used for specimens with low unit weight. When the specimen was half completed, a check on the unit weight of soil matrix was made. If the unit weight of soil matrix was to high, the ring was emptied and preparation was started over. If the unit weight of soil matrix was too low, it was shaken on the vibrating table until the desired unit was achieved.

After the proper amount of sand and shredded tires had been placed in the shear ring, the surface was leveled and the top plate was placed on the specimen. Distance from the upper surface of the top plate to the top of the shear ring was measured. If the unit weight of the soil matrix was too high (which rarely happened for medium and high unit weight tests), the sample was rebuilt. If the specimen was too loose, it was subjected to additional vibration and concurrently the distance from the top plate to the top of the ring was measured. When the appropriate unit weight of soil matrix was reached, the vibrator was shut off. Most of the samples

prepared at medium and high unit weight needed additional vibration. For specimens with medium unit weight of the soil matrix, only a few seconds of vibration were needed. For specimens with high unit weight of soil matrix, up to one minute of vibration was needed. After the proper unit weight of soil matrix was obtained, the shear ring was lifted by hand and placed gently into the loading frame.

3.6 DEFINITION OF FAILURE

Two definitions of failure were used because most specimens did not exhibit a peak shear stress after being sheared 2.54 cm. Typical graphs of shear stress vs. displacement are shown in Figure 3.11. Some samples tested at confining stresses near 0 kPa did peak at displacements less than 2.54 cm. In these cases, failure was defined as the peak shear stress (Fig 3.11a). If the sample did not peak, the shear stress at 2.54 cm of displacement was called the peak shear stress even though a peak had not actually occurred (Fig. 3.11b).

SECTION 4

RESULTS AND DISCUSSION

4.1 INITIAL INVESTIGATION

4.1.1 Factorial Design

A two-level factorial design was used to isolate important factors influencing the shear strength of mixtures of sand and shredded waste tires. Factors studied in the first phase of experimentation were reinforcement content, length of reinforcement, orientation of reinforcement, unit weight of the soil matrix, and confining stress. The measured response was peak shear strength or shear strength at a displacement of 2.54 cm, with the greater value recorded as the shear strength.

A half-fraction design was used. The 2^{4-1} experiment, which required 16 tests, allowed isolation of main effects but confounded the 2/3 factor, and 4 factor interactions. A randomized design with two blocks was used to avoid confounding the analysis with systematic errors. Jass® (Joiner Associates Inc., 1986), a statistical analysis software package, was used to generate the experimental design (Table 4.1).

4.1.2 Levels Studied

Table 4.2 is a summary of the levels at which the factors were studied. To investigate the effect of reinforcement content on shear strength, the reinforcement contents of 10% and 30% (by volume) were used. The upper bound of 30% reinforcement content was selected because it was the maximum amount of reinforcement that could be placed randomly in the shear ring. The lower bound

Table 4.1. Design for 2^{4-1} Initial Experiment.

Run	Block	Reinforcement Content	Shred Length	Orientation	Unit Weight of the Soil Matrix	Confining Stress
1	1	+	+	-	-	+
2	1	+	+	+	-	-
3	1	+	+	-	+	-
4	1	-	-	+	+	+
5	1	-	-	-	+	-
6	1	-	-	+	-	-
7	1	-	-	-	-	+
8	1	+	+	+	+	+
9	2	-	+	+	+	-
10	2	+	-	-	-	-
11	2	+	-	+	+	-
12	2	-	+	+	-	+
13	2	-	+	-	-	-
14	2	+	-	+	-	+
15	2	-	+	-	+	+
16	2	+	-	-	+	+

Table 4.2. Factors and Levels for Half-Fraction Factorial.

Factor	**Level 1 (+)**	**Level 2 (-)**
Reinforcement Content	10% by Volume	30% by Volume
Length of Reinforcement	10 to 15 cm	Up to 5 cm Long
Orientation	Vertical	Random
Unit Weight of the Soil Matrix	14.7 kN/m^3	16.8 kN/m^3
Confining Stress	25.5 kPa	6.2 kPa

(10% reinforcement content) was selected because visual inspections showed that few shreds crossed the shear plane when this quantity of reinforcement was used.

The effect of length of reinforcement on shear strength was also investigated. The maximum shred length was 15 cm, which is one-half the diameter of the shear ring. The writer believed that tests using reinforcement longer than 15 cm would have been confounded by boundary effects. Two groups were studied in the initial investigation: (1) shreds with lengths ranging from 10 to 15 cm (hereafter called "15 cm reinforcement") and (2) with lengths of shreds up to 5 cm (hereafter called "5 cm reinforcement").

To study the influence of reinforcement orientation on shear strength, two levels (random and vertical) were studied. Random orientation was selected because the writer believed that random orientations are most likely to occur in a field application. Vertical orientation of the tire shreds was selected because it was the easiest preferred orientation to maintain during preparation of the test specimens.

The influence of unit weight of the soil matrix (γ_{sm}) was evaluated at two levels, low and high (14.7 and 16.8 kN/m^3). The low γ_{sm} was less than the minimum dry unit weight of Portage sand (15.5 kN/m^3). This was possible because addition of bulky shredded tires resulted in more void space (Fig. 4.1). It was not possible to fill some of these voids with sand. Thus, the average unit weight of the soil matrix was less than the minimum unit weight.

4.1.3 Results of Half-Fraction Factorial

Table 4.3 summarizes the results of the experiment; Jass® (Joiner Associates Inc. 1986) was used to analyze the half-fraction factorial. The effects were calculated using Yates's algorithm (Box et al., 1978). The variance of an effect

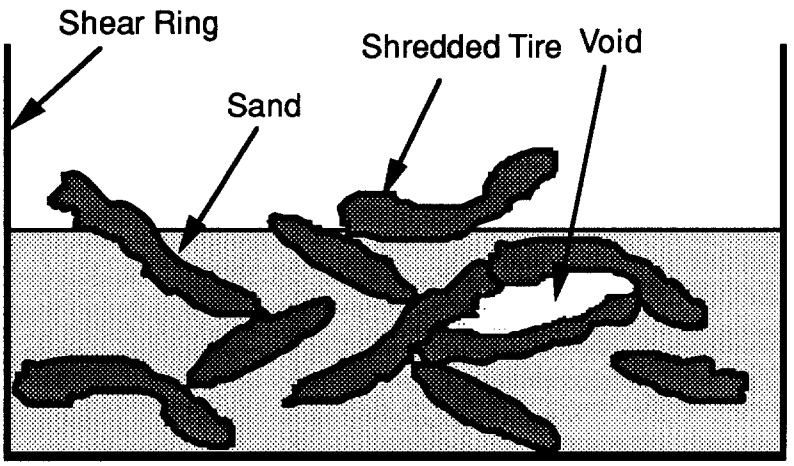

Fig. 4.1. Illustration of Formation of Voids in Specimens.

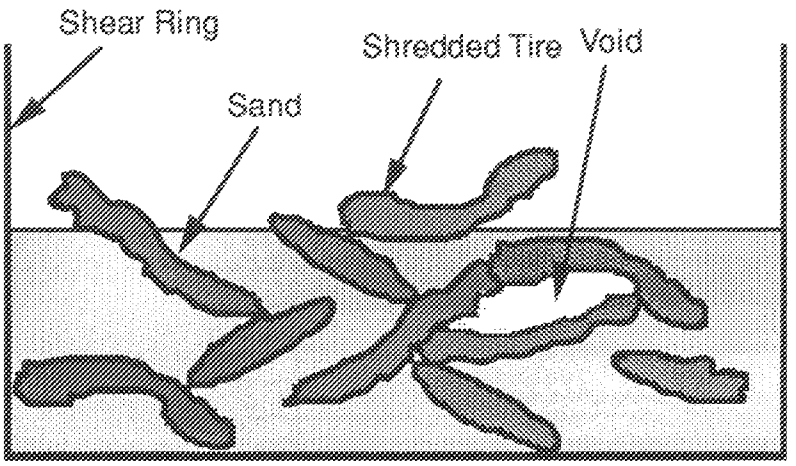

Fig. 4.1. Illustration of Formation of Voids in Specimens.

Table 4.3. Measured Response from Half-Fraction Factorial.

Run	Measured Response, Peak Shear Strength [kPa]
1	37.9
2	18.6
3	8.3
4	37.2
5	11.0
6	20.7
7	55.2
8	32.4
9	32.4
10	13.8
11	9.7
12	78.6
13	22.8
14	29.0
15	42.1
16	19.3

was estimated assuming that higher order interactions were negligible. A t-ratio was calculated to evaluate the significance of each factor using the average of all effects, variance, and effect of each factor. Results of the analysis of variance are shown in Table 4.4.

The t-ratio for 9 degrees of freedom is 2.262 for a 95% confidence level (Box et al., 1978). Thus, for a factor to be considered significant at the 95% confidence level, the absolute value of the t-ratio must be greater than 2.262. Three factors were found to be significant: reinforcement content, γ_{sm}, and confining stress. Results from the experiment showed that differences in blocks, length of reinforcement, and orientation were not significant.

Results from the half-fraction factorial were used to direct further testing. The effect of reinforcement orientation (random and vertical) on shear strength was not considered further because it was not found to be significant. However, length of reinforcement was studied further because the difference between the t-statistic for length and the critical t (2.262) was small (Table 4.4). This decision was also made, in part, because the writer believed that shred length should be significant and to disregard it based on the results of 16 direct shear tests seemed pre-mature.

4.2 DEVELOPMENT OF STRENGTH ENVELOPES

4.2.1 Testing Program

A testing program was designed to determine the strength envelopes for sand reinforced with shredded waste tires. Three significant factors identified from the initial half-fraction factorial (reinforcement content, unit weight of soil matrix, and confining stress) were studied in addition to length of reinforcement. To evaluate these four factors, testing was expanded to 3 levels for reinforcement content, unit weight of soil matrix, and length of reinforcement. Three factors, at 3 levels can be

Table 4.4. Results of Half-Fraction Factorial.

Factor	Effect	Standard Error of Effect	t-Ratio	Significant
Average	4.250	0.323	13.165	-
Block	-0.475	0.646	-0.736	No
Reinforcement Content	-2.375	0.646	-3.678	Yes
Length of Shred	1.400	0.646	2.168	No
Orientation	0.875	0.646	1.355	No
Unit Weight of Soil Matrix	-1.525	0.646	-2.362	Yes
Confining Stress	3.525	0.646	5.460	Yes

defined as a 3^3 experiment, which requires testing of 27 different mix designs. A summary of the parameters and the levels at which they were tested is listed in Table 4.5.

Confining stresses were varied from 0 to 112 kPa. For mixes of sand and shredded waste tires exhibiting a bi-linear strength envelope, a minimum of 4 different confining stresses were required to define the envelope. Typically, 2 initial tests were performed, with one test conducted at a confining stress less than 20 kPa and the other test conducted at a confining stress more than 60 kPa. These two points were graphed with the Mohr-Coulomb envelope for un-reinforced sand and a preliminary envelope for the reinforced sand was drawn (Fig 4.2). Confining stresses for the third and fourth tests were selected to fill in points needed to substantiate the preliminary strength envelope. If the results of the third and fourth tests fit with the preliminary envelope reasonably well, no further testing was conducted. If the results of the four tests did not permit an envelope to be developed, additional tests were conducted at confining stresses where more data was needed to define the strength envelop.

Table 4.6 is a list of all mixes tested. A unique 9-digit code was assigned to each test conducted. The symbol n specifies a variable parameter in the mix design, which in this case is confining stress (Table 4.6). The middle numbers (10, 20, and 30) specify the percentage of reinforcement by volume. The numbers 5, 10, and 15 specify the maximum length of reinforcement in centimeters. The letters L, M, and H specify whether the unit weight of soil matrix is low, medium, or high (14.7, 15.7, or 16.8 kN/m^3). The "R" indicates that the reinforcement was randomly oriented.

Table 4.5. Summary of Testing Parameters.

Parameter	Levels
Reinforcement Content	10%
	20%
	30%
Reinforcement Orientation	Random
	Vertical
Length of Reinforcement	≤ 5 cm
	5 to 10 cm
	10 to 15 cm
Unit Weight of the Soil Matrix γ_{sm}	(low) 14.7 kN/m^3
	(medium) 15.7 kN/m^3
	(high) 16.8 kN/m^3
Confining Stress	0 to 112 kPa

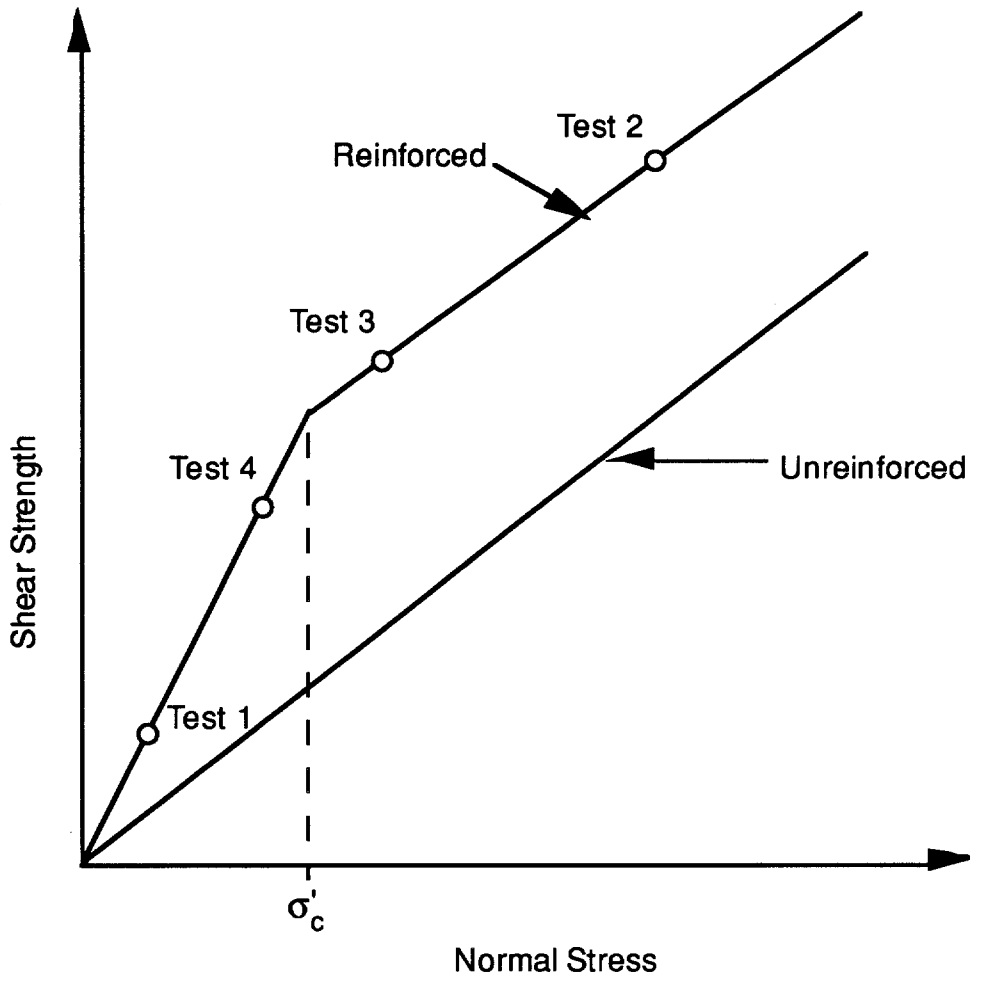

Fig. 4.2. Testing Sequence to Define Strength Envelope.

Table 4.6. Summary of Mixes Tested.

Mix #	Reinforcement Content [%]	Length of Reinforcement [cm]	Unit Weight of the Soil Matrix [kN/m^3]	Orientation
Sn3015LR	30	10 - 15	14.7	random
Sn3015MR	30	10 - 15	15.7	random
Sn3015HR	30	10 - 15	16.8	random
Sn2015LR	20	10 - 15	14.7	random
Sn2015MR	20	10 - 15	15.7	random
Sn2015HR	20	10 - 15	16.8	random
Sn1015LR	10	10 - 15	14.7	random
Sn1015MR	10	10 - 15	15.7	random
Sn1015HR	10	10 - 15	16.8	random
Sn3010LR	30	5 - 10	14.7	random
Sn3010MR	30	5 - 10	15.7	random
Sn3010HR	30	5 - 10	16.8	random
Sn2010LR	20	5 - 10	14.7	random
Sn2010MR	20	5 - 10	15.7	random
Sn2010HR	20	5 - 10	16.8	random
Sn1010LR	10	5 - 10	14.7	random
Sn1010MR	10	5 - 10	15.7	random
Sn1010HR	10	5 - 10	16.8	random
Sn305LR	30	≤ 5	14.7	random
Sn305MR	30	≤ 5	15.7	random
Sn305HR	30	≤ 5	16.8	random
Sn205LR	20	≤ 5	14.7	random
Sn205MR	20	≤ 5	15.7	random
Sn205HR	20	≤ 5	16.8	random
Sn105LR	10	≤ 5	14.7	random
Sn105MR	10	≤ 5	15.7	random
Sn105HR	10	≤ 5	16.8	random

4.2.2 Repeatability

To assess repeatability, a set of tests was performed using a mixture having a reinforcement content = 30%, length of reinforcement = 5 cm, and unit weight of the soil matrix = 16.8 kN/m^3. Three months later, five replicate tests were conducted using the same mixture at a confining stress equal to 6.9 kPa. A second set of five tests was conducted on specimens with a confining stress equal to 48.3 kPa. The confining stresses for the replicate tests were selected so that the tests would be conducted above and below the critical confining stress. Results from the replicate tests were used to establish the variability expected in shear strength above and below the critical confining stress. A second strength envelope was developed for the mixture.

Results of the tests are shown in Fig. 4.3. At a confining stress of 6.9 kPa, the shear strength ranged from 16 to 18 kPa. At a confining stress of 48.3 kPa, the shear strength ranged from 58 to 64 kPa. The range of critical confining stresses determined from the tests was from 24 to 33 kPa and the range of initial friction angles determined from the tests was from 61 to 65^o. The writer believes that these small ranges indicate that the test results are repeatable, at least for the mix design tested.

4.3 STRENGTH PARAMETERS AND ENVELOPES

4.3.1 Effect of Mix Design on Critical Confining Stress

Only mixes with high γ_{sm} (16.8 kN/m^3) had bi-linear strength envelopes. The only exception was a single mix having a γ_{sm} of 15.7 kN/m^3. The effect of mix design on critical confining stress was evaluated in terms of shred length and reinforcement content. A graph of critical confining stress versus shred length is shown in Fig. 4.4. No trends exists with respect to the effect of shred length on

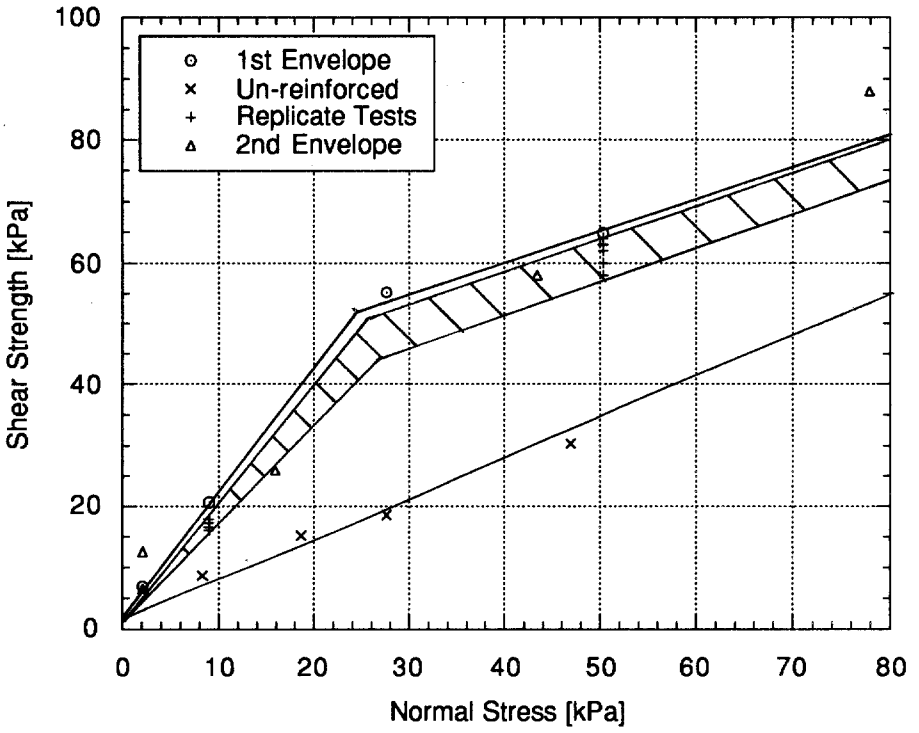

Figure 4.3. Repeatability of Strength Envelopes.

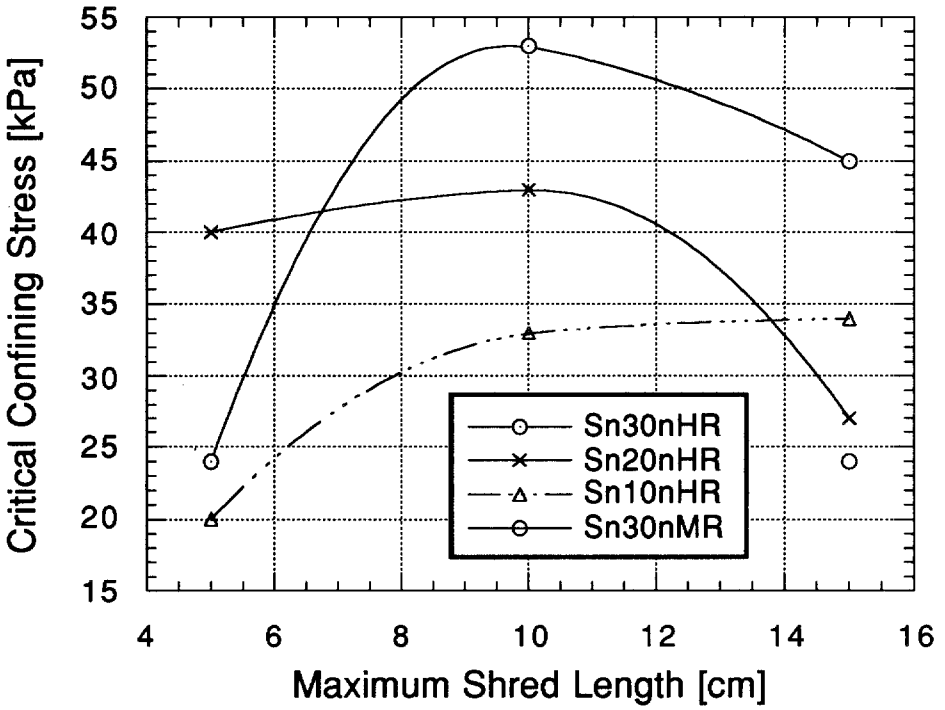

Figure 4.4. Critical Confining Stress vs. Maximum Length of Shred.

critical confining stress. For mixtures with a reinforcement content equal to 10%, the critical confining stress increased from 20 kPa to 33 kPa when the length of reinforcement was increased from 5 cm to 10 cm. However, when the length of reinforcement was increased from 10 to 15 cm, the critical confining stress only increased from 33 kPa to 34 kPa, which is much smaller than the range of repeatability discussed in Section 4.2.2.

For mixes with reinforcement contents of 20%, the critical confining stress decreased with an increase in shred length. The mix with a reinforcement content of 20% and a length of reinforcement of 5 cm had a critical confining stress of 40 kPa. When the length of reinforcement was increased from 5 cm to 10 cm, the critical confining stress increased from 40 kPa to 43 kPa which is much less than the range of repeatability discussed in 4.2. For the mix with 20% reinforcement content and 15 cm reinforcement, the critical confining stress was 27 kPa, a decrease of 16 kPa in comparison to the mix with 10 cm reinforcement.

For mixes having a reinforcement content of 30%, the critical confining stress for the mix with 5 cm reinforcement was 24 kPa. When the length of reinforcement was increased from 5 cm to 10 cm, the critical confining stress increased to 53 kPa. The critical confining stress for the mix with 30% reinforcement content with 15 cm reinforcement was not determined. Tests on this mix design were conducted at confining stresses up to 44 kPa. Testing at higher confining stresses would have overloaded the machine.

A critical confining stress of 24 kPa was measured for the mixture having a reinforcement content of 30%, length of reinforcement of 15 cm, and a γ_{sm} of 15.7 kN/m^3. For mixes having 15 cm reinforcement, this mix had the lowest critical confining stress.

Table 4.8 lists the samples that had bi-linear strength envelopes and the critical confining stress for each mix. Table 4.9 summarizes the average critical confining stress for each length of reinforcement and Table 4.10 is a summary of the average critical confining stress by reinforcement content. The average critical confining stress does not appear to depend on length of reinforcement or reinforcement content. Furthermore, the maximum and minimum average critical confining stress differ by only 15 kPa, which is close to the error in critical confining stress (9 kPa) observed in the repeatability tests (Section 4.2). Thus, critical confining stress does not appear to depend on reinforcement content or length. Perhaps the average critical confining stress from all mixes (34 kPa) provides the best estimate of the critical confining stress for these mixes.

4.3.2 Effect of Reinforcement Content on Initial Friction Angle

A graph of initial friction angle (ϕ_1') vs. reinforcement content is shown in Figure 4.5. All specimens reinforced with shredded waste tires had a higher initial friction angle than the friction angle for un-reinforced sand. Furthermore the initial friction angle increased with increasing reinforcement content.

There are two distinct bands shown in Fig. 4.5. The lower band is for samples that had low or medium γ_{sm}. The upper band corresponds to specimens having high γ_{sm}. Friction angles for specimens with low and medium γ_{sm} were similar at reinforcement contents of 0% because the minimum dry unit weight of Portage sand was 15.6 kN/m^3 and medium unit weight of the soil matrix was 15.7 kN/m^3.

A more practical analysis of the effect of reinforcement content on initial friction angle can be made by analyzing the average ϕ_1' for a given γ_{sm} and reinforcement content. Average ϕ_1' for low, medium, and high ϕ_1' are shown in

Table 4.8. Samples with Bi-Linear Strength Envelopes.

Mix #	Critical Confining Stress [kPa]
Sn305HR	24
Sn205HR	40
Sn105HR	20
Sn3010HR	53
Sn2010HR	43
Sn1010HR	33
Sn3015MR	24
Sn3015HR	>40
Sn2015HR	27
Sn1015HR	34

Table 4.9. Average Critical Confining Stress for Lengths of Reinforcement Studied.

Reinforcement Length [cm]	Average Critical Confining Stress [kPa]
5	28
10	43
15	33

Table 4.10. Average Critical Confining Stress for Reinforcement Contents Studied.

Reinforcement Content [%]	Average Critical Confining Stress [kPa]
10	29
20	37
30	37

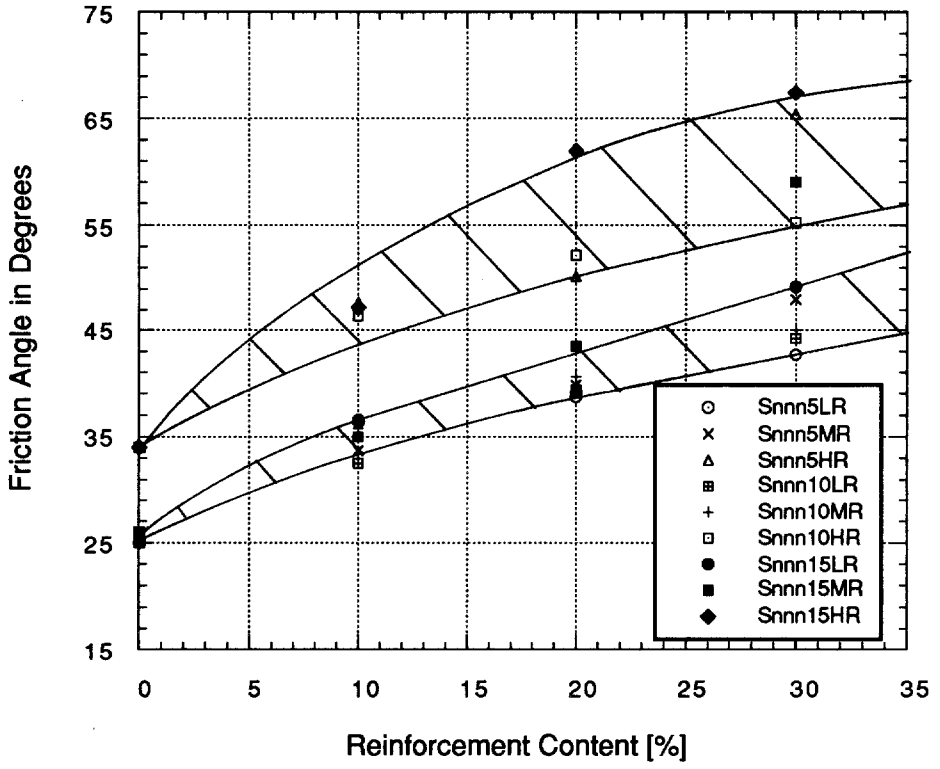

Figure 4.5. Friction Angle vs. Reinforcement Content for all Mixes Tested.

Figure 4.6. From Figure 4.6, it appears that the relationship between reinforcement content and ϕ_1' is approximately linear.

The strength envelopes for the group of mixes having length of reinforcement of 10 cm, high γ_{sm}, and varying reinforcement content are shown in Fig. 4.7. Results from this group of mixes are typical of the results of varying reinforcement content. Increased reinforcement content increased both ϕ_1' and shear strength. The strength envelopes for the other groups of mixes tested are shown in Appendix A1.

4.3.3 Effect of Length of Reinforcement on Initial Friction Angle

A graph of ϕ_1' vs. maximum length of reinforcement is shown in Fig. 4.8. No trend in ϕ_1' with respect to length of reinforcement was observed. Instead, the data are distributed over a broad band (ϕ_1'=34 to 66°) with higher ϕ_1' corresponding to mixes with high γ_{sm} and higher reinforcement contents. As shown in Table 4.11, the range of average values of ϕ_1' is less than experimental error (Section 4.2).

Because volume of reinforcement was controlled in this study, increasing the length of reinforcement had two effects. When the length of reinforcement was increased, the number of reinforcing elements decreased because the volume of reinforcement remained constant. This would result in fewer shreds crossing the shear plane. However, longer reinforcing elements had more free length to become mobilized with the sand. Thus, the longer shreds probably had higher pullout resistance. Possibly, the effect of increasing the length of reinforcement was balanced by the resulting reduction in the number of reinforcing elements crossing the shear plane and thus, no increase in ϕ_1' occurred.

Figures 4.9 and 4.10 are strength envelopes of groups of mixes (i.e. only one parameter of the mix was varied) having the same mixture parameters except for length of reinforcement. Results shown in Fig. 4.9 for the group of mixes with a

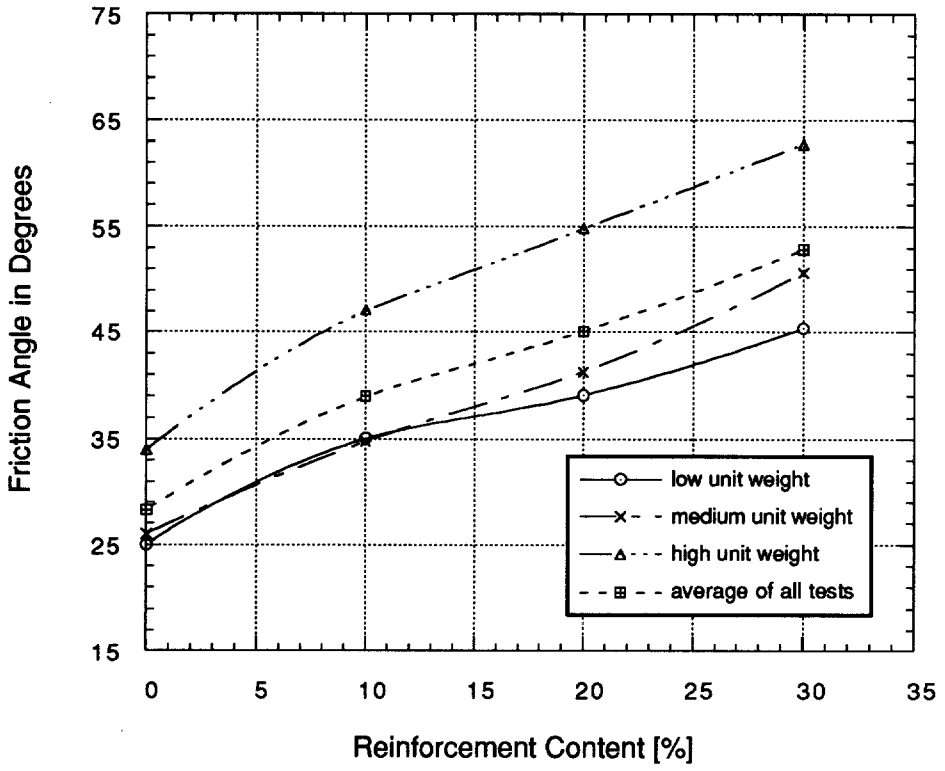

Figure 4.6. Average Friction Angle vs. Reinforcement Content.

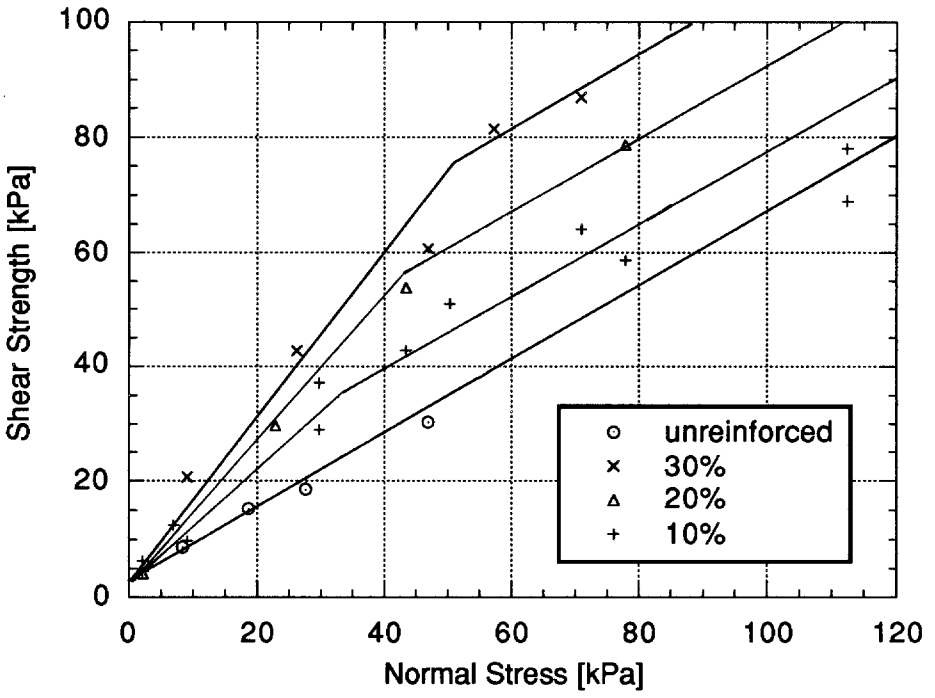

Figure 4.7. Strength Envelope for Mix with Length of Reinforcement=10 cm, High Unit Weight of the Soil Matrix, and Varying Reinforcement Content.

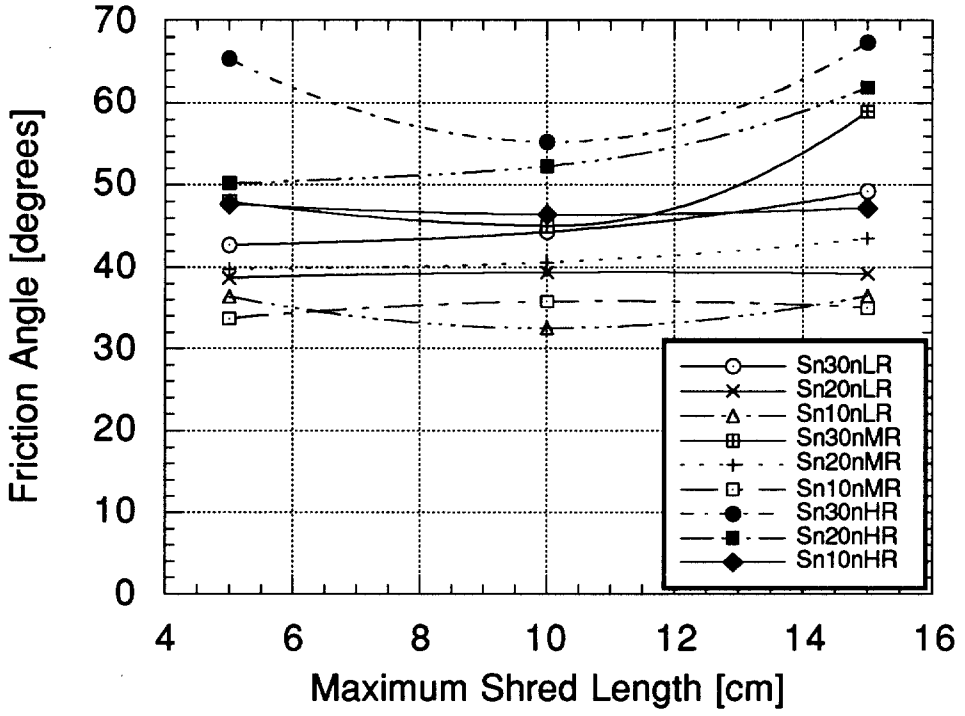

Figure 4.8. Initial Friction Angle vs. Length of Reinforcement.

Table 4.11. Average ϕ_1' for Lengths of Reinforcement Studied.

Maximum Length of Reinforcement [cm]	**Average ϕ_1' [degrees]**
5	48
10	44
15	49
all lengths studied	

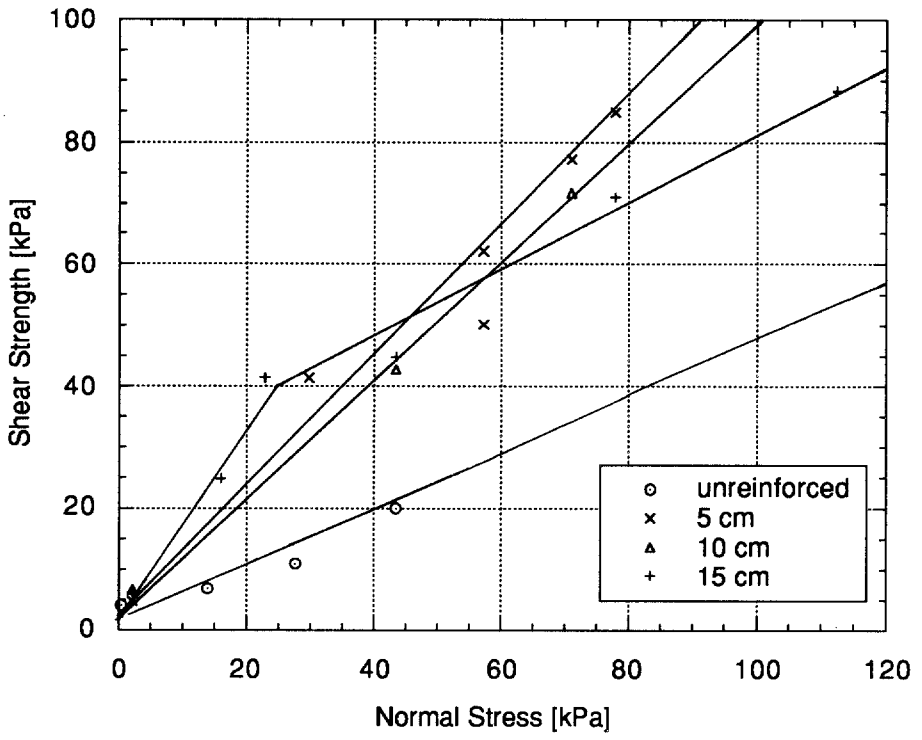

Figure 4.9. Strength Envelope for Mix with Reinforcement Content=30%, Medium Unit Weight of the Soil Matrix, and Varying Reinforcement Length.

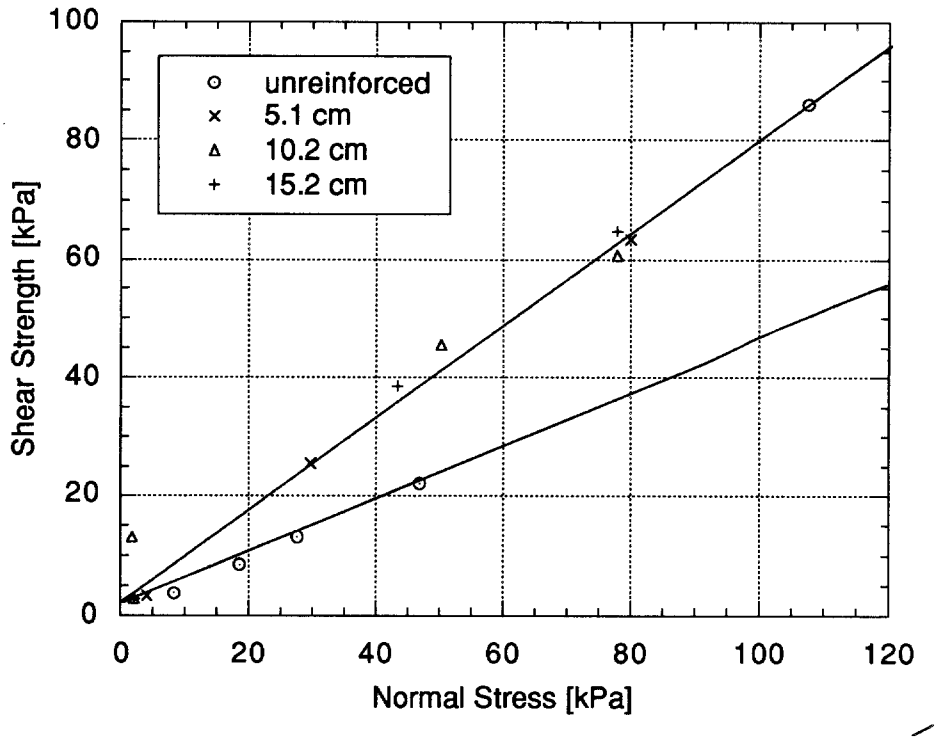

Figure 4.10. Strength Envelope for Mix with Reinforcement Content=20%, Low Unit Weight of the Soil Matrix, and Varying Reinforcement Length.

reinforcement content of 30%, medium γ_{sm}, and varying length of reinforcement indicate that ϕ_1' for the mixture with 15 cm reinforcement is greater than ϕ_1' for the mixture with 5 cm reinforcement. Initial friction angles for both of these mixes is greater than ϕ_1' of the mixture with 10 cm reinforcement. Conversely, results shown in Fig 4.10 for the group of mixes with a reinforcement content of 20%, low γ_{sm}, and varying reinforcement indicate that length of reinforcement had no effect on ϕ_1'. Results from analysis of these two groups, in addition to those shown in Appendix A1, indicate that length of reinforcement has no apparent effect on the strength envelopes.

4.3.4 Effect of Unit Weight of Soil Matrix on Initial Friction Angle

Unit weight of the soil matrix was found to have a significant effect on initial friction angle. The strength envelopes for the group of mixes having a reinforcement content of 30%, length of reinforcement of 15 cm, and varying γ_{sm}, are shown in Fig. 4.11. Results from this group of results, in addition to those shown in Appendix A1, indicate that increasing γ_{sm} increases ϕ_1'.

As shown in Fig. 4.12, the initial friction angle of all mixes increased significantly when the unit weight of soil matrix was increased. The average increase in ϕ_1' resulting from an increase in γ_{sm} from 14.7 kN/m^3 (low γ_{sm}) to 16.8 kN/m^3 (high γ_{sm}) was 15^o. Increases in ϕ_1' resulting from increases in unit weight of soil matrix from 14.7 kN/m^3 (low γ_{sm}) to 15.7 kN/m^3 (medium γ_{sm}) resulted in a much smaller increase in ϕ_1' (2.5^o). Thus, to obtain the maximum benefit from reinforcement using tire shreds, the soil matrix should be made as dense as possible.

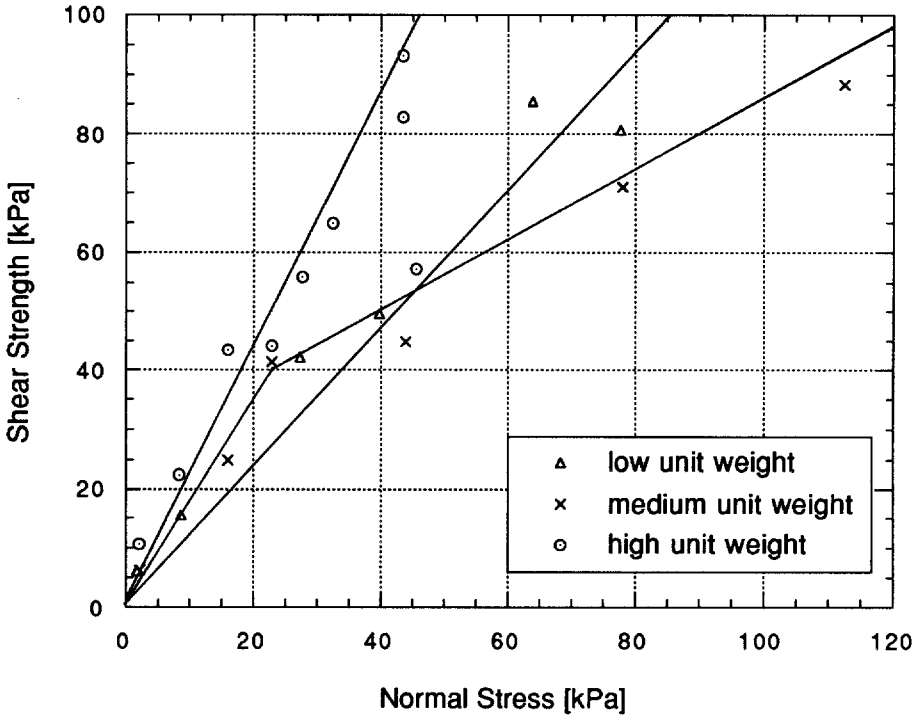

Figure 4.11. Strength Envelope for Mix with Reinforcement Content=30%, Length of Reinforcement=15 cm, and Varying Unit Weight of the Soil Matrix.

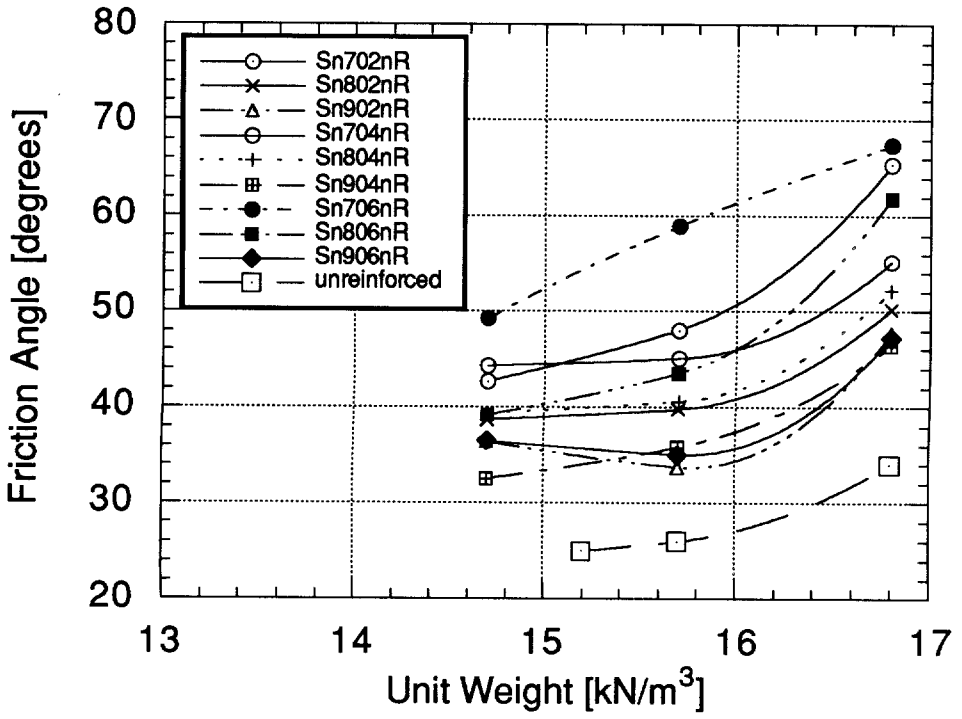

Figure 4.12. Initial Friction Angle vs. Unit Weight of the Soil Matrix.

4.3.5 Importance of ϕ_1' and σ_c'

As shown in Fig. 4.11, critical confining stress is as important as ϕ_1' in determining the shear strength of mixture of sand and shredded waste tires. For example, ϕ_1' for the mixture with medium γ_{sm} is 10° greater than ϕ_1' for mixture with low γ_{sm}. However, at confining stresses greater than 50 kPa, the mixture with low γ_{sm} is stronger than mixture with high γ_{sm}. From this comparison, it is apparent that in practical applications of soil reinforced with shredded waste tires, the operating confining stress would influence mix selection.

4.4 OTHER RESULTS FROM DIRECT SHEAR TESTS

4.4.1 Modulus

Modulus from each test was calculated at 50% of peak stress. Because strain is not determined in a direct shear test, the units of modulus are reported here as stress per unit displacement (kPa/cm).

Four groups of data were analyzed to investigate the effect of reinforcement content on modulus. No trends existed for any of the data analyzed. Additionally, five groups of data were analyzed to investigate the effect of length of reinforcement on modulus. Again, no trends were found.

The effect of unit weight of the soil matrix of reinforced sand on modulus is the same as that for un-reinforced sand. That is, increasing the unit weight increases the modulus. The graph of modulus vs. γ_{sm} for the group of specimens shown in Fig. 4.13 is typical of the responses that were observed.

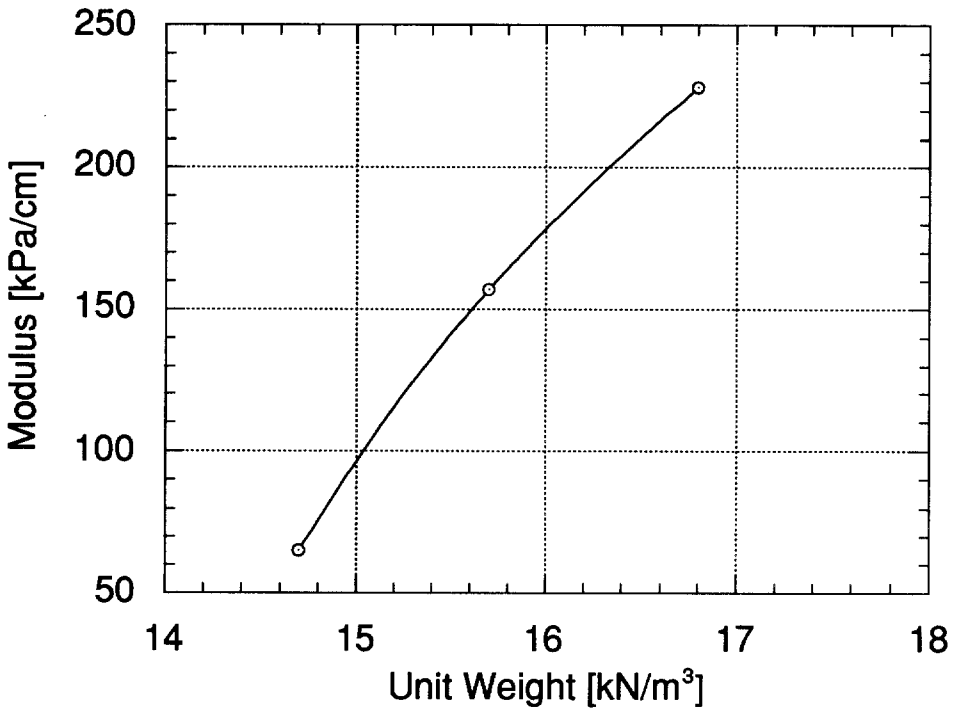

4.13. Modulus vs. Unit Weight for Group of Mixes with Reinforcement Content of 20%, Length of Reinforcement of 5 cm, Randomly Oriented Reinforcement, and Tested at a Confining Stress of 75.9 kPa.

4.4.2 Volume Change

4.4.2.1 *Effect of Reinforcement Content on Volume Change*

For samples that dilated during shear, increasing reinforcement content resulted in increased dilation at the end of the test. Graphs of volumetric strain vs. horizontal displacement for two different mixes are shown in Fig. 4.14. For the group with σ=25.5 kPa, length of reinforcement=5 cm, and unit weight of the soil matrix=16.8 kN/m^3 (Fig. 4.14a), the specimen with reinforcement content=30% dilated 0.01. The specimen with reinforcement content=20% dilated 0.006, and the specimen with reinforcement content equal to 10% dilated 0.004.

Similar results were seen for the group with σ=25.5 kPa, length of reinforcement=15 cm, and unit weight of the soil matrix=16.8 kN/m^3 (Fig. 14b). The specimen with a reinforcement content of 30% dilated 0.01 after being sheared 1.7 cm. If this specimen had been sheared 2.5 cm, it likely would have dilated 0.14 (this test was terminated a displacement equal to 1.7 cm). The specimen with reinforcement content equal to 20% dilated 0.009 and the sample with reinforcement content equal to 10% dilated 0.006.

From these two groups of data, it appears that when γ_{sm} was high, increased reinforcement content increased dilation. This is possibly the result of the shear zone expanding because of increased reinforcement content. This may occur because there is less room for the shredded tires crossing the shear plane to move about when the reinforcement content is increased. As the shredded tires move, they contact other pieces of reinforcement that do not cross the shear plane and force them to move. When shredded tires away from the shear zone move, the sand away from the shear plane must also sheared. Because more sand is active in the shear zone, more dilation occurs during shearing. For samples that compressed during shear (i.e., specimens with low or medium γ_{sm}), there was no clear trend as to

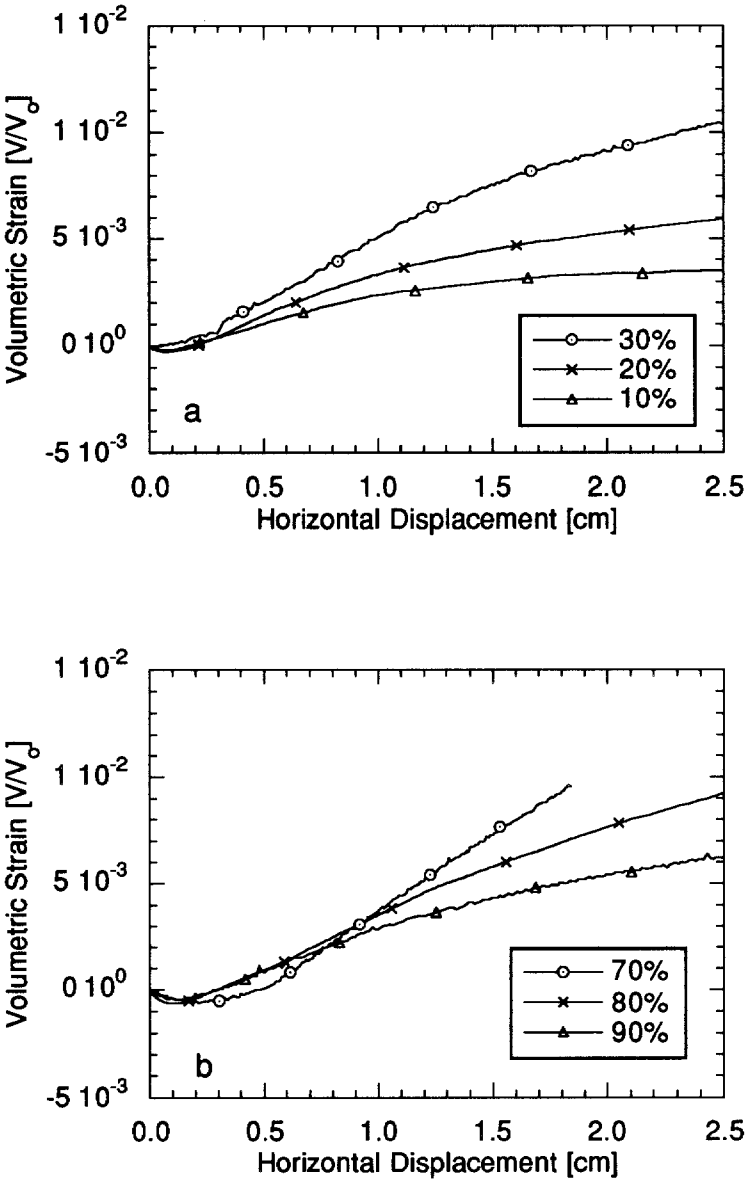

Figure 4.14. (a) Mix Group with σ=25.5 kPa, Length of Reinforcement=5 cm, and Unit Weight of the Soil matrix=16.8 kN/m^3. (b) Mix Group with σ=25.5 kPa, Length of Reinforcement=15 cm, and Unit Weight of the soil Matrix=16.8 kN/m^3.

the effect of reinforcement content on volumetric strain for the two groups of data analyzed.

4.4.2.2 *Effect of Length of Reinforcement on Volume Change*

For specimens that dilated during shear, longer reinforcement resulted in greater dilation at the end of the test. For the group analyzed, σ=75.9 kPa, reinforcement content=20%, and unit weight of the soil matrix=16.8 kN/m^3 (Fig. 4.15). The specimen with length of reinforcement=15 cm dilated 0.0043. The specimen with reinforcement length of 10 cm dilated 0.002, and the specimen with reinforcement length=5 cm dilated 0.0015.

This is possibly the result of the shear zone expanding because longer reinforcement crossing the shear plane may influence a greater volume of sand. Because more sand is active in the shear zone, more dilation occurs during shear. For samples that settled during shear, the effect of the length of reinforcement on settlement was not clear for the 3 groups of mixes analyzed.

4.4.2.3 *Effect of Unit Weight of the Soil Matrix on Volume Change*

The effect of γ_{sm} on volume change at the end of the test for reinforced sand was similar to that for un-reinforced sand. For the 5 groups of data analyzed, samples with high γ_{sm} dilated during shear and samples with low and medium γ_{sm} compressed (Fig. 4.16).

4.5 RESULTS OF DIRECT SHEAR TESTS ON PURE TIRE SHREDS

Strength envelopes were developed for specimens of pure shredded tires (i.e., reinforcement content=100%) and are shown in Figure 4.17. The envelopes

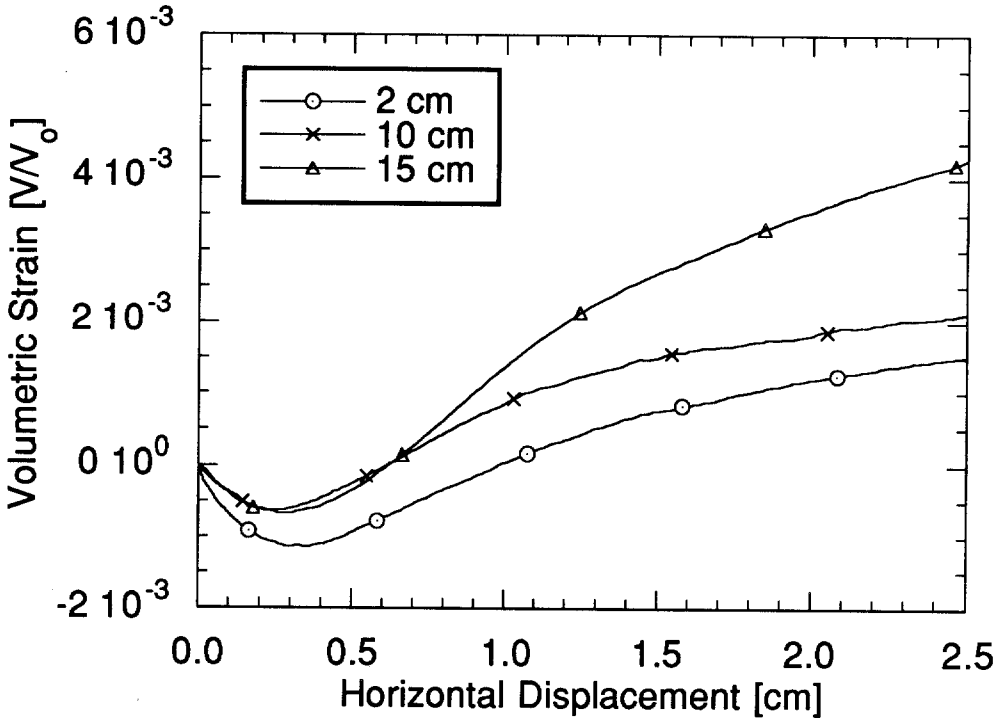

Figure 4.15. Volumetric Strain vs. Displacement for Specimen having σ=75.9 kPa, Reinforcement Content=20%, and Unit Weight of the Soil Matrix=16.8 kN/m^3.

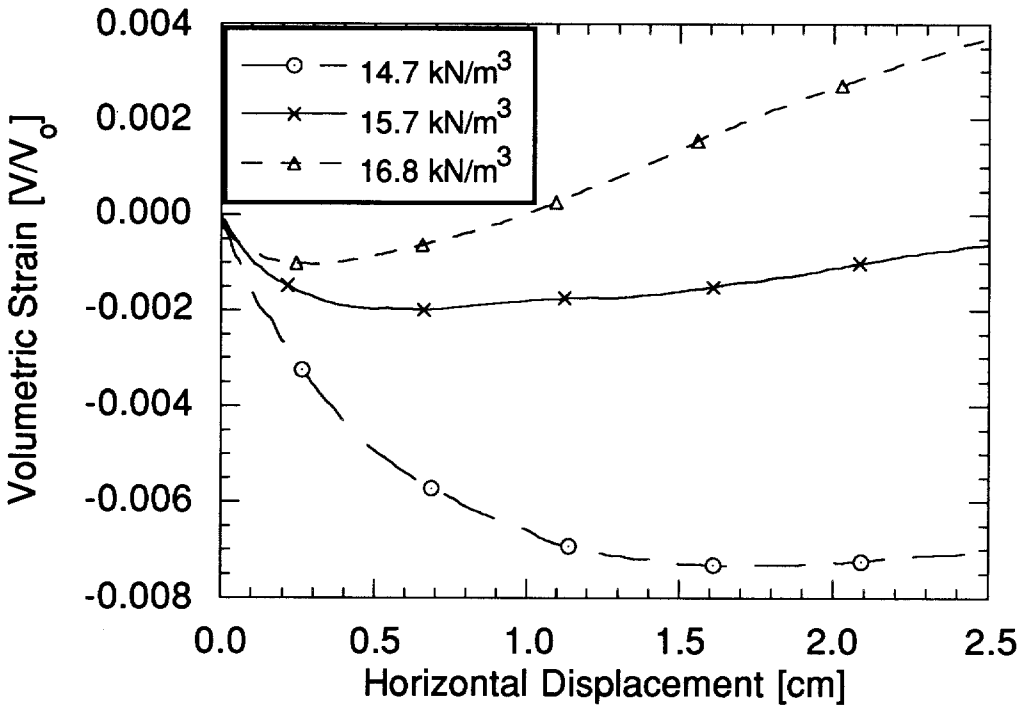

Figure 4.16. Volumetric Strain vs. Displacement for Specimen having σ=41.4 kPa, with Reinforcement Content=30%, and Length of Reinforcement=10 cm.

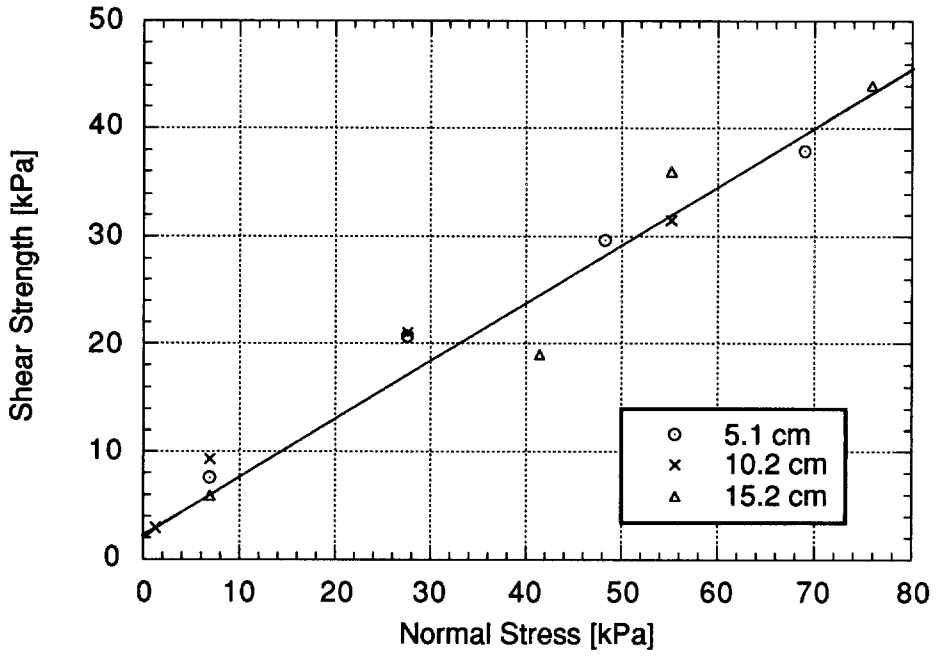

Figure 4.17. Strength Envelope for Pure Shredded Tires.

did not vary when the length of the shredded tires was varied. For the shredded tires used in this study, ϕ_1' was 30°.

A typical shear stress vs. displacement curve for pure shredded tires is shown in Fig. 4.18. All specimens, regardless of length of reinforcement or confining stress, showed similar response. None of the pure shredded tire specimens peaked during shearing. Because of the high compressibility of these specimens, measurement of volumetric strain during shear was not possible.

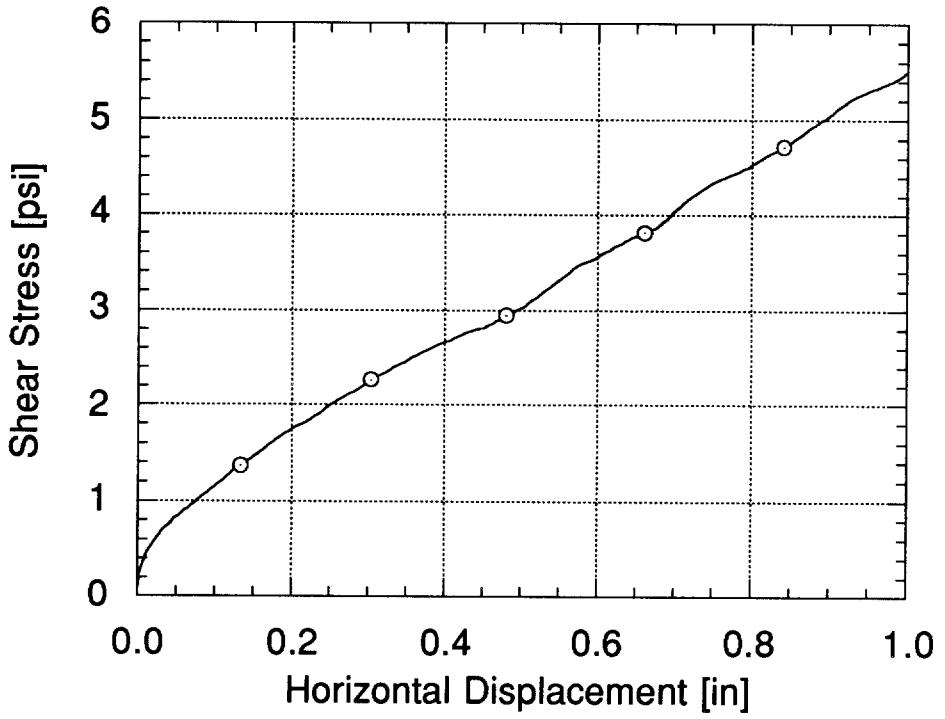

Figure 4.18. Shear Stress vs. Horizontal Displacement for Pure Shredded Tires at Confining Stress=69 kPa.

SECTION 5

COMPARISON OF STRENGTH ENVELOPES OBTAINED BY TESTING AND BY PREDICTION WITH A THEORETICAL MODEL

5.1 ASSUMPTIONS

A theoretical model to predict the static response of sands reinforced with randomly distributed fibers was developed by Maher and Gray (1990). The assumptions of the model are:

(1) The length (L) and diameter (d) of the reinforcing fibers are constant.

(2) The smaller portion (X*) of a fiber that lies on either side of a failure plane is uniformly distributed between zero and half of the length of the fiber.

(3) Reinforcing fibers nave an equal probability of making all possible angles with any fixed axis (i.e., the shear plane in direct shear tests).

(4) The fibers in the soil mass and their points of intersection between the fibers and the failure plane is randomly distributed and following a Poisson process.

(5) Sand-fiber composites have a bi-linear failure envelope.

To meet the requirements of the first assumption it was assumed that the average length of reinforcement in each group (e.g. 5 cm, 10 cm, and 15 cm) could be used to represent the length of the reinforcement in the model. The diameter of the reinforcement in each group was assumed to equal the "diameter" of the shredded tires in each group. Because the shredded tires were rectangular in shape, an "effective diameter" was used that corresponded to a circular cross-section with equal area. This process required judgment by the experimenter and was probably not free of error.

5.2 EQUATIONS

Two basic equations are used to predict the strength envelope of sand reinforced with randomly oriented inclusions. Equation 5.1 is used to calculate the increase in shear strength (ΔS_R) for confining stresses less than the critical confining stress:

$$\Delta S_R = N_s\left(\pi\frac{d^2}{4}\right)(2\sigma_{conf}\tan\delta)(\sin\omega + \cos\omega\tan\phi)(\zeta) \qquad (5.1)$$

where N_s is in Eq. 5.2, d is the diameter of reinforcement, σ_{conf} is the confining stress, δ is the friction angle between the soil and fiber, ω is the angle of shear distortion, ϕ is the angle of internal friction of sand, and ζ is an empirical coefficient that accounts for sand granulometry and fiber properties on ΔS_R. The parameter N_s is:

$$N_S = \frac{2\beta_f}{\pi d^2} \qquad (5.2)$$

where β_f is the reinforcement content by volume. The angle of shear distortion is:

$$\omega = \tan^{-1}\frac{x}{z} \qquad (5.3)$$

where x is the shear distortion and z is the thickness of the shear zone.

Because the thickness of shear zone was unknown, the width of shear zone was assumed to equal the average length of reinforcement. This assumption was made because the minimum width of sand above and below the shear plane that would be influenced by the reinforcement should equal the average length of

reinforcement. The shear distortion was 2.54 (maximum displacement in the direct shear tests).

For confining stresses greater than the critical confining stress (σ_c), the increase in shear strength is (Maher and Gray, 1990):

$$\Delta S_R = N_s\left(\pi\frac{d^2}{4}\right)(2\sigma_c \tan\delta)(\sin\omega + \cos\omega\tan\phi)(\zeta) \qquad (5.4)$$

where the parameters in Eq. 5.4 have the same meaning as those in Eq. 5.1.

5.3 APPLICATION

5.3.1 Calculating ζ

With the exception ζ, all variables in Eqs. 5.1 through 5.4 were known or could be estimated. According to Maher and Gray (1990), ζ is a factor that accounts for the influence of sand granulometry, fiber properties, and also includes the effects of aspect ratio of the fibers. In essence, ζ is a fitting parameter.

To determine ζ for Portage sand reinforced with shredded waste tires, one strength envelope was selected from each group and the measured increase in shear strength was used to back-calculate ζ. A group of strength envelopes consisted of test results from three mixes that had only one parameter of the mix varied. Because ζ is a factor that accounts for characteristics of the sand and reinforcement properties, test results were grouped by reinforcement content.

The strength envelope corresponding to a mix having 20% reinforcement content was used from each group to calculate ζ. Mixes with 20% reinforcement content were used because these mixes represent an "average mix" from each group and it is likely that they yield the most representative value of ζ.

5.3.2 Sample Calculation

The increase in shear strength at critical confining stress was 32.4 kPa for the mix with 20% reinforcement content, length of reinforcement=15 cm, unit weight of soil matrix=16.8 kN/m^3, and randomly oriented reinforcement (Fig. 5.1). The angle of friction at the interface between sand with a unit weight of 16.8 kN/m^3 and a shredded tire was 39^o (see Table 3.3). The average diameter of the 15 cm reinforcement was 2.8 cm. The angle of shear distortion (ω) was 11.5^o. The angle of internal friction of sand with a unit weight of 16.8 kN/m^3 was 34^o.

The value of ζ, 8.6, for the group of mixes having length of reinforcement=15 cm, unit weight of soil matrix=16.8 kN/m^3, and reinforcement oriented randomly was 8.6. Once ζ was known, the increase in shear strength (ΔS_R) at confining stresses less than or equal to critical confining stress could be predicted for mixes having reinforcement contents other than 20%. The shear strength of reinforced sand was the obtained by adding ΔS_R to the shear strength of un-reinforced sand. The predicted shear strength of reinforced sand was used to back calculate ϕ_1 for the mixture.

5.3.3 Comparison

Experimental results and predictions based on the model are listed in Table 5.1. The confining stress listed in Table 5.1 was the stress at which the results were compared. On average, the model predicts tanϕ_1 to be 0.04 higher than the experimentally obtained tan ϕ_1. In many cases, however, the difference in tanϕ_1 was greater than 10%.

Strength envelopes obtained experimentally and by prediction are shown in Fig. 5.2. They represent the best (Fig. 5.2a) and worst (Fig 5.2b) fits with respect to tanϕ_1. Strength envelopes for all of the comparisons listed in Table 5.1 are shown

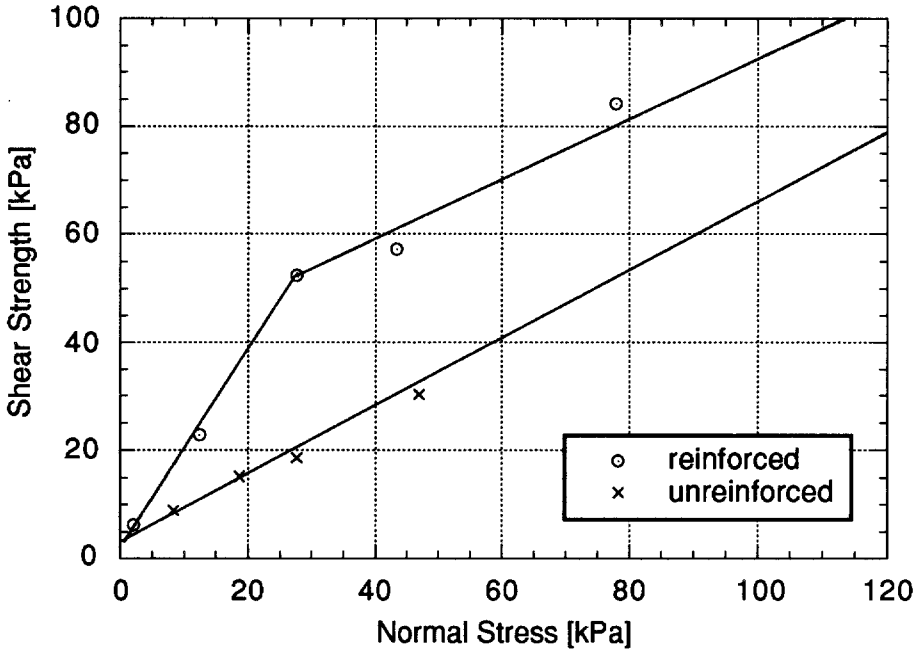

Figure 5.1. Strength Envelope for Mix with Reinforcement Content=20%, Length of Reinforcement=15 cm, and Unit Weight of the Soil Matrix=16.8 kN/m^3.

Table 5.1. Comparison of Experimental Results and Predictions from Model.

Mix #	Confining Stress [kPa]	Experimental ϕ_1 [degrees]	Model ϕ_1 [degrees]	Percent Difference in tan ϕ_1	ζ
Sn305LR	50	43	44	3.6	2.7
Sn105LR	50	36	32	-14	2.7
Sn305MR	50	48	45	10	2.8
Sn105MR	50	34	30	14	2.8
Sn305HR	24	65	56	-31	3.0
Sn105HR	20	48	43	-16	3.0
Sn3010LR	50	44	45	3.5	3.4
Sn1010LR	50	33	33	0.0	3.4
Sn3010MR	50	45	46	3.6	3.5
Sn1010MR	50	36	34	-7.2	3.5
Sn3010HR	53	55	58	12.1	3.9
Sn1010HR	33	46	44	-6.7	3.9
Sn3015LR	50	49	56	2.9	7.8
Sn1015LR	50	37	39	-7.5	7.8
Sn3015MR	24	59	49	-31	5.0
Sn1015MR	50	35	36	3.8	5.0
Sn3015HR	45	67	68	5.1	8.6
Sn1015HR	34	47	52	19.4	8.6

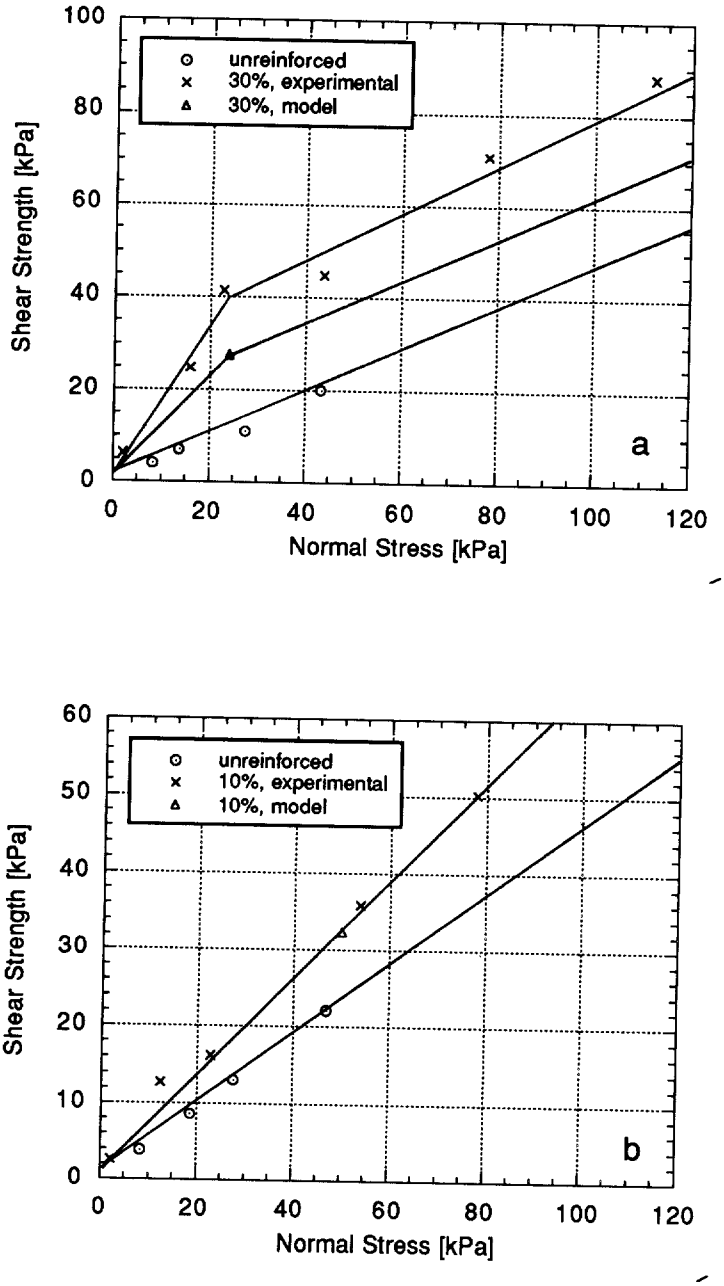

Figure 5.2. (a) Worst Fit (reinforcement content=30%, length of reinforcement=15 cm, and unit weight of the soil matrix=15.7 kN/m^3. (b) Best Fit (reinforcement content=10%, length of reinforcement=10 cm, and unit weight of the soil matrix=14.7 kN/m^3).

in Appendix A2. For the best case there was no difference in ϕ_1 from the experimental results and predicted with the model (Fig. 5.2b). For the mix with the worst fit (Fig 5.2a), the difference in ϕ_1 from experimental results and model prediction was 10º (experimental results and model predictions of $\tan\phi_1$ differed by 31%).

Values of ζ were studied to determine if there were any trends as to the effects of soil matrix unit weight and reinforcement length on ζ. From results presented in Table 5.1, it appears that increasing the unit weight of the soil matrix increases ζ. Over the range of unit weights tested, ζ for length of reinforcement=5 cm increased from 2.7 to 3.0. Results from group of tests with 10 cm reinforcement increased from 3.4 to 3.9 over the range of unit weights tested. Results from the group of tests with 15 cm indicate that ζ increased from 7.8 to 8.6 over the range of unit weights tested. However, for the group with 15 cm reinforcement, ζ for the specimens with medium soil matrix unit weight (15.7 kN/m^3) was lower than ζ for the specimen with low unit weight of the soil matrix (the worst fit between experimental results and predictions with the model also occurred with this specimen).

From the results presented in Table 5.1, it appears that increasing the length of reinforcement increased ζ. The average value of ζ for length of reinforcement=5 cm was 2.8 and for length of reinforcement=10 cm, the average value of ζ was 3.6. The average value of ζ for length of reinforcement=15 cm was 7.1.

5.4 ANALYSIS

The applicability of the model by Maher and Gray (1990) for predicting the strength of sand reinforced with shredded waste tires is limited. The greatest limiting factor is determination of the empirical coefficient ζ. To use the model, a

strength envelope of the mixture of sand and shredded waste tires has to be developed to determine the critical confining stress and back-calculate ζ.

It appears that for sand reinforced with shredded waste tires, the model by Maher and Gray (1990) can be used to approximately predict strength envelopes for mixes with different reinforcement contents based on results of direct shear tests performed at a single reinforcement content. Predictions of this sort would be useful in design. However, once a mix is selected additional tests should be conducted to verify that the strength predicted from the model can be realized.

SECTION 6
SUMMARY AND CONCLUSIONS

The feasibility of reinforcing soil with shredded waste tires was investigated in this study. Shredded waste tires were mixed with Portage sand and tested in a direct shear machine. The influence of four factors (reinforcement content, length of reinforcement, unit weight of the soil matrix, and orientation of reinforcement) were studied. The tests showed that reinforcing sand with shredded waste tires improves it shear strength. The following conclusions were made based on the test results:

1. Addition of shredded waste tires to Portage sand increased its shear strength by as much as much as 3.5 times over un-reinforced sand. The largest increase occurred for a mixture of sand and shredded waste tires having a reinforcement content of 30% (by volume), length of reinforcement of 15 cm, and unit weight of the soil matrix of 1 6.8 kN/m^3. This mixture had an initial friction angle of 67^o and a critical confining stress greater than 45 kPa. The angle of internal friction for un-reinforced Portage sand (at the same unit weight) was 34^o .

2. Initial friction angle was found to increase with increased reinforcement content. The relationship between initial friction angle and reinforcement content was approximately linear. However, the increase in friction angle occurred only at stresses less than the critical confining stress.

3. No clear trend was found for the effect of increasing reinforcement content on critical confining stress. The average critical confining stress for the mixtures tested was 34 kPa.

4. Length of reinforcement was not found to be a significant factor affecting values of the initial friction angle.

5. Unit weight of the soil matrix was found to be an important parameter affecting the initial friction angle of reinforced soil. Mixtures with a unit weight of the soil matrix of 16.8 kN/m^3 had an initial friction angle that was 15^o higher (on average) than the friction angle for reinforced specimens having a unit weight of the soil matrix of 15.7 kN/m^3. It was also found that increasing the unit weight of the soil matrix increased the modulus of the reinforced soil.

5. Increased reinforcement content was found to increase dilation of reinforced soil having a unit weight of the soil matrix of 16.8 kN/m^3. Increasing the length of reinforcement was also found to increase dilation when the unit weight of soil matrix was 16.8 kN/m^3. This is possibly the result of expansion of the shear zone.

6. Results of tests performed on pure shredded tires indicate that there is no difference in friction angle between different lengths of shredded tires. The friction angle for pure shredded tires was 30^o.

7. A theoretical model to predict the strength of sand reinforced with randomly distributed fibers was used. Experimental results and predictions from the model were compared. On average, the experimental results and predictions of the model for $\tan\phi'$ were within 0.5%. However, in many cases, the difference in $\tan\phi'$ was more than 10%.

The results of this study suggest that shredded waste tires my be useful as soil reinforcement in highway fills, leachate collection systems on steep slopes, and other applications where strong and lightweight fill would be useful. Further study is needed, however, to: (1) determine economic aspects of using shredded waste tires as soil reinforcement, (2) determine the effectiveness shredded waste tires as reinforcement in cohesive and fine grained soils, and (3) determine if results obtained in the laboratory are representative of what can be achieved in field applications.

REFERENCES

Andersland, O. B., and Khattak, A. S. (1979). "Shear Strength of Kaolinite/Fiber Soil Mixtures." Proceedings of the International Conference on Soil Reinforcement. Vol. 1, Paris, pp. 11-16.

Arenicz, R.M., and Chowdhury, R. N. (1988). "Laboratory Investigation of Earth Walls Simultaneously Reinforced by Strips and Random Reinforcement." Geotechnical Testing Journal. ASTM, Vol. 11, No. 4, December, pp. 241-247.

Bader, C. D. (1992). "Where Will All the Tires Go?." Municipal Solid Waste Management. Vol. 2, No. 7, pp. 26-34.

Benson, C. H., and Khire, M. V. (1992). "Soil Reinforcement with Strips of Reclaimed HDPE." Journal of Geotechnical Engineering, ASCE, in press.

Bosscher, P. J., Edil, T. B., and Eldin, N. (1992). "Construction and Performance of a Shredded Waste Tire Test Embankment." Transportation Research Record, No. 1345, pp. 44-52.

Edil, T. B, and Bosscher, P. J. (1992). "Development of Engineering Criteria for Shredded Waste Tires in Highway Applications." Final Report, Wisconsin Department of Transportation. Research-Report GT-92-9.

Eldin and Senouci (1992). "Use of Scrap Tires in Road Construction." Journal of Construction Engineering, Vol. 118, No. 3, pp. 561-576.

Fletcher, C. S., and Humphrey, W. K. (1991), "California Bearing Ratio Improvement of Remolded Soils by the Addition of Polypropylene Fiber Reinforcement." Proceedings of the 70th Annual Meeting of the Transportation Research Board. Washington, D.C., January.

Freitag, D. R. (1986). "Soil Randomly Reinforced with Fibers." Journal of Geotechnical Engineering, ASCE, Vol. 112, No. 8, August, pp. 823-826.

Gray, D. H., and Ohashi, H. (1983), "Mechanics of Fiber Reinforcement in Sand." Journal of Geotechnical Engineering, ASCE, Vol 109, No. 3, pp. 335-353.

Gray, D. H., and Lieser (1982). "Biotechnical Slope Protection." Prentice-Hall, NJ.

Gray, D. H., and Maher, M. H. (1989). "Admixture Stabilization of Sands with Random Fibers." Proceedings of the 12th International Conference on Soil Mechanics and Foundation Engineering. Vol. 2, pp. 1363-1366. Rio De Janeiro.

Gray, D. H., and Al-Refeai, T. (1986). "Behavior of Fabric-versus Fiber-Reinforced Sand." Journal of Geotechnical Engineering, ASCE, Vol. 112, No. 8, August, pp. 804-820.

Hall, T. J. (1991), "Reuse of Shredded Tire Material for Leachagte Collection Systems." Proceedings of the 14th Annual Madison Waste Conference. Madison, WI.

Hoare, D. J. (1979). "Laboratory Study of Granular Soils Reinforced with Randomly Oriented Discrete Fibers." Proceedings of the International Conference on Soil Reinforcement, Vol. 1, Paris, pp. 47-52.

Humphrey, D. N., and Manion, S. M. (1992). Properties of Tire Chips for Lightweight Fill." Proceedings of the Conference on Grouting, Soil Improvement and Geosynthetics, ASCE Special Publication No. 30, Vol. 2, pp. 1344-1355. New Orleans, LA.

Ahmed, Imtiaz (1991). "Use of Waste Materials in Highway Construction." Indiana Department of Transportation, Project No. C-36-50K.

Joiner Associates Inc. (1986). "Jass," software. Madison, WI

Jewell, R. A. and Wroth, C. P. (1987), "Direct Shear Tests on Reinforced Sand," Geotechnique, 37, No. 1, pp. 53-68.

Koerner, Robert M. (1990). "Designing with Geosynthetics." Prentice-Hall Inc. New Jersey.

Lawton E. C., Khire, M. V., and Fox, N. S. (1992), "Reinforcement of Soils By Multi-Oriented Geosynthetic Inclusions." Journal of Geotechnical Engineering, ASCE Vol 119, No. 2, February, pp. 257-274.

Lee, K. L., Adams, B. D., and Vagneron, J. M. (1973). "Reinforced Earth Retaining Walls." Journal of Soil Mechanics and Foundation Division, ASCE, Vol. 99, No. 10, pp. 745-.764

Maher, M. H. and Gray, D. H. (1989). "Static Response of Sands Reinforced with Randomly Distributed Fibers." Jounal of Geotechnical Engineering, ASCE, Vol 116, No. 11, pp 1661-1677.

Maher, M. H., and Woods, R. D. (1990), "Dynamic Response of Sand Reinforced with Randomly Distributed Fibers." Journal of Geotechnical Engineering. ASCE, Vol. 116, No. 7, pp. 1116-1131.

McGown, A., et al. (1985). "Soil Strengthening Using Randomly Distributed Mesh Elements." Proceedings of the 11th International Converence on Soil Mechanics and Foundation Engineering, Vol 5, San Francisco, pp. 1735-1738.

McGown, A., et al. (1978). "Effect of Inclusion Properties on the Behavior of Sand," Geotechnique, Vol. 28, No. 3, pp. 327-346.

Minnesota Pollution Control Agency (1992). "Waste Tires in Subgrade Road Beds," a report on the Environmental Study of the Use of Shredded Waste Tires for roadway Subgrade Support. Waste Tire Management Unit, Minnesota Pollution Control Agency. St. Paul, MN

Noorany, I., and Uzdavines, M. (1989), "Dynamic Behavior of Saturated Sand Reinforced with Geosynthetic Fibers." Proceedings of Geosynthetics '89, San Diego, Vol. 2, pp. 385-396.

Park, J. K., Kim J. Y., and Edil, T. B. (1993). "Removal of Organic Compounds in Landfills by Shredded Scrap Vehicle Tires." Green 93, an Internation Symposium on Geotechnics Related to the Environment. Bolton, UK.

Saran, S., Talwar, D., and Vaish, U. (1978). "Some Aspects of Engineering Behaviour of Reinforced Earth." Proceedings of the Symposium on Soil Reinforcing and Stabilizing Techniques, NSWIT/NSW University, pp. 40-49.

Shewbridge, S. E. and Sitar, N. (1989). "Deformation Characteristics of Reinforced Sand in Direct Shear." Journal of Geotechnical Engineering, ASCE, Vol. 115, No. 8, pp. 1134-1147.

Verma, B. P. and Char, A. N. R. (1978). "Triaxial Tests on Reinforced Sand." Proceedings of the Symposium on Soil Reinforcing and Stabilizing Techniques, NSWIT/NSW University, pp. 29-39.

Validyne Engineering Corp. "Easy Sense" software. Northridge, CA 91324.

Vidal (1969). The Principle of Reinforced Earth. Highway Research Record, No. 282

APPENDIX A

SUPPLEMENTAL RESULTS

SECTION A1

STRENGTH ENVELOPES FOR SPECIMENS TESTED

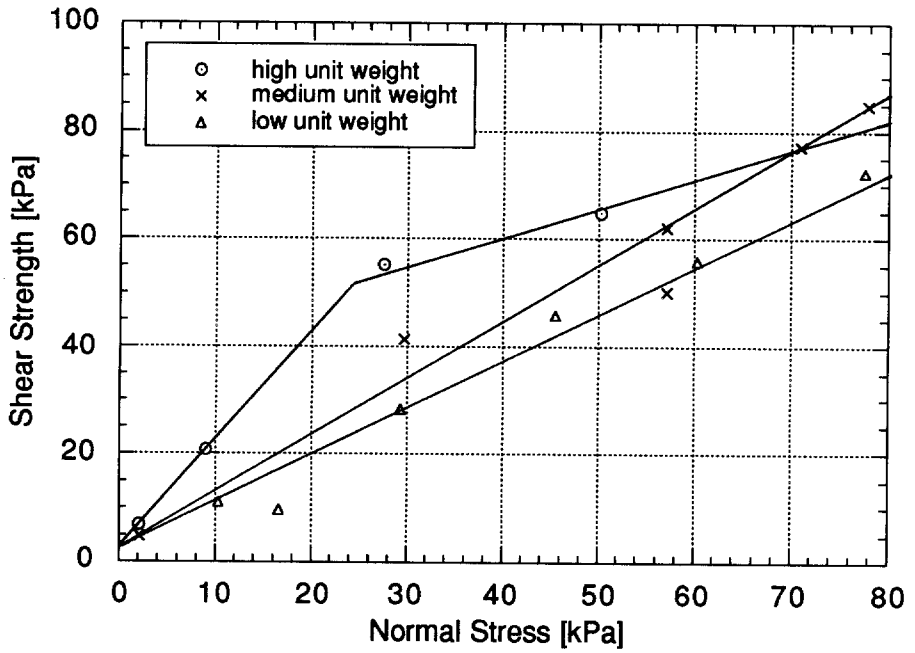

Figure A1.1. Failure Envelope for the Group of Mixes having Reinforcement Content=30%, Length of Reinforcement=5 cm, Randomly Oriented Reinforcement, and Variable Unit Weight of the Soil Matrix.

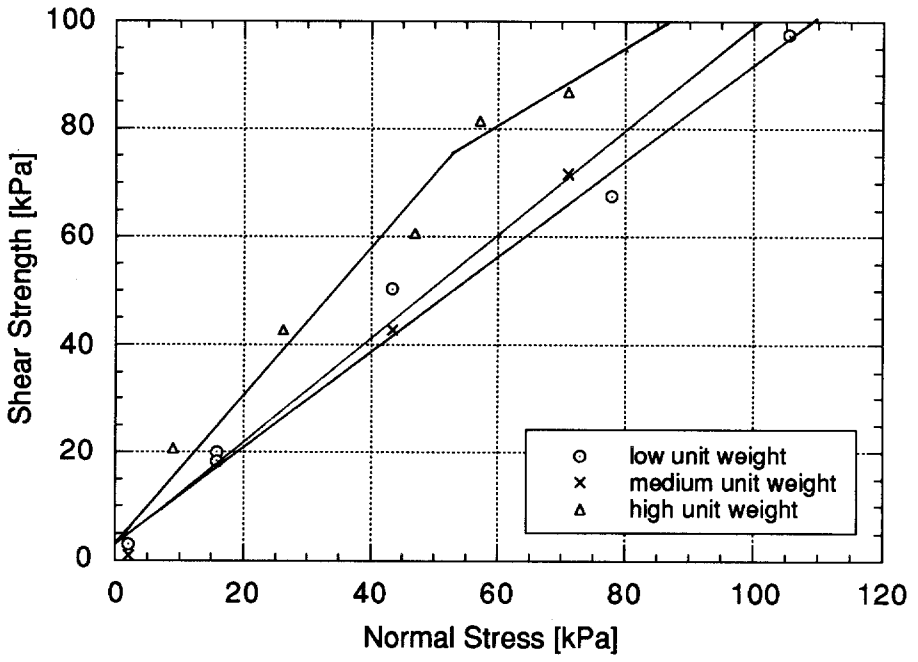

Figure A1.2. Failure Envelope for the Group of Mixes having Reinforcement Content=30%, Length of Reinforcement=10 cm, Randomly Oriented Reinforcement, and Variable Unit Weight of the Soil Matrix.

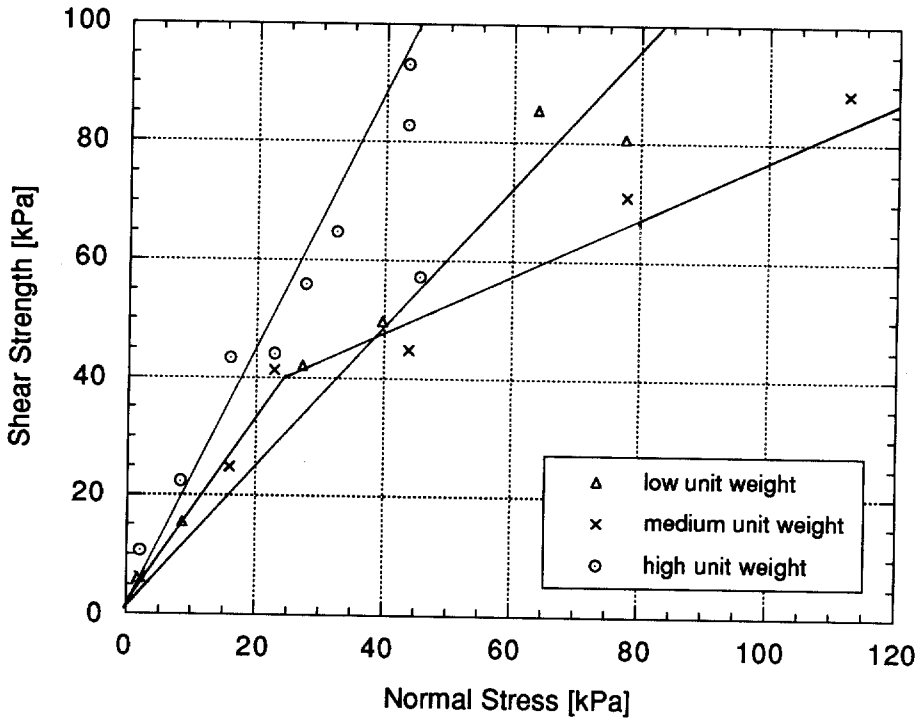

Figure A1.3. Failure Envelope for the Group of Mixes having Reinforcement Content=30%, Length of Reinforcement=15 cm, Randomly Oriented Reinforcement, and Variable Unit Weight of the Soil Matrix.

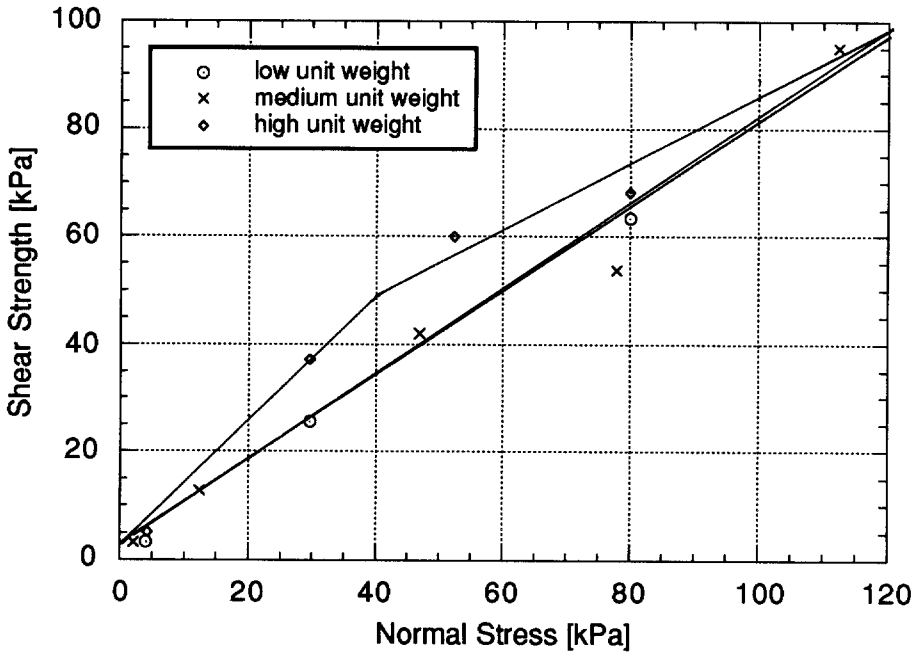

Figure A1.4. Failure Envelope for the Group of Mixes having Reinforcement Content=20%, Length of Reinforcement=5 cm, Randomly Oriented Reinforcement, and Variable Unit Weight of the Soil Matrix.

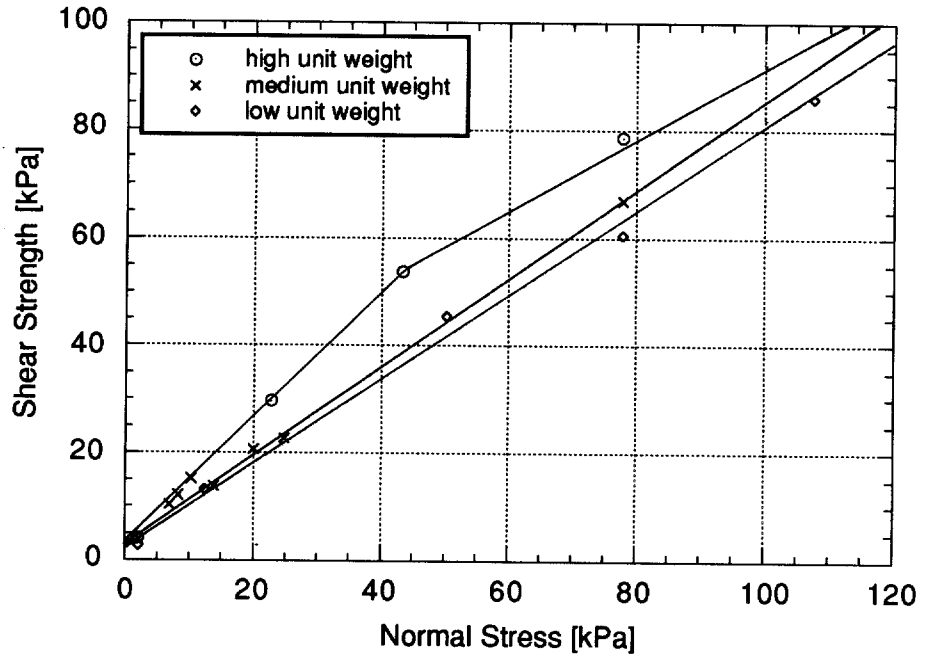

Figure A1.5. Failure Envelope for the Group of Mixes having Reinforcement Content=20%, Length of Reinforcement=10 cm, Randomly Oriented Reinforcement, and Variable Unit Weight of the Soil Matrix.

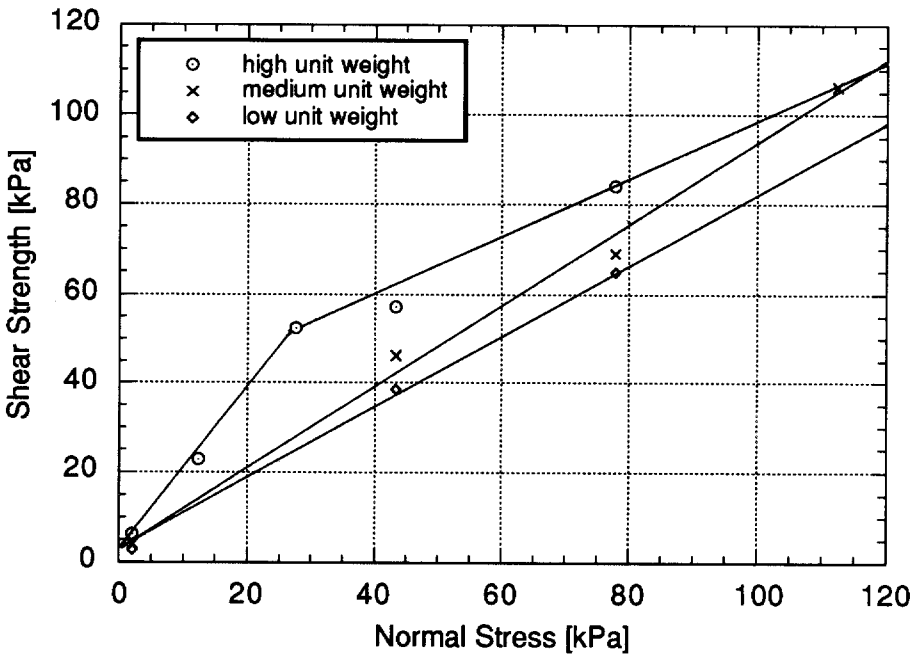

Figure A1.6. Failure Envelope for the Group of Mixes having Reinforcement Content=20%, Length of Reinforcement=15 cm, Randomly Oriented Reinforcement, and Variable Unit Weight of the Soil Matrix.

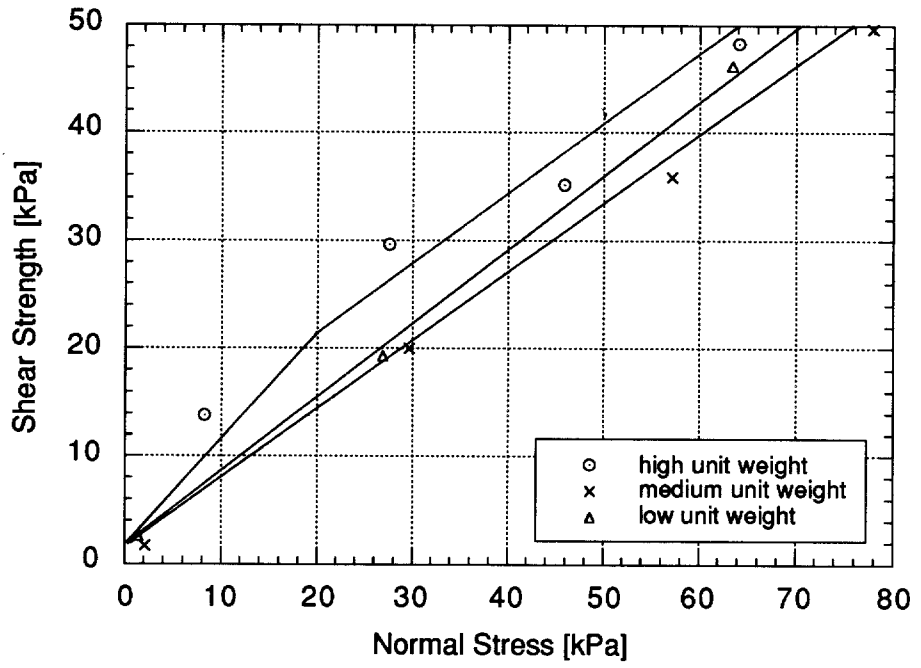

Figure A1.7. Failure Envelope for the Group of Mixes having Reinforcement Content=10%, Length of Reinforcement=5 cm, Randomly Oriented Reinforcement, and Variable Unit Weight of the Soil Matrix.

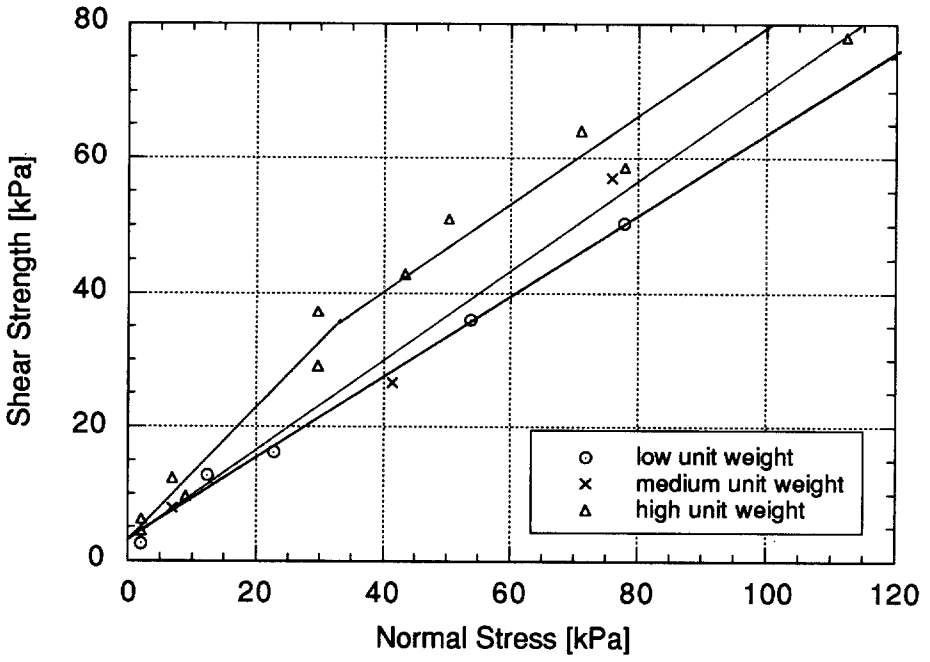

Figure A1.8. Failure Envelope for the Group of Mixes having Reinforcement Content=10%, Length of Reinforcement=10 cm, Randomly Oriented Reinforcement, and Variable Unit Weight of the Soil Matrix.

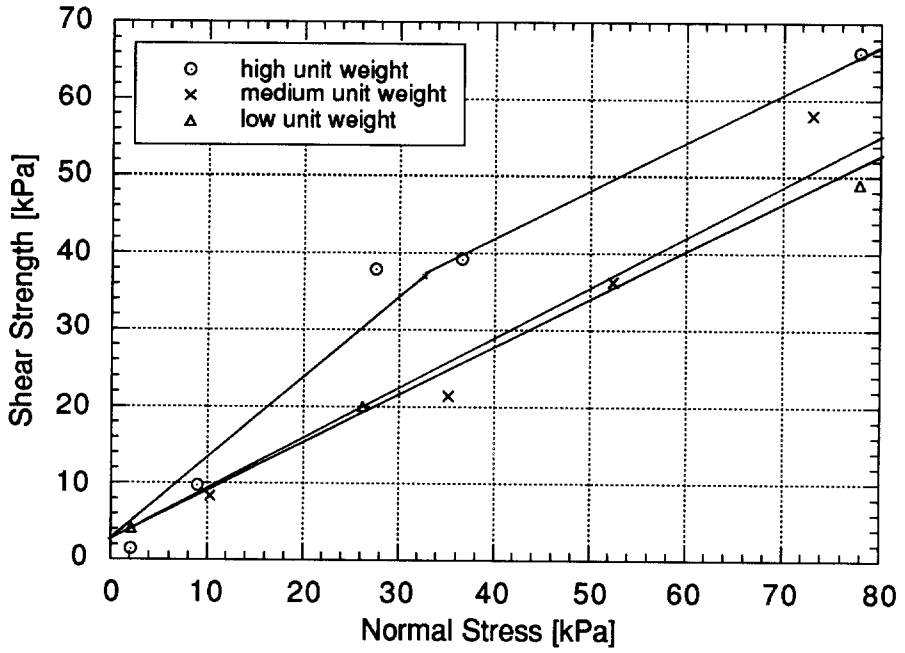

Figure A1.9. Failure Envelope for the Group of Mixes having Reinforcement Content=10%, Length of Reinforcement=15 cm, Randomly Oriented Reinforcement, and Variable Unit Weight of the Soil Matrix.

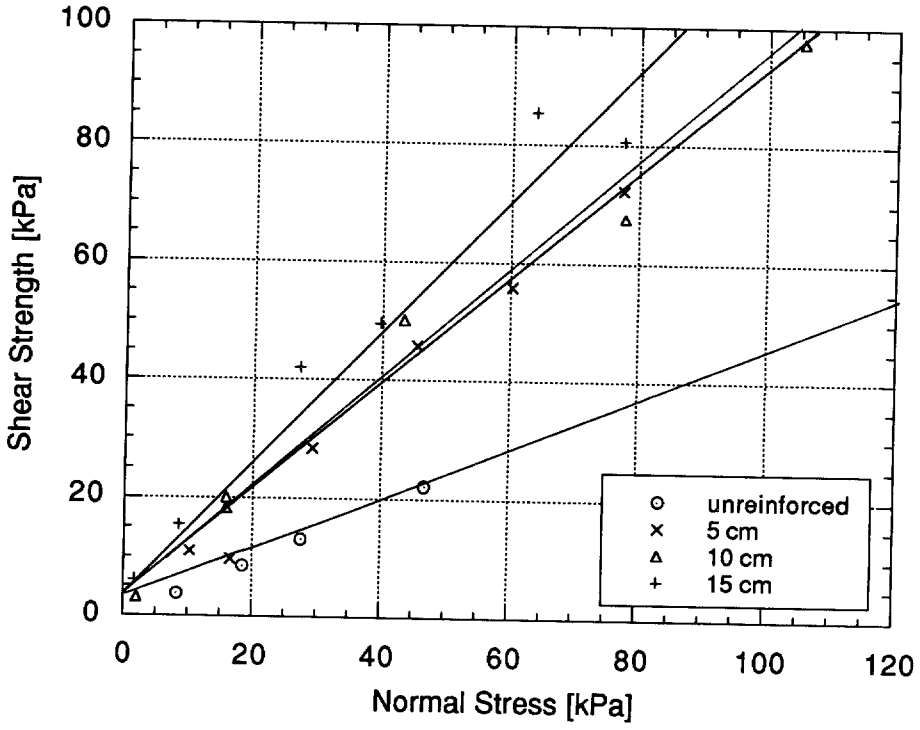

Figure A1.10. Failure Envelope for the Group of Mixes having Reinforcement Content=30%, Unit Weight of the Soil Matrix=14.7 kN/m^3, Randomly Oriented Reinforcement, and Variable Length of Reinforcement.

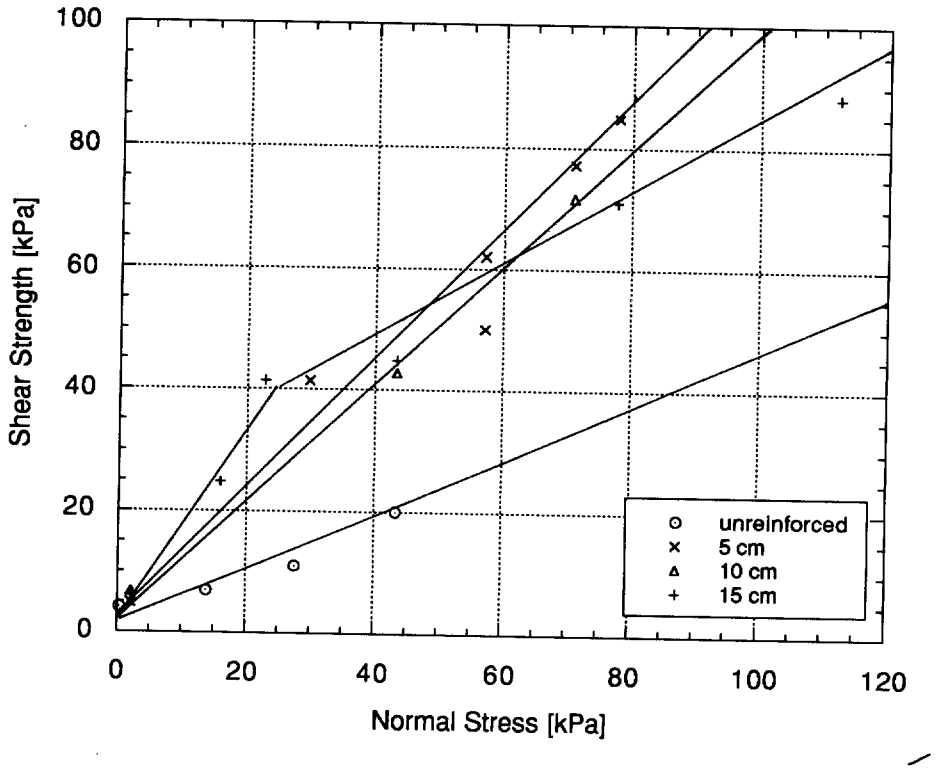

Figure A1.11. Failure Envelope for the Group of Mixes having Reinforcement Content=30%, Unit Weight of the Soil Matrix=15.7 kN/m^3, Randomly Oriented Reinforcement, and Variable Length of Reinforcement.

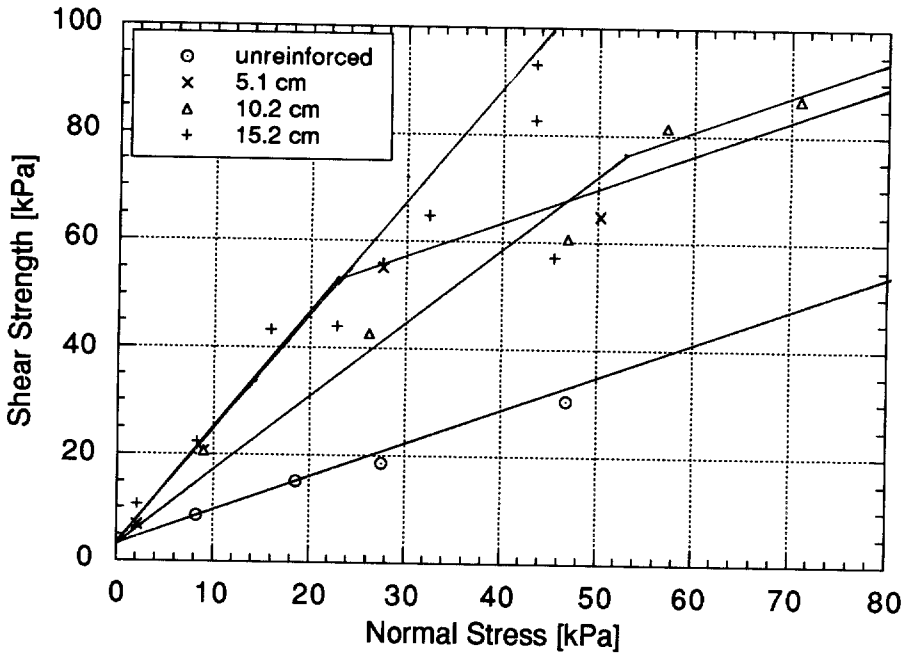

Figure A1.12. Failure Envelope for the Group of Mixes having Reinforcement Content=30%, Unit Weight of the Soil Matrix=16.8 kN/m^3, Randomly Oriented Reinforcement, and Variable Length of Reinforcement.

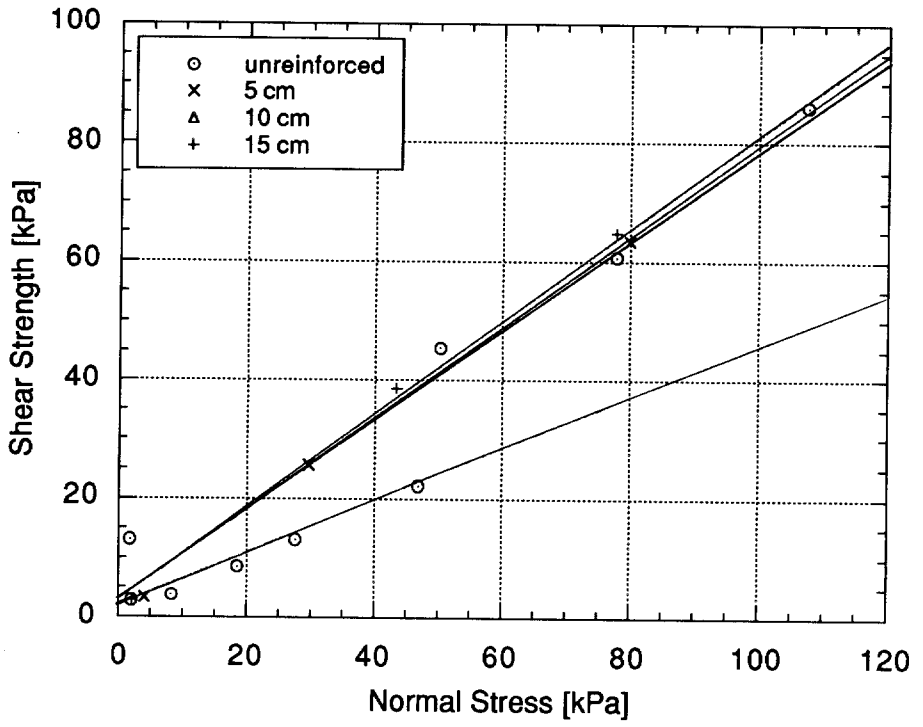

Figure A1.13. Failure Envelope for the Group of Mixes having Reinforcement Content=20%, Unit Weight of the Soil Matrix=14.7 kN/m^3, Randomly Oriented Reinforcement, and Variable Length of Reinforcement.

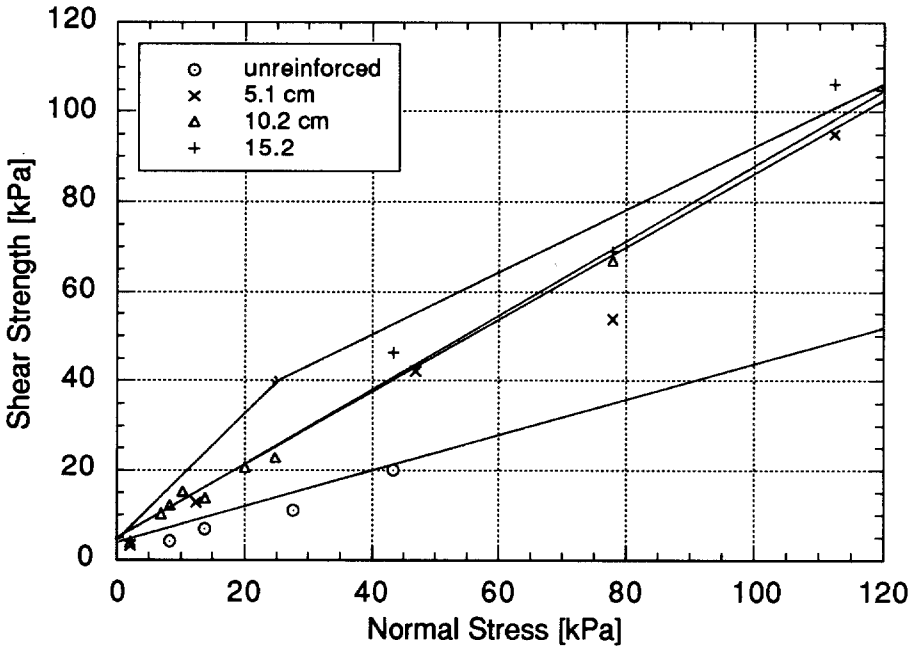

Figure A1.14. Failure Envelope for the Group of Mixes having Reinforcement Content=20%, Unit Weight of the Soil Matrix=15.7 kN/m^3, Randomly Oriented Reinforcement, and Variable Length of Reinforcement.

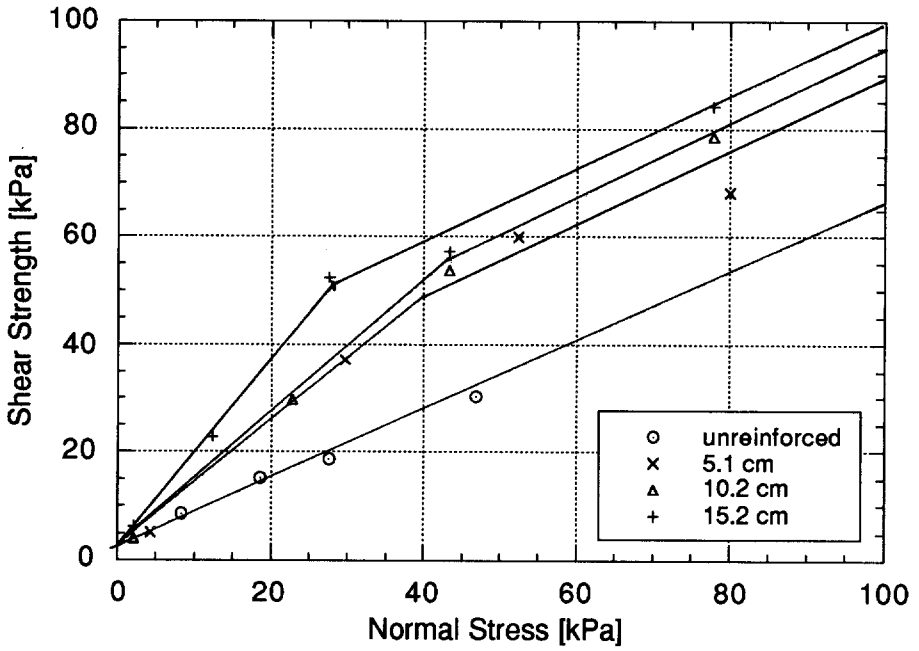

Figure A1.15. Failure Envelope for the Group of Mixes having Reinforcement Content=20%, Unit Weight of the Soil Matrix=16.8 kN/m^3, Randomly Oriented Reinforcement, and Variable Length of Reinforcement.

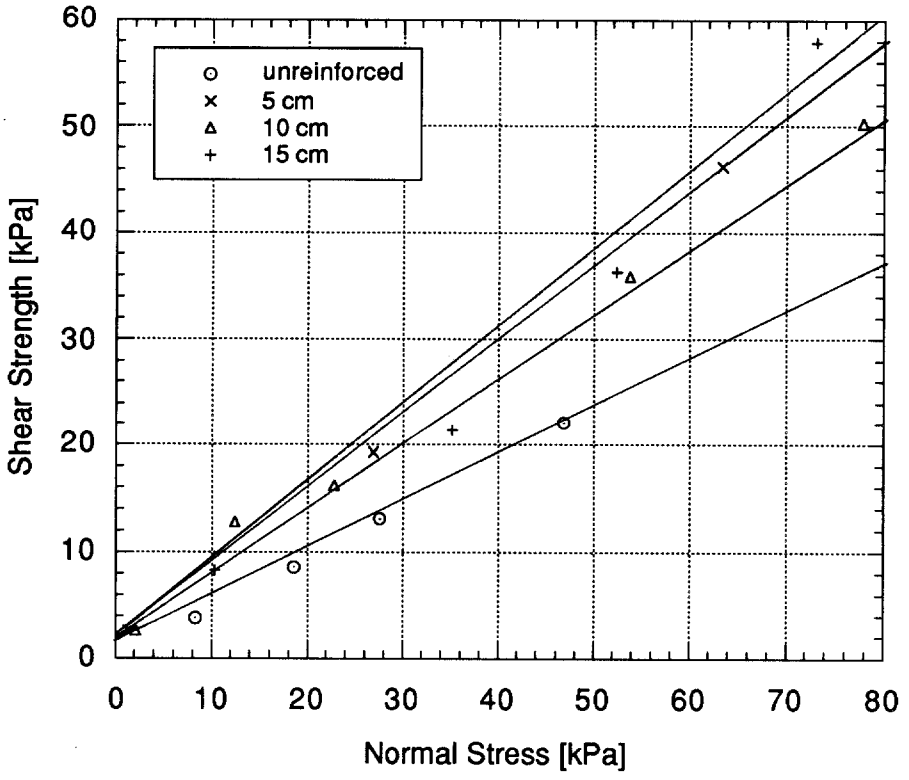

Figure A1.16. Failure Envelope for the Group of Mixes having Reinforcement Content=10%, Unit Weight of the Soil Matrix=14.7 kN/m^3, Randomly Oriented Reinforcement, and Variable Length of Reinforcement.

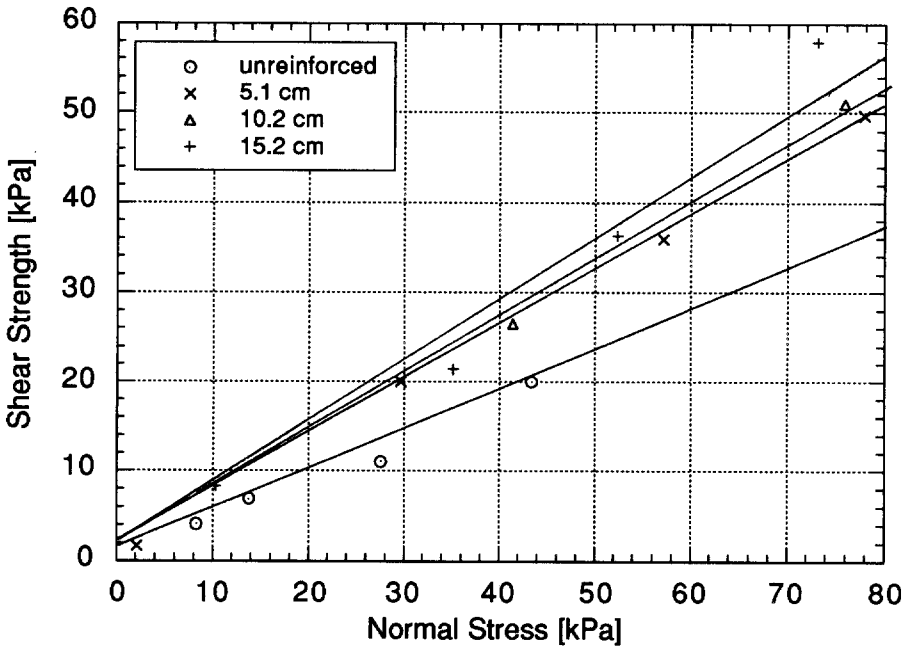

Figure A1.17. Failure Envelope for the Group of Mixes having Reinforcement Content=10%, Unit Weight of the Soil Matrix=15.7 kN/m^3, Randomly Oriented Reinforcement, and Variable Length of Reinforcement.

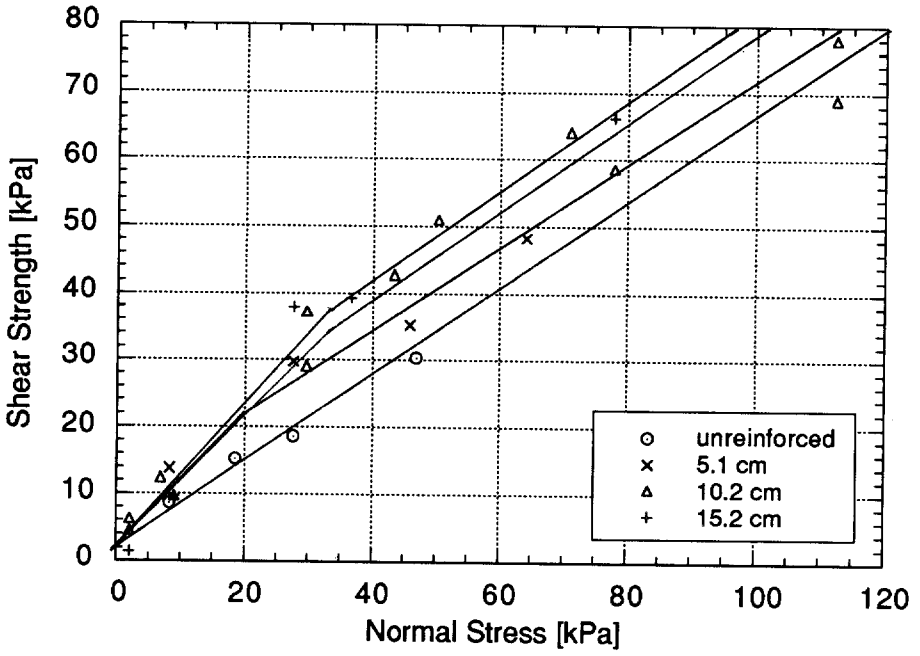

Figure A1.18. Failure Envelope for the Group of Mixes having Reinforcement Content=10%, Unit Weight of the Soil Matrix=16.8 kN/m^3, Randomly Oriented Reinforcement, and Variable Length of Reinforcement.

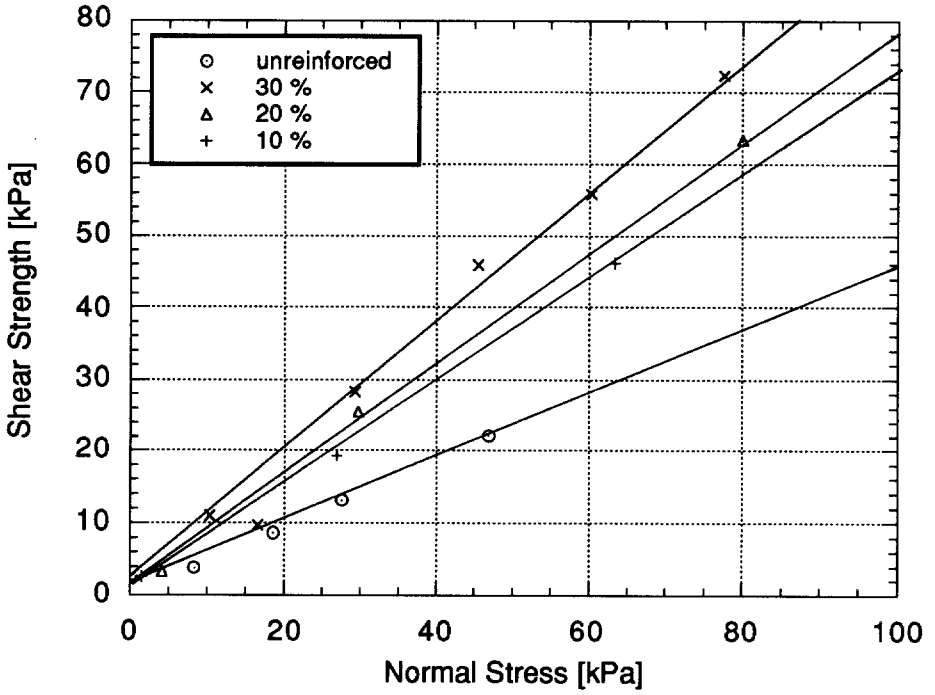

Figure A1.19. Failure Envelope for the Group of Mixes having Length of Reinforcement=5 cm, Unit Weight of the Soil Matrix=14.7 kN/m^3, Randomly Oriented Reinforcement, and Variable Reinforcement Content.

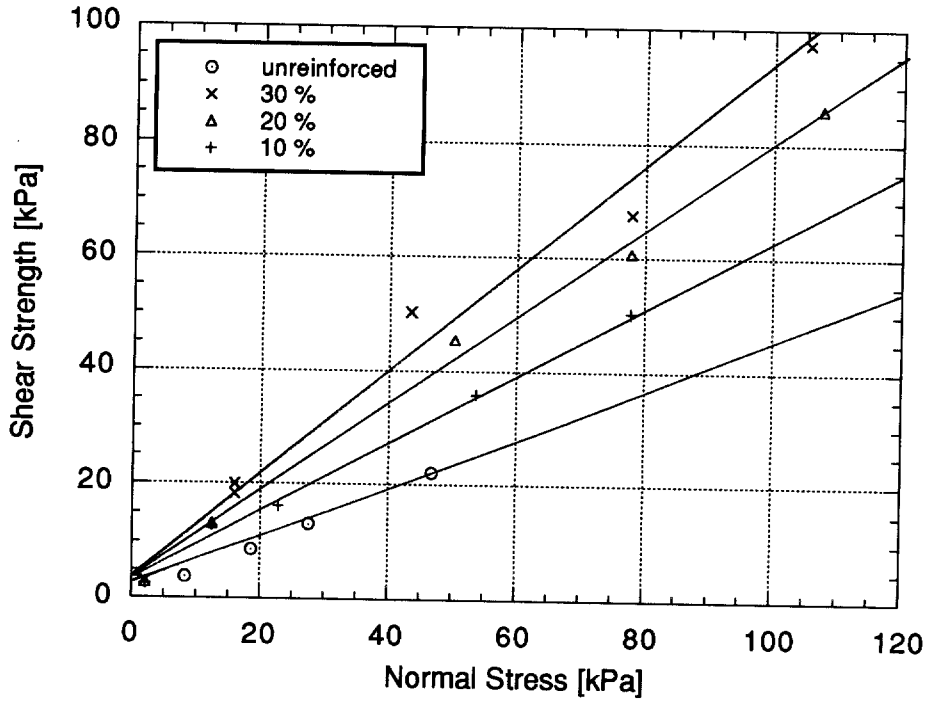

Figure A1.20. Failure Envelope for the Group of Mixes having Length of Reinforcement=10 cm, Unit Weight of the Soil Matrix=14.7 kN/m^3, Randomly Oriented Reinforcement, and Variable Reinforcement Content.

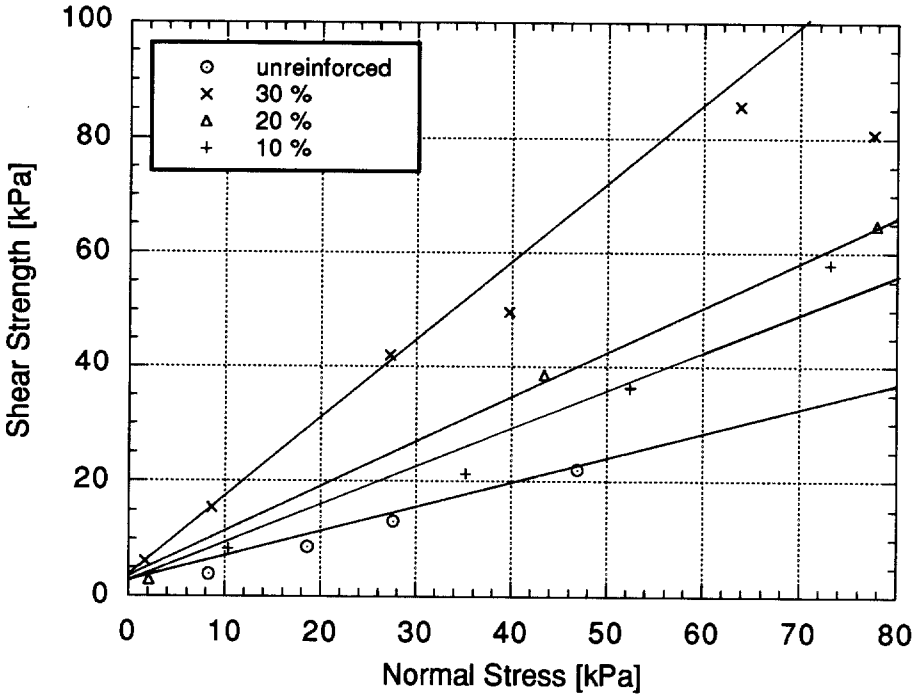

Figure A1.21. Failure Envelope for the Group of Mixes having Length of Reinforcement=15 cm, Unit Weight of the Soil Matrix=14.7 kN/m^3, Randomly Oriented Reinforcement, and Variable Reinforcement Content.

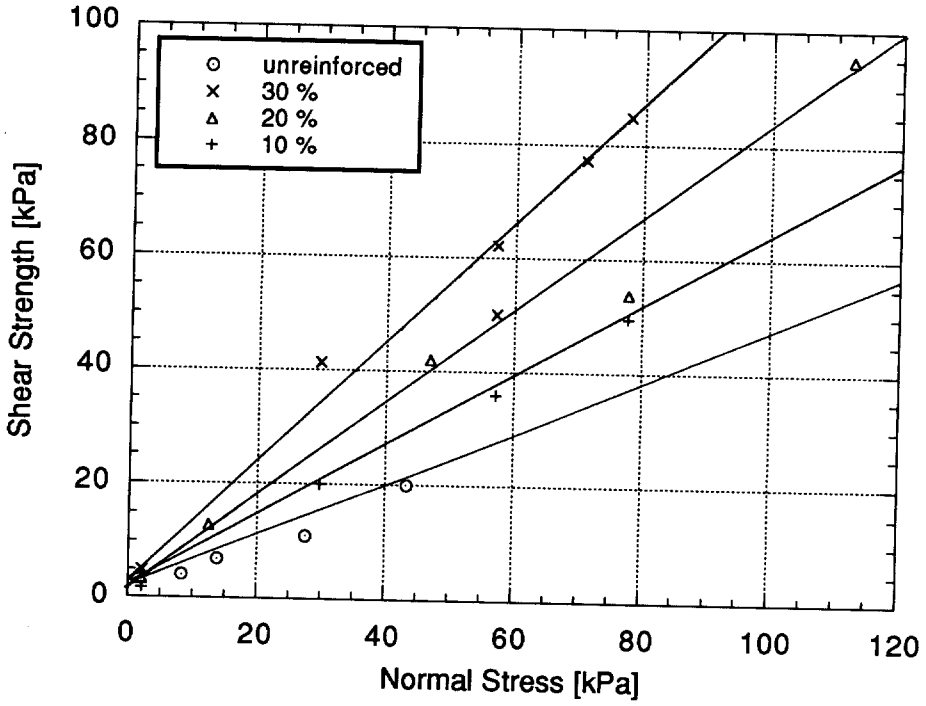

Figure A1.22. Failure Envelope for the Group of Mixes having Length of Reinforcement=5 cm, Unit Weight of the Soil Matrix=15.7 kN/m^3, Randomly Oriented Reinforcement, and Variable Reinforcement Content.

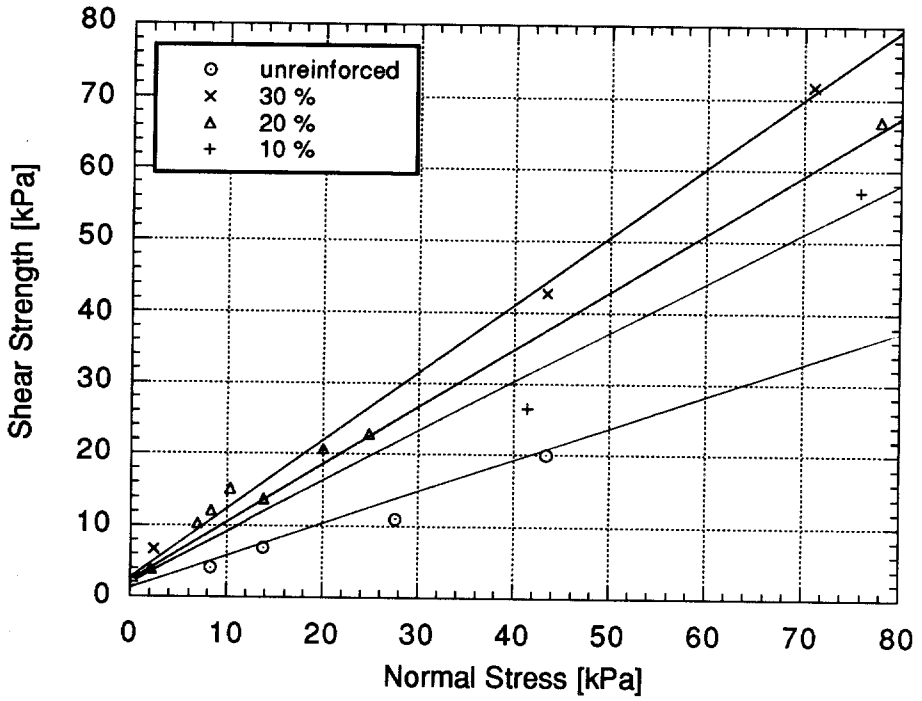

Figure A1.23. Failure Envelope for the Group of Mixes having Length of Reinforcement=10 cm, Unit Weight of the Soil Matrix=15.7 kN/m^3, Randomly Oriented Reinforcement, and Variable Reinforcement Content.

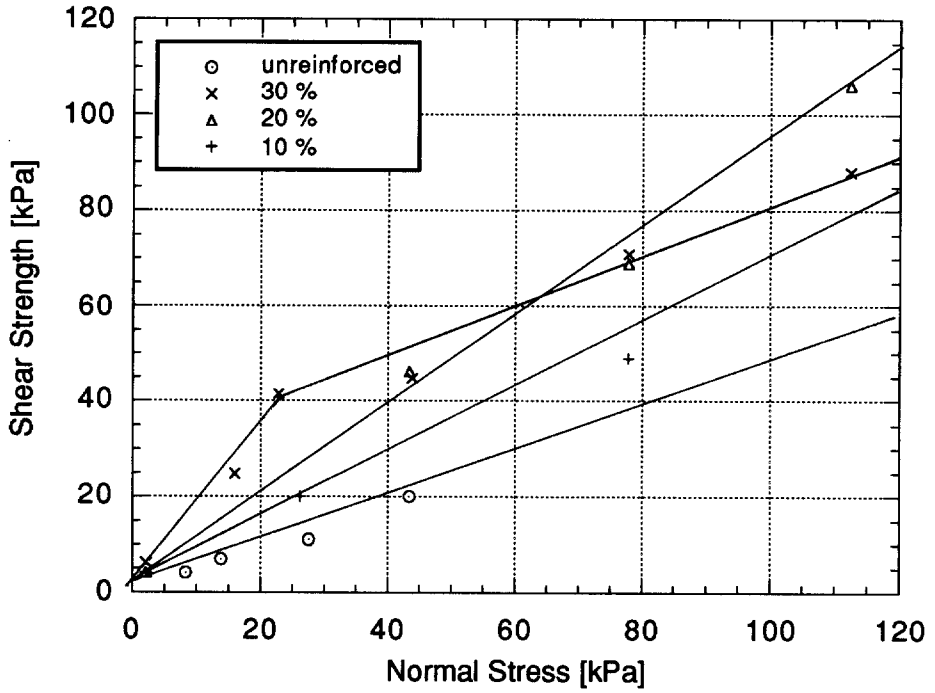

Figure A1.24. Failure Envelope for the Group of Mixes having Length of Reinforcement=15 cm, Unit Weight of the Soil Matrix=15.7 kN/m^3, Randomly Oriented Reinforcement, and Variable Reinforcement Content.

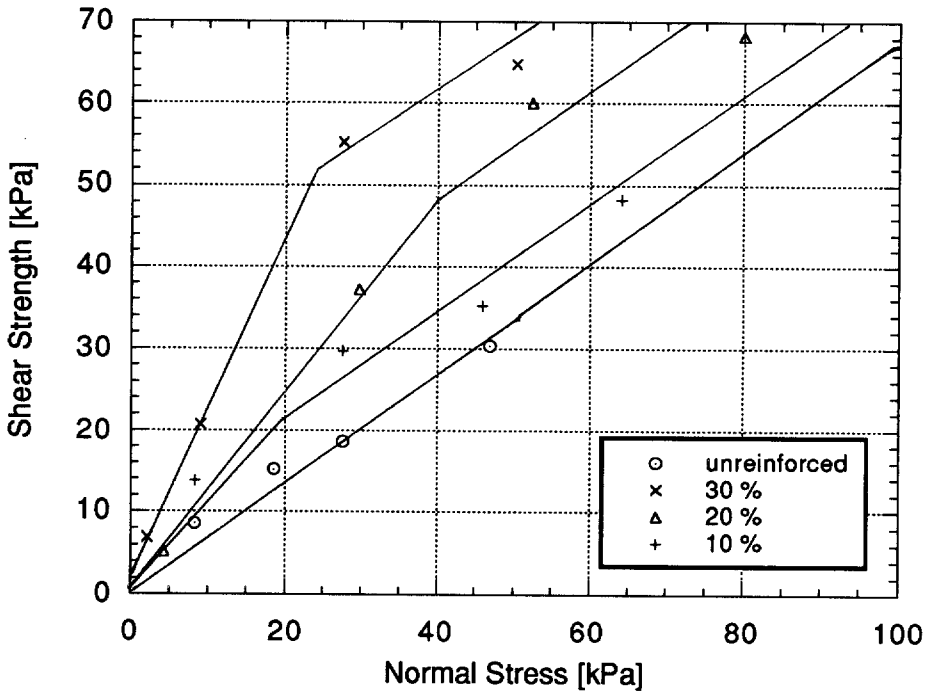

Figure A1.25. Failure Envelope for the Group of Mixes having Length of Reinforcement=5 cm, Unit Weight of the Soil Matrix=16.8 kN/m^3, Randomly Oriented Reinforcement, and Variable Reinforcement Content.

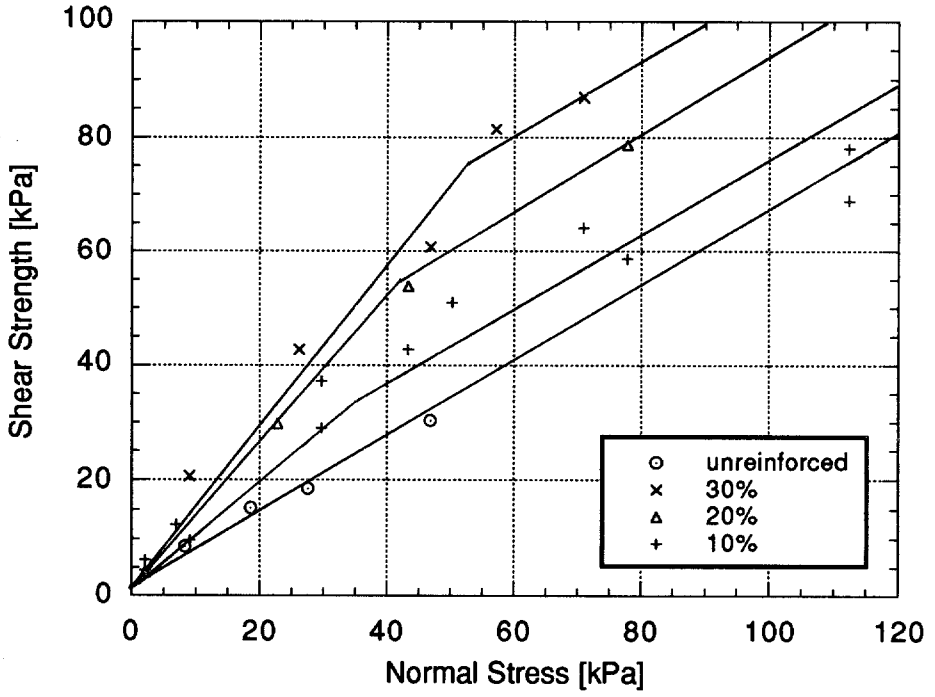

Figure A1.26. Failure Envelope for the Group of Mixes having Length of Reinforcement=10 cm, Unit Weight of the Soil Matrix=16.8 kN/m^3, Randomly Oriented Reinforcement, and Variable Reinforcement Content.

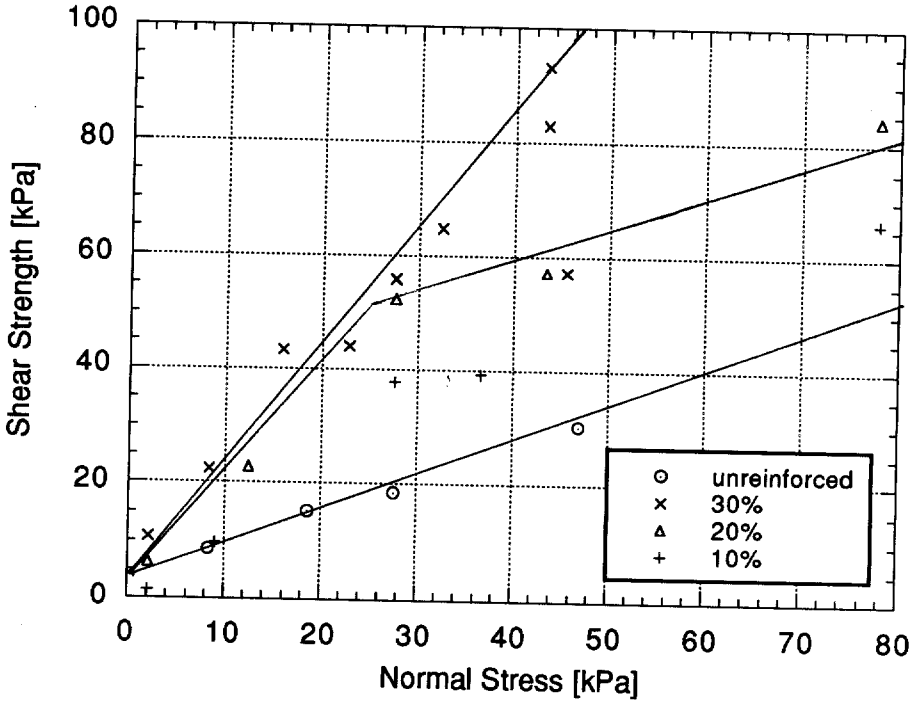

Figure A1.27. Failure Envelope for the Group of Mixes having Length of Reinforcement=15 cm, Unit Weight of the Soil Matrix=16.8 kN/m^3, Randomly Oriented Reinforcement, and Variable Reinforcement Content.

Table A1.1. Table of Strength Envelope Results.

Mix #	ϕ_1'	σ_c
Sn305LR	42.7	-
Sn205LR	38.7	-
Sn105LR	36.4	-
Sn305MR	48.0	-
Sn205MR	39.8	-
Sn105MR	33.7	-
Sn305HR	65.4	24.0
Sn205HR	50.2	40.0
Sn105HR	47.7	20
Sn3010LR	44.3	-
Sn2010LR	39.4	-
Sn1010LR	32.5	-
Sn3010MR	45.0	-
Sn2010MR	40.6	-
Sn1010MR	35.8	-
Sn3010HR	55.2	53
Sn2010HR	52.2	43
Sn1010HR	46.4	33
Sn3015LR	49.2	-
Sn2015LR	39.2	-
Sn1015LR	36.5	-
Sn3015MR	59.0	24.0
Sn2015MR	43.5	-
Sn1015MR	35.0	-
Sn3015HR	67.4	>40
Sn2015HR	61.9	27.0
Sn1015HR	47.2	34.0

SECTION A2

EXPERIMENTAL RESULTS AND PREDICTIONS BY MODEL FOR SPECIMENS TESTED

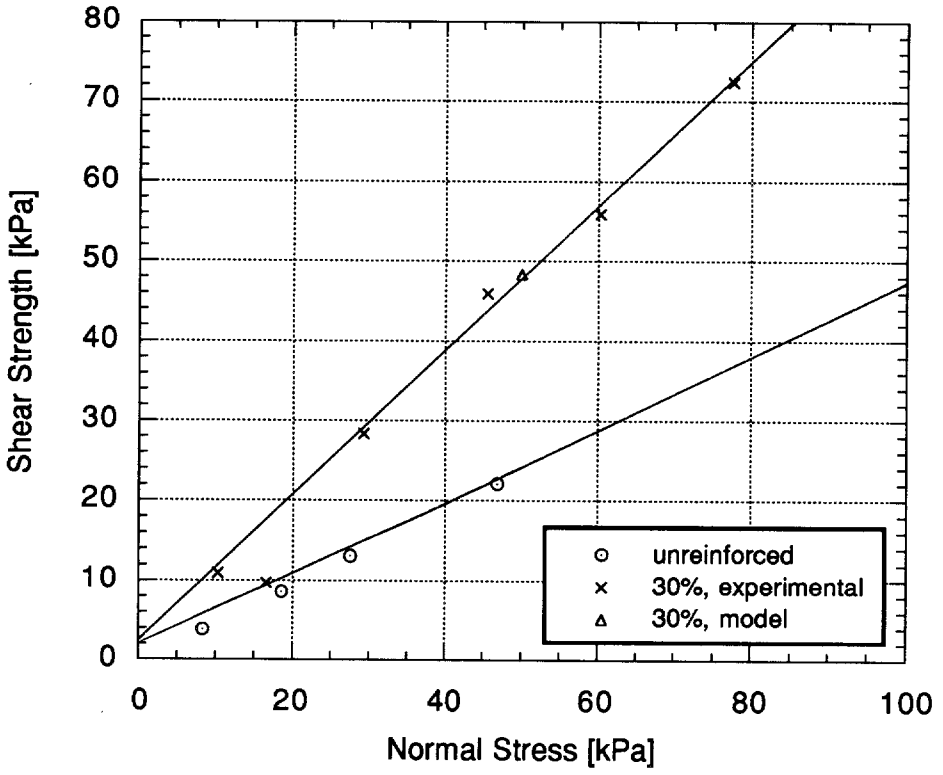

Figure A2.1. Experimental and Model Prediction for Specimen with reinforcement content=30%, Length of Reinforcement=5 cm, Unit Weight of the Soil Matrix=14.7 kN/m^3, and Randomly Oriented Reinforcement.

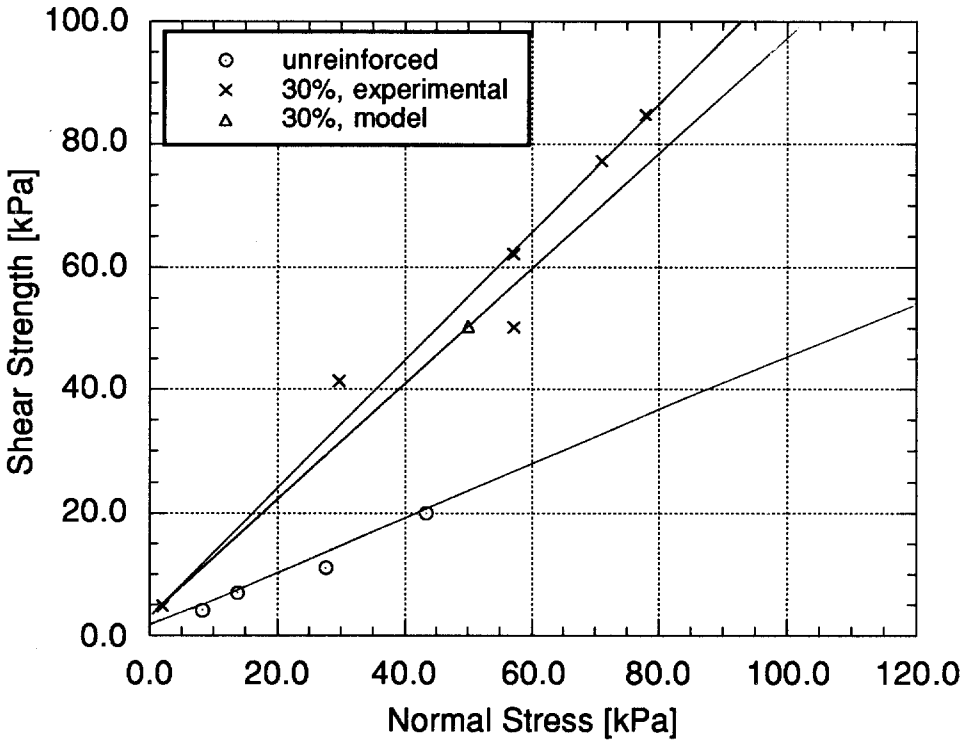

Figure A2.2. Experimental and Model Prediction for Specimen with reinforcement content=30%, Length of Reinforcement=5 cm, Unit Weight of the Soil Matrix=15.7 kN/m^3, and Randomly Oriented Reinforcement.

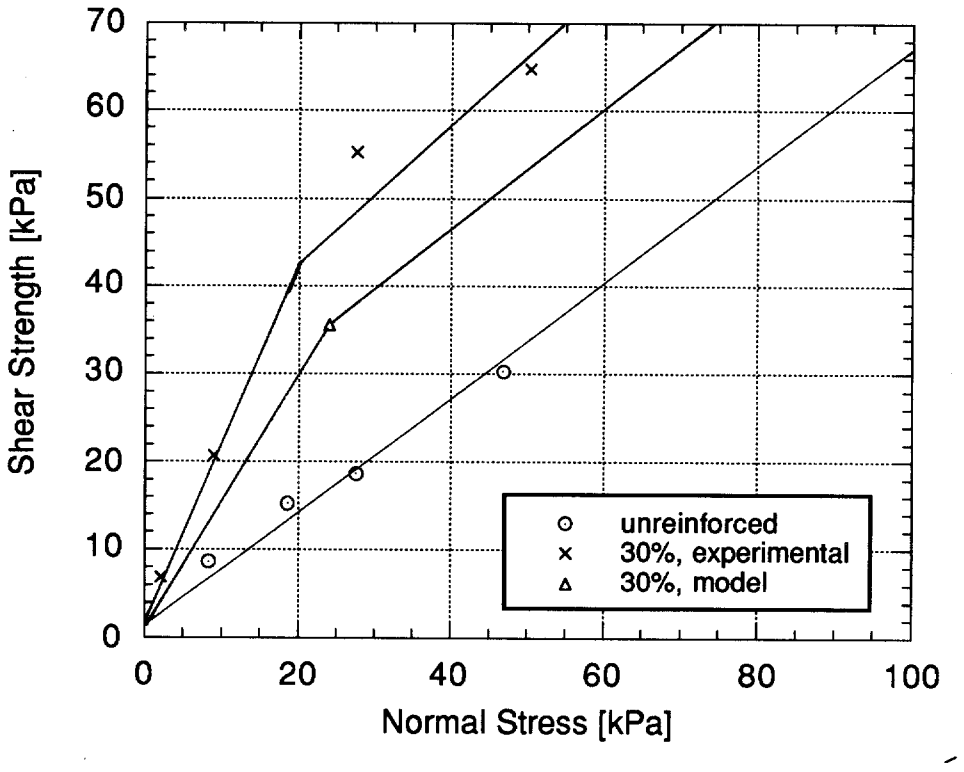

Figure A2.3. Experimental and Model Prediction for Specimen with reinforcement content=30%, Length of Reinforcement=5 cm, Unit Weight of the Soil Matrix=16.8 kN/m^3, and Randomly Oriented Reinforcement.

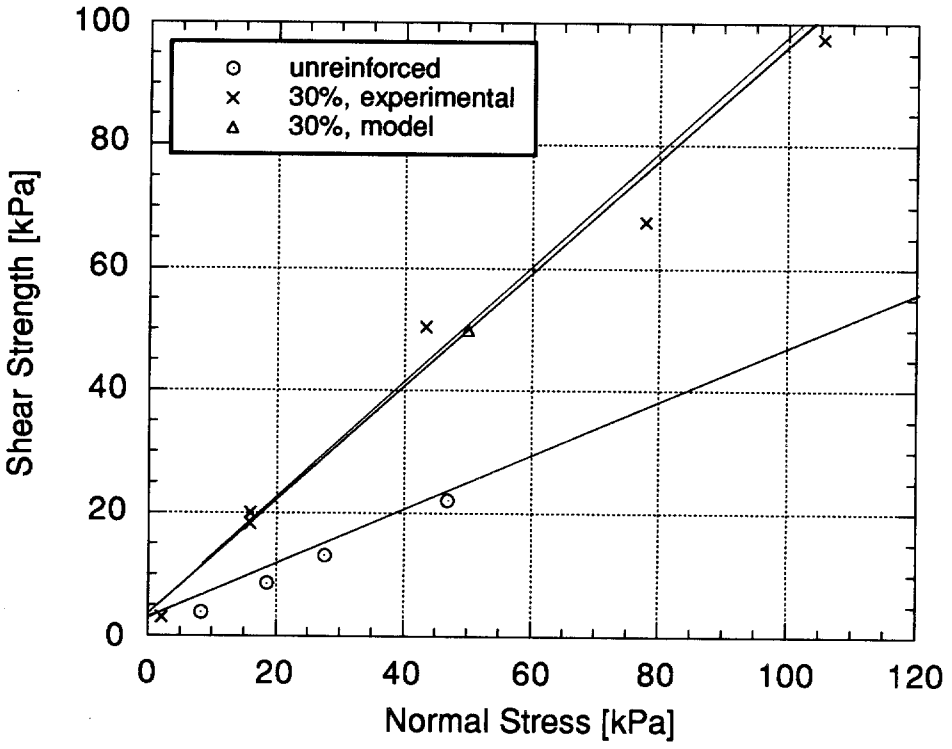

Figure A2.4. Experimental and Model Prediction for Specimen with reinforcement content=30%, Length of Reinforcement=10 cm, Unit Weight of the Soil Matrix=14.7 kN/m^3, and Randomly Oriented Reinforcement.

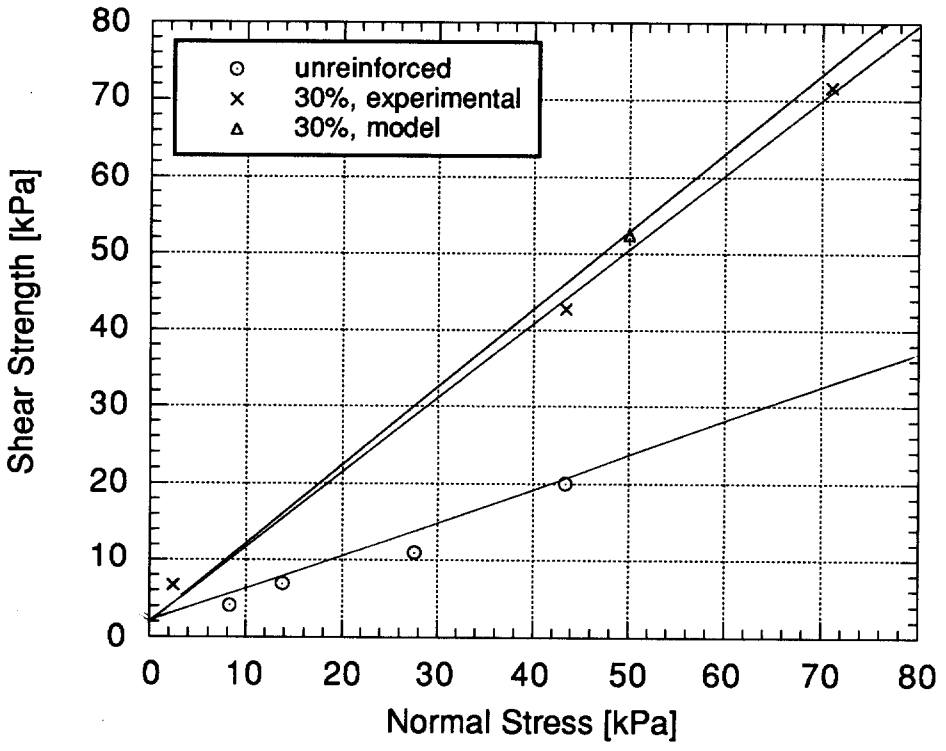

Figure A2.5. Experimental and Model Prediction for Specimen with reinforcement content=30%, Length of Reinforcement=10 cm, Unit Weight of the Soil Matrix=15.7 kN/m^3, and Randomly Oriented Reinforcement.

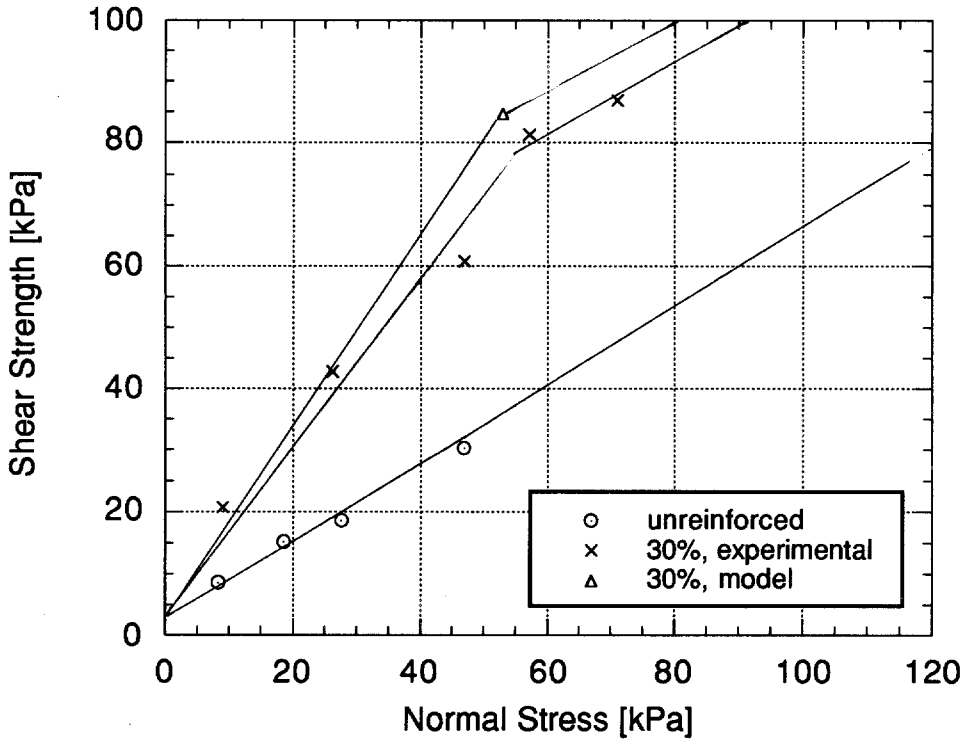

Figure A2.6. Experimental and Model Prediction for Specimen with reinforcement content=30%, Length of Reinforcement=10 cm, Unit Weight of the Soil Matrix=16.8 kN/m^3, and Randomly Oriented Reinforcement.

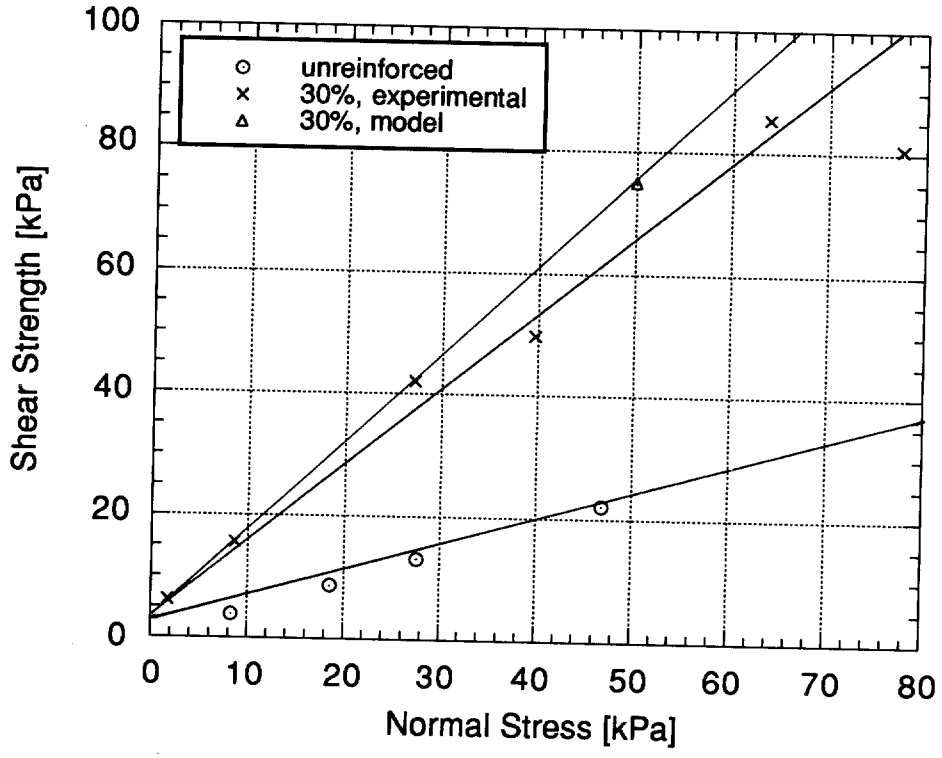

Figure A2.7. Experimental and Model Prediction for Specimen with reinforcement content=30%, Length of Reinforcement=15 cm, Unit Weight of the Soil Matrix=14.7 kN/m^3, and Randomly Oriented Reinforcement.

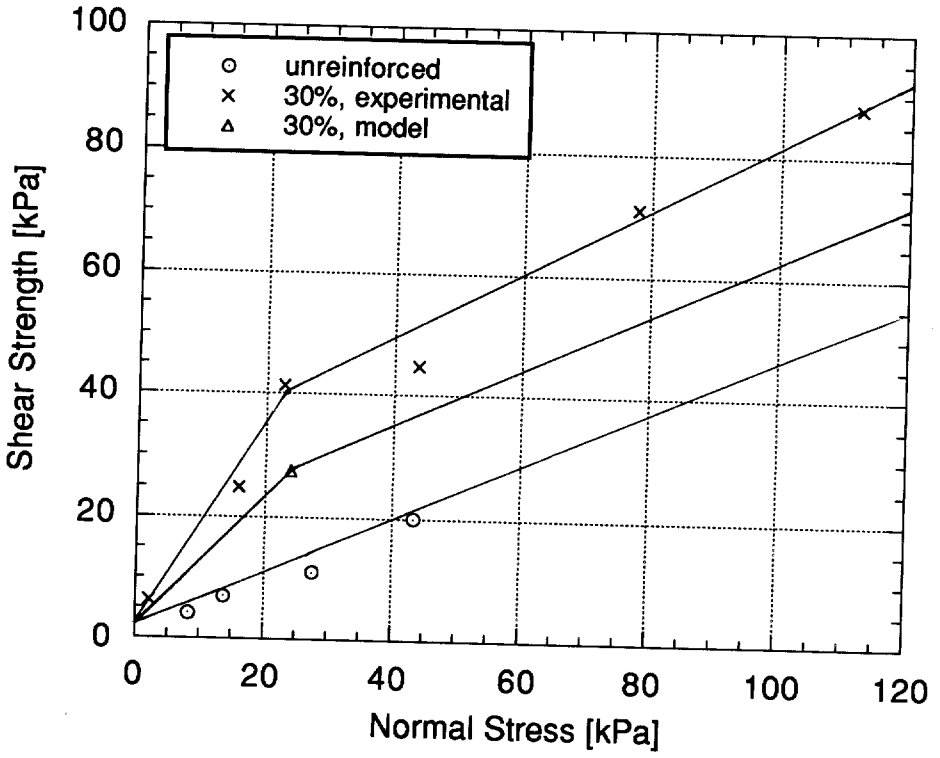

Figure A2.8. Experimental and Model Prediction for Specimen with reinforcement content=30%, Length of Reinforcement=15 cm, Unit Weight of the Soil Matrix=15.7 kN/m^3, and Randomly Oriented Reinforcement.

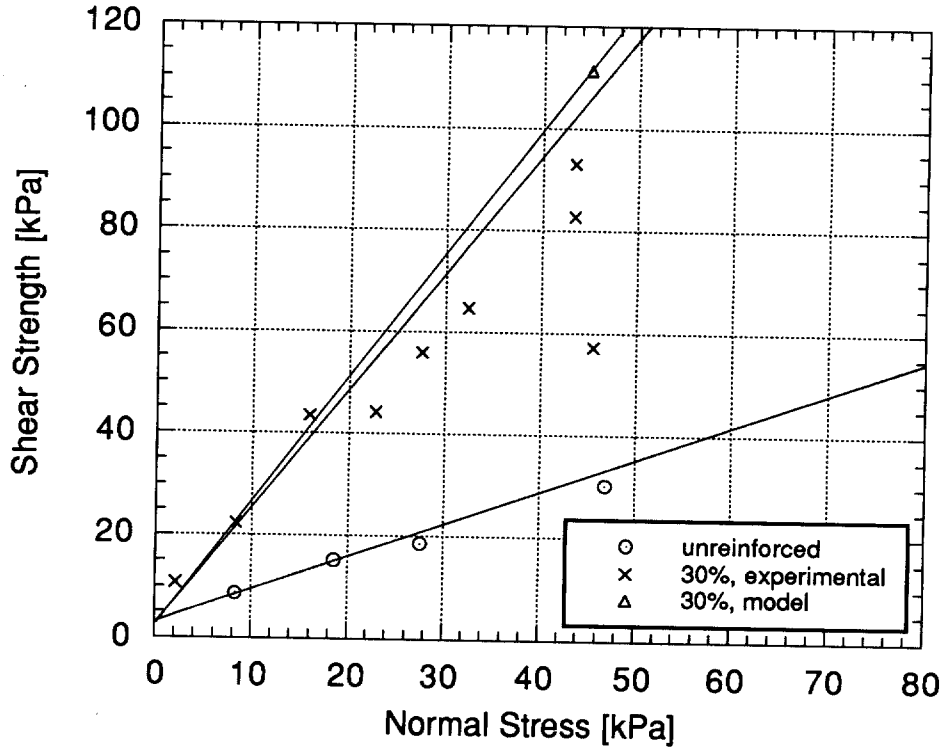

Figure A2.9. Experimental and Model Prediction for Specimen with reinforcement content=30%, Length of Reinforcement=15 cm, Unit Weight of the Soil Matrix=16.8 kN/m^3, and Randomly Oriented Reinforcement.

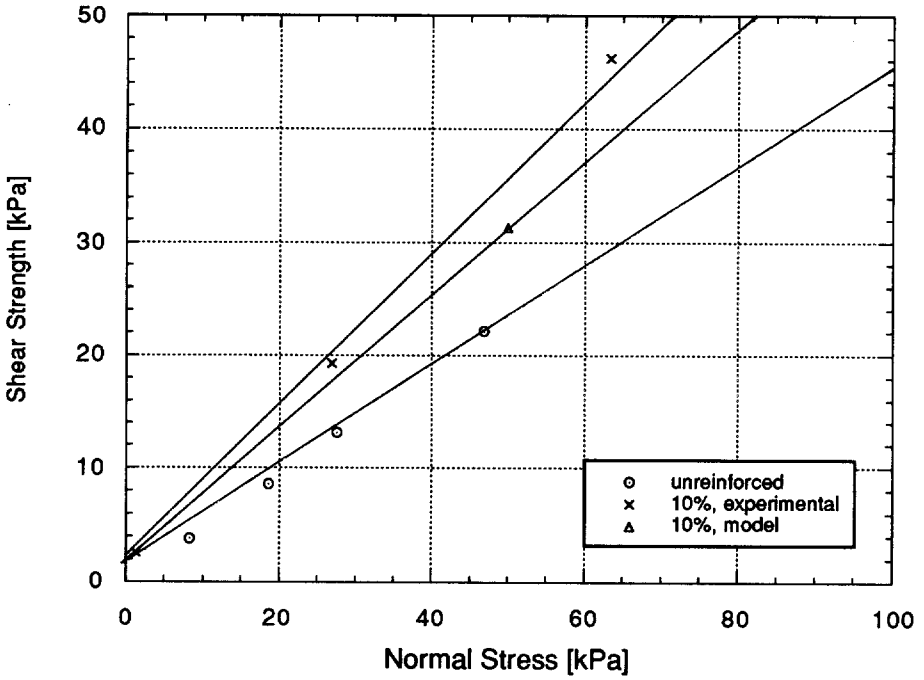

Figure A2.10. Experimental and Model Prediction for Specimen with reinforcement content=10%, Length of Reinforcement=5 cm, Unit Weight of the Soil Matrix=14.7 kN/m^3, and Randomly Oriented Reinforcement.

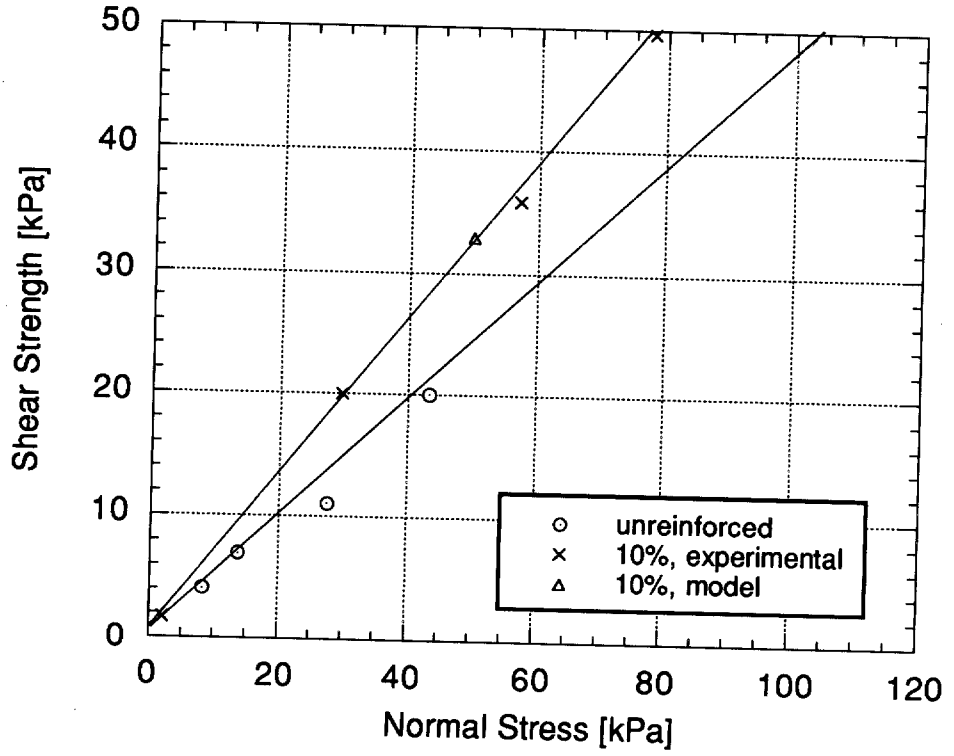

Figure A2.11. Experimental and Model Prediction for Specimen with reinforcement content=10%, Length of Reinforcement=5 cm, Unit Weight of the Soil Matrix=15.7 kN/m^3, and Randomly Oriented Reinforcement.

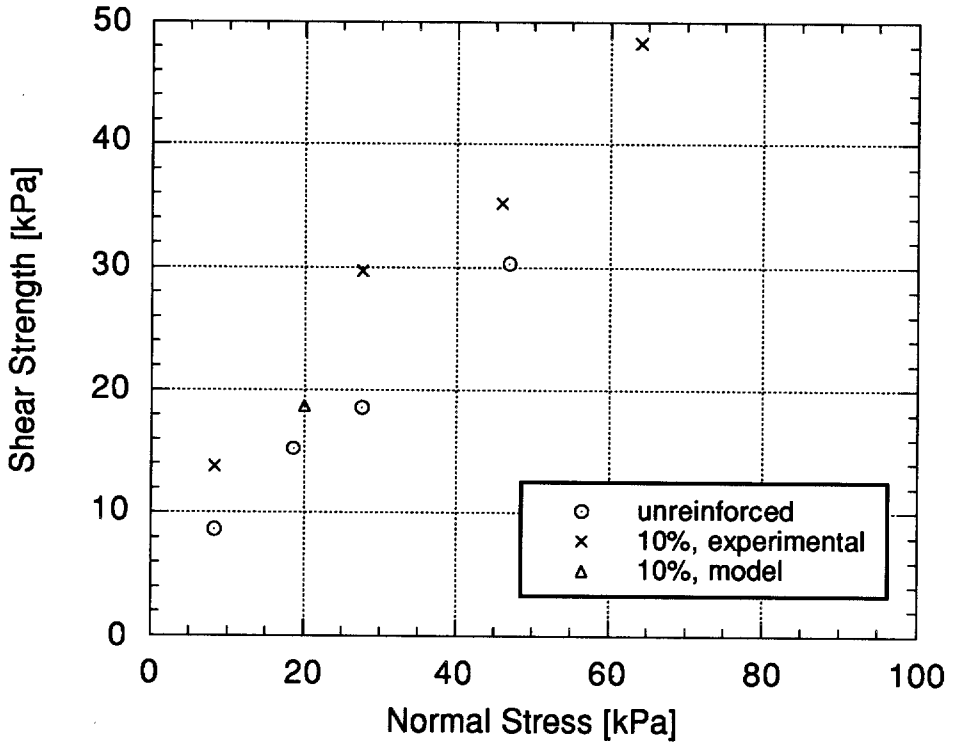

Figure A2.12. Experimental and Model Prediction for Specimen with reinforcement content=10%, Length of Reinforcement=5 cm, Unit Weight of the Soil Matrix=16.8 kN/m^3, and Randomly Oriented Reinforcement.

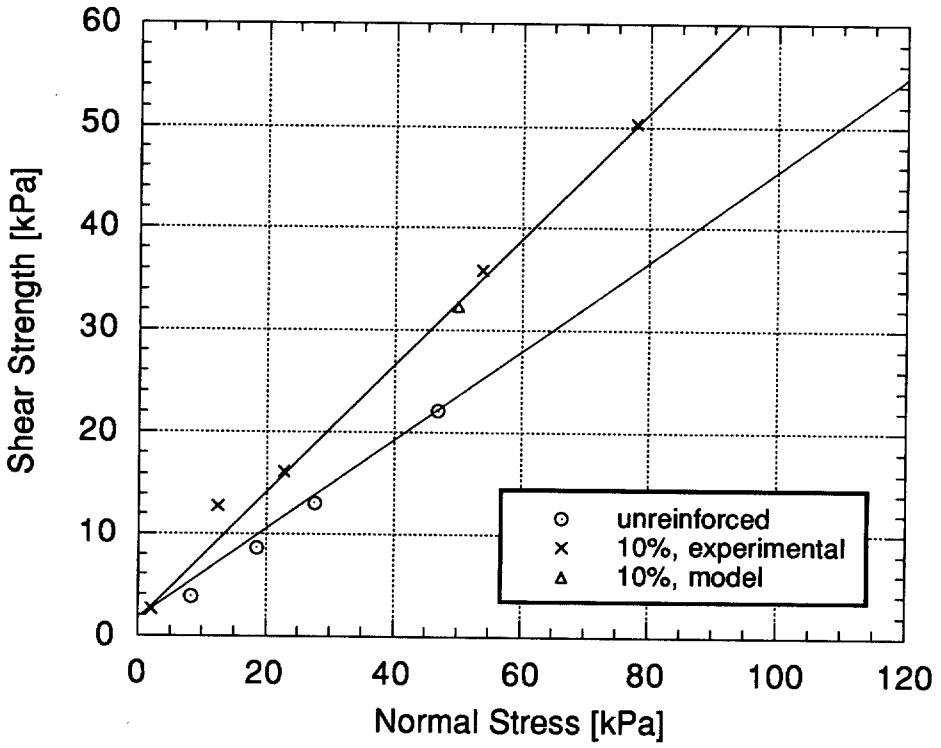

Figure A2.13. Experimental and Model Prediction for Specimen with reinforcement content=10%, Length of Reinforcement=10 cm, Unit Weight of the Soil Matrix=14.7 kN/m^3, and Randomly Oriented Reinforcement.

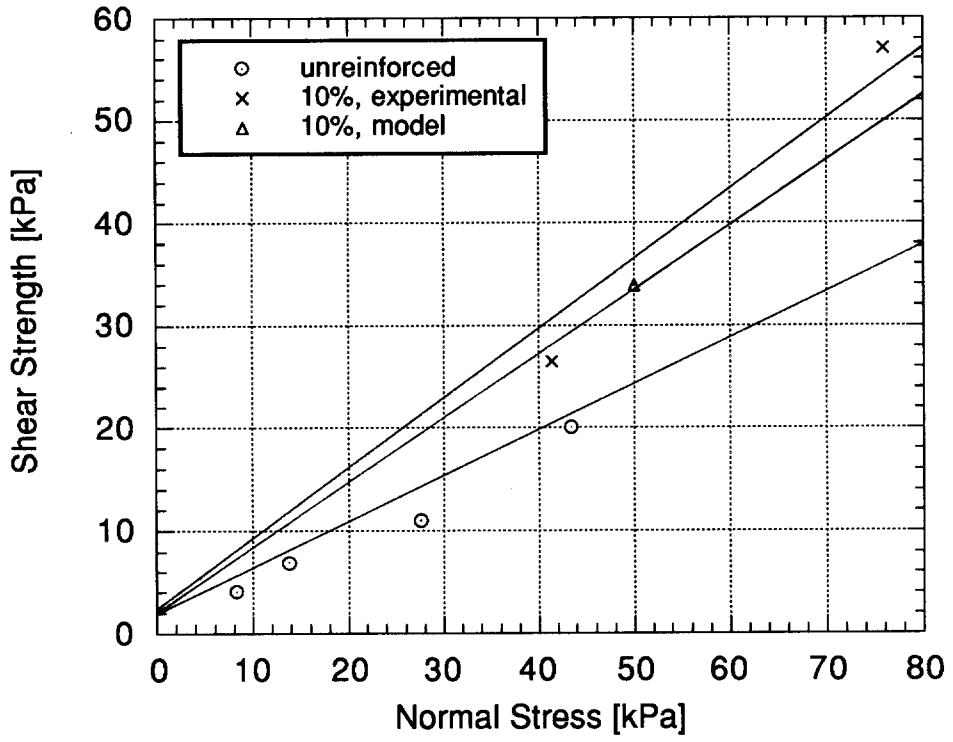

Figure A2.14. Experimental and Model Prediction for Specimen with reinforcement content=10%, Length of Reinforcement=10 cm, Unit Weight of the Soil Matrix=15.7 kN/m^3, and Randomly Oriented Reinforcement.

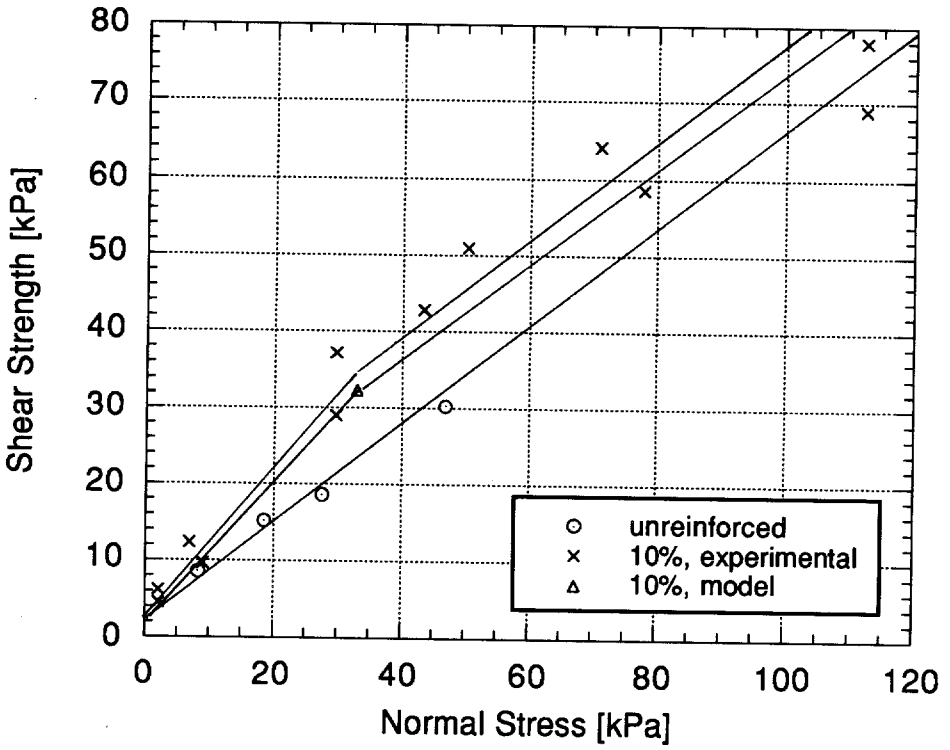

Figure A2.15. Experimental and Model Prediction for Specimen with reinforcement content=10%, Length of Reinforcement=10 cm, Unit Weight of the Soil Matrix=16.8 kN/m^3, and Randomly Oriented Reinforcement.

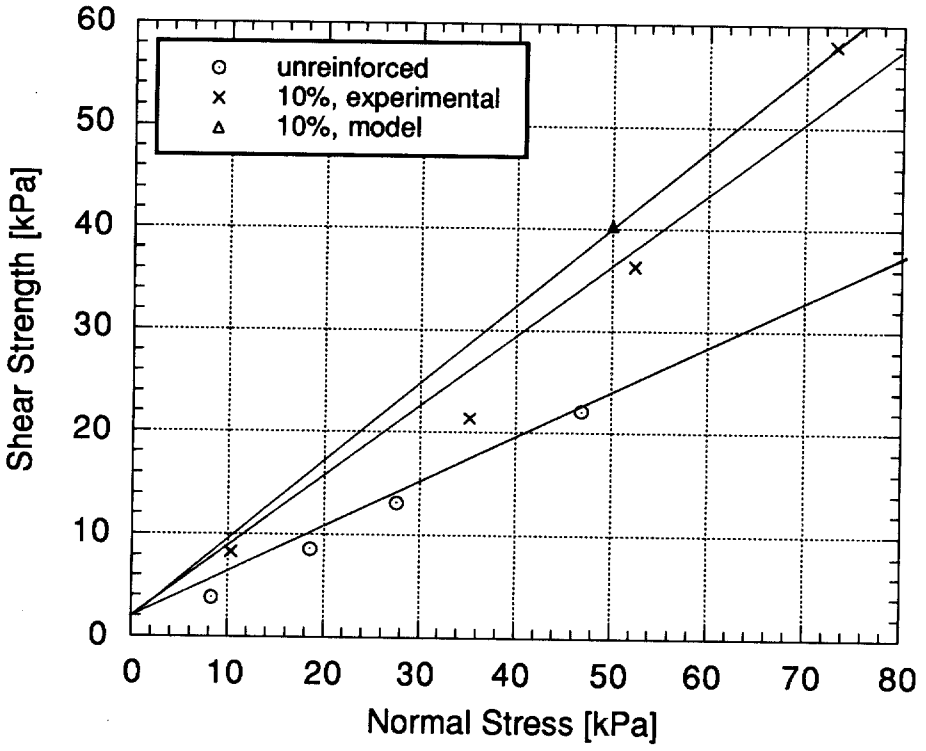

Figure A2.16. Experimental and Model Prediction for Specimen with reinforcement content=10%, Length of Reinforcement=15 cm, Unit Weight of the Soil Matrix=14.7 kN/m^3, and Randomly Oriented Reinforcement.

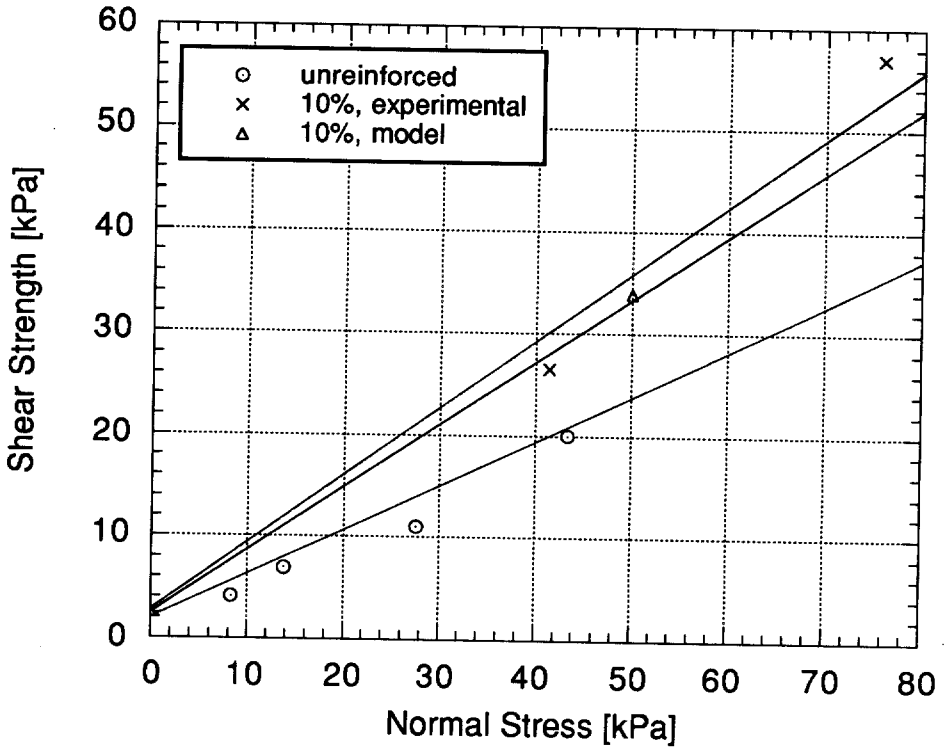

Figure A2.17. Experimental and Model Prediction for Specimen with reinforcement content=10%, Length of Reinforcement=15 cm, Unit Weight of the Soil Matrix=15.7 kN/m^3, and Randomly Oriented Reinforcement.

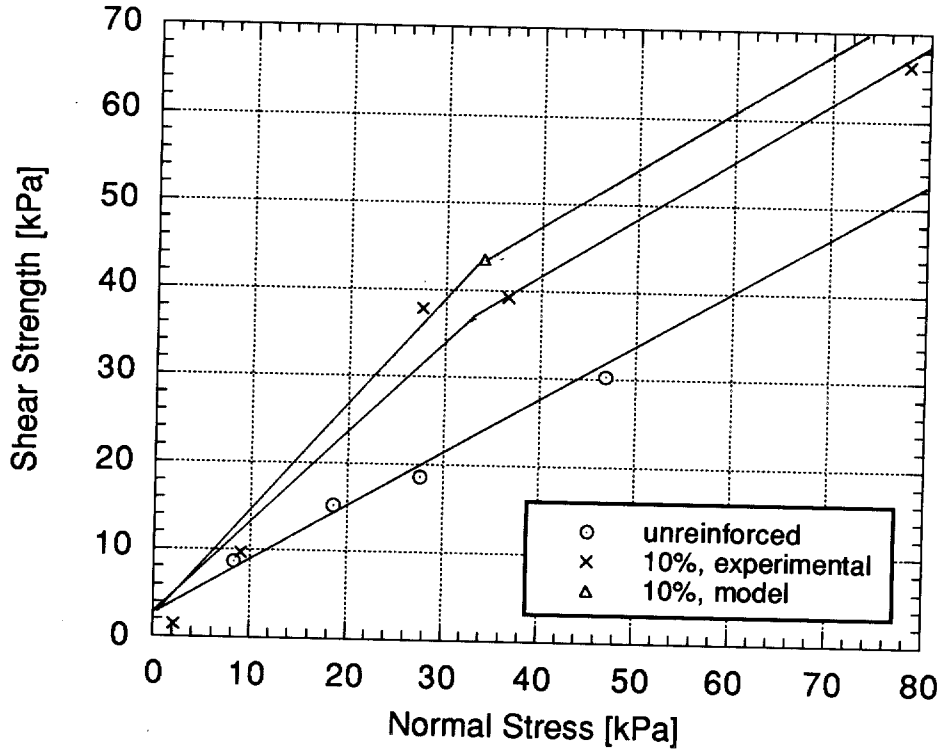

Figure A2.18. Experimental and Model Prediction for Specimen with reinforcement content=10%, Length of Reinforcement=15 cm, Unit Weight of the Soil Matrix=16.8 kN/m^3, and Randomly Oriented Reinforcement.

SHEAR STRENGTH OF SAND REINFORCED WITH SHREDDED WASTE TIRES

Approved

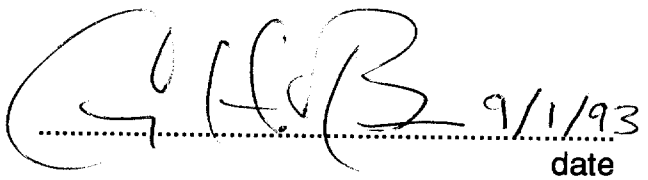

9/1/93
date

Craig H. Benson, Assistant Professor